Potential solutions for certain hurdles of the implementation of exosomes in drug delivery

2018

Tokushima University

Faculty of Pharmaceutical Sciences

Sherif Emam Abdallah Emam

Table of contents

LIST OF TABLES

LIST OF FIGURES

List of abbreviations

Abs	Antibodies
ANOVA	Analysis of variance
APC	Allophycocyanin fluorophore
B16BL6	Murine melanoma cell line
BALB/c	Albino laboratory-bred strain of the house mouse with genotype c
BBB	Blood brain barrier
BCA	Bicinchoninic acid assay
BSA	bovine serum albumin
C26	Murine colorectal cancer cell line; colon 26
CD (9, 19, 29, 63 and 81)	Cluster of differentiation (9, 19, 29, 63 and 81)
CDE	Caveolin-dependent endocytosis
CHOL	Cholesterol
CL	Cationic bare liposomes
CL1	Cationic liposomes composed of HSPC/CHOL/DC-6-14 (2/1/0.2)
CL2	Cationic liposomes composed of DOPE/DC-6-14 (2/1)
CL3	Cationic liposomes composed of DOPE/DOTAP (2/1)
CL4	cationic liposomes composed of DOPE/DC-Chol (2/1)
CME	Clathrin-mediated endocytosis
CPZ	Chlorpromazine
DC(s)	Tumor associated dendritic cell(s)
DC-6-14	O,O′-ditetradecanoyl-N-(alpha-trimethyl ammonio acetyl) diethanolamine chloride
DC-Chol	3ß-[N-(N',N'-dimethylaminoethane)-carbamoyl] cholesterol

	hydrochloride
DiI	1,1'-Dioctadecyl-3,3,3',3'-Tetramethylindocarbocyanine Perchlorate; DiIC18(3)
DiR	1,1'-Dioctadecyl-3,3,3',3'-Tetramethylindotricarbocyanine Iodide; DiIC18(7)
DLD-1	Human colorectal cancer cell line
DNA	Deoxyribonucleic acid
DOPE	1,2-dioleoyl-*sn*-glycero-3-phosphoethanolamine
DOTAP	1,2-dioleoyl-3-trimethylammonium-propane, chloride salt
DTT	1,4-dithiothreitol
EDTA	Ethylenediaminetetraacetic acid
EGF	Epidermal growth factor
EGFR	Epidermal growth factor receptor
EPR	Enhanced permeation and retention
ESCRT	Endosomal sorting complex required for transport
EV(s)	Extracellular vesicle(s)
Exo(s)	Exosome(s)
exo-FBS	Exosome-depleted fetal bovine serum
exo-N	Exosomes harvested under no liposomal stimulation
exo-S1	Exosomes harvested under liposomal stimulation with HSPC-based cationic liposomes
exo-S2	Exosomes harvested under liposomal stimulation with DOPE-based cationic liposomes
FBS	Normal fetal bovine serum
FITC	Fluorescein-5-isothiocyanate
HEPES	N-(2-hydroxyethyl) piperazineN′-2-ethanesulfonic acid
HRP	Horseradish peroxidase

Hsp	Heat-shock protein
HSPC	hydrogenated soy phosphatidylcholine
HSPGs	Heparin sulphate proteoglycans
IgG	Immunoglobulin G
IgM	Immunoglobulin M
ILVs	Intraluminal vesicles
iRGD	9-amino acid cyclic arginylglycylaspartic acid*, cyclo RGD* (CRGDKGPDC-NH_2)
LSM	Laser scanning confocal microscope
miRNA	Micro ribonucleic acid
MKN45	Human gastric cancer cell line
$mPEG_{2000}$-DSPE	1,2-distearoylsn-glycero-3-phosphoethanol-amine-n-[methoxy (polyethyleneglycol)-2000]
MPS	Mononuclear phagocyte system
MS	Mass spectrometry
MUC1	Mucin 1
NL	neutral bare liposomes
PBS	Phosphate buffered saline
PEG	Polyethylene glycol
RPMI1640	Roswell Park Memorial Institute medium 1640
SDS-PAGE	Sodium dodecyl sulfate polyacrylamide gel electrophoresis
siRNA	Small interfering ribonucleic acid
TAM(s)	Tumor associated macrophage(s)
TBST 0.05%	Tris-buffered saline with 0.05% Tween 20
Tris base	Tris(hydroxymethyl)aminomethane; 2-Amino-2-(hydroxymethyl)-1,3-propanediol

TSG101	Tumor susceptibility gene 101
TSPAN8	Tetraspanin 8

Abstract

Exosomes (Exos) are nano-sized extracellular vesicles (EVs) which are secreted by various cell types including tumor cells. The potential usage of Exos (EVs) as delivery vehicles particularly to tumor is promising and increasingly expanding due to their credentials, such as *in vivo* stability due to their endogenous origin, their innate ability to carry macromolecules to target cells, the presence of a set of uptake-related surface proteins on their surface which can also be engineered for targeting specific cell types. Although these characteristics reveal the preponderance of cancer cell-derived Exos (EVs) as drug delivery system to tumor, many challenges for that emerging field still exist. For instance, the low yield of secreted Exos (EVs), uncertain uptake mechanism, unpredictable Exo (EV) biodistribution and poor specific cell-targeting of systemically administered Exos (EVs) hinders their implementation in tumor targeting delivery. Hence, the aim of this research was to try to overcome such hurdles.

To increase Exo yield, I attempted to stimulate tumor cells via the addition of liposomes *in vitro*. Neutral-, cationic-bare or PEGylated liposomes were incubated with four different tumor cell lines. The stimulatory effect of liposomes on Exo secretion and cellular uptake propensity of the collected Exos by autologous cells or allogeneic cells was evaluated. Both neutral- and cationic-bare liposomes enhanced Exo secretion in a dose-dependent manner. Fluid cationic liposomes provided the strongest stimulation. Surprisingly, the PEGylation of bare liposomes diminished Exo secretion. Exos harvested in the presence of fluid cationic liposomes showed increased cellular uptake, but solid cationic liposomes did not.

Then, to see if the incubation of cells with liposomes would change the biological properties of these Exos, I investigated the surface proteins and the uptake

mechanism of the harvested Exos. Interestingly, Exos induced by solid cationic liposomes lacked some major exosome marker proteins such as CD9, flotillin-1, annexin-A2 and EGF, and subsequently showed lower levels of cellular uptake upon re-incubation with donor cancer cells. However, Exos induced under normal condition and by fluid cationic liposomes, displayed the entire spectrum of proteins, and exhibited higher uptake by the donor cancer cells. Although endocytosis was the major uptake pathway of Exos by tumor cells, endocytosis could occur via more than one mechanism. Higher Exo uptake was observed in donor cells than in allogenic cells, indicating that donor cells might interact specifically with their Exos and avidly internalize them.

Later on, to enhance Exos circulation time and hence their tumor accumulation, PEGylation of Exos was conducted. Then, the biodistribution of intravenously injected PEGylated Exos, namely autologous C26-Exos and allogeneic B16BL6-Exos, were evaluated in C26 tumor bearing mice. Both Exos were remarkably accumulated in the tumor tissue. In addition, the tumor accumulation of autologous Exos was more predominant than that of allogeneic Exos. In addition to the detected Exo uptake by tumor cells, their uptake by certain tumor-infiltrating immune cells was observed. The uptake of autologous Exos by tumor-associated macrophages (TAMs) and T cells was more prominent than allogeneic Exos, while no significant difference was noticed between the uptake propensities for both Exos types by tumor-infiltrating dendritic cells (DCs) and B cells.

Overall, the obtained findings indicate that the physicochemical properties of liposomes determine whether they will act as a stimulant or as a depressant on Exo secretion from tumor cells. In addition, liposomes of varying physicochemical properties might control the characteristics of secreted Exos such as the expression of Exos proteins and Exos uptake. Finally, PEGylated autologous cancer cell-derived Exos

can be a promising delivery platform to target tumor cells as well as tumor-infiltrating immune cells and that may be fruitfully exploited in cancer therapeutics and diagnostics.

Background and rationale

Drug delivery systems (DDS) with nanoparticles have been exploited to improve the delivery of therapeutic agents to the target cell or tissue or organ. DDS have been widely investigated and have shown a breakthrough in the treatment strategies of numerous diseases. However, due to the unavoidable side effects of the artificial DDS, trials to develop alternative natural DDS have been tremendously evolved **(Tominaga et al., 2015)**. One of the potential natural DDS is extracellular vesicles (EVs) which are mainly classified into three groups; exosomes (Exos), microvesicles and apoptotic bodies. Such classification depends on vesicle size and biogenesis **(Barile and Vassalli, 2017)**. Exos are homogenous vesicles which their size varies from 30 nm to 150-200 nm and have specific surface markers (CD9, CD63, CD81 and TSG101). These vesicles are formed within endosomes and released from these endosomes after their maturation and fusion with cell plasma membrane **(Hannafon and Ding, 2013; Whiteside, 2017)**. While, microvesicles, also called microparticles or shedding vesicles, are heterogeneous vesicles (200-1000 nm) and are generated by direct budding or shedding from cell plasma membrane **(Whiteside, 2017)**. The last class is apoptotic bodies which are larger (1000-5000 nm) and produced during cell death by fractionation or karyorrhexis of cell content **(Whiteside, 2017)**. These classes can be isolated via differential centrifugation at approximately 2,000, 10,000 and 100,000 x g for apoptotic bodies, microvesicles and Exos respectively **(Barile and Vassalli, 2017)**. These natural nanoparticles, EVs (Exos), have lipid bilayer structures composed of proteins, lipids and RNAs **(Keerthikumar et al., 2016)**. This unique structure reflects the versatility in the potential implementations of these natural DDS for fitting with various therapeutic targets.

Exos can be harnessed in drug delivery for different diseases, particularly in cancer therapy. Exos have several characteristic credentials as drug delivery carriers **(Johnsen et al., 2014; Stremersch et al., 2016; Vader et al., 2016; Jiang and Gao, 2017; Lu et al., 2017)**, for example;

1) Mediating cell – cell communications, they are released from one cell and taken up by another cell.
2) Their innate ability to transfer their cargo (proteins and RNA molecules) to the recipient cell indicates their potential use in delivering various types of therapeutic agents.
3) Their endogenous origin is supposed to mitigate their removal by the immune system; they can be isolated from the biological fluids of the patient and then injected to the same patient to deliver different therapeutic agents.
4) Their ability in targeting specific cell or tissue via their surface proteins (cell or tissue tropism).
5) Their *in vivo* stability in blood circulation.
6) Their ability in crossing biological barriers such as blood brain barrier (BBB).
7) Their nano size is also supposed to reduce their detection by the immune system and in addition to enhance their accumulation in tumors via enhanced permeation and retention effect (EPR).
8) Having surface proteins (tetraspanins, integrins, etc) which contribute to their release, cellular uptake and targeting.
9) The amenability for engineering their cargo or surface characters expands their versatility.
10) The ability to protect their cargo against degradation.
11) Reasonable storage condition.

Accordingly, Exos have been exploited in different therapeutic implementations for different diseases such as cancer, neurological and inflammatory disorders. For cancer, several researchers have investigated Exos as drug delivery in cancer therapy either in unmodified form or bioengineered with specific ligands (such as GE11, iRGD) to deliver chemotherapeutic agents (such as paclitaxel and doxorubicin) or nucleic acids (such as miRNA and siRNA) to target tumor **(Ohno et al., 2013; Y. Tian et al., 2014b; Kim et al., 2016; Kamerkar et al., 2017)**. For instance, intravenously administered mesenchymal stem cell-derived Exos showed a long-circulating property via expressing CD47 which reduced Exo clearance by phagocytes and accordingly had a predominant ability in delivering siRNA to pancreatic tumor, compared to liposome **(Kamerkar et al., 2017)**. Similarly, intravenously administered GE-11 positive Exos substantially delivered miRNA to EGFR- expressing cancer cell **(Ohno et al., 2013)**. Another example, intravenously administered iRGD-Exos had the ability to deliver doxorubicin to integrin-expressing cancer cells **(Y. Tian et al., 2014b)**. Furthermore, intranasally administered paclitaxel containing Exos could prominently suppress pulmonary metastases in mice **(Kim et al., 2016)**.

While, due to Exos are the predominant ability of Exos to cross BBB, unmodified or bioengineered Exos have been exploited in delivering therapeutic agents (such as siRNA, antioxidants and anticancers) to the brain for treating different diseases (such as Alzheimer's, Parkinson's, other brain-inflammatory disorders and brain cancer) **(Alvarez-Erviti et al., 2011; Zhuang et al., 2011; Haney et al., 2015; Yang et al., 2015)**. For example, Doxorubicin-encapsulated Exos could cross BBB and suppress the growth of brain tumor after their injection into the blood circulation of zebrafish model **(Yang et al., 2015)**. Another example, intranasally

administered catalase-encapsulated Exos could cross BBB and target neurons treating the inflammatory activities in Parkinson's disease mouse model **(Haney et al., 2015)**. Similarly, intranasally administered curcumin-encapsulated Exos had the ability to cross BBB and relieve brain inflammatory activities in an induced inflammation mouse model **(Zhuang et al., 2011)**. Intravenously administered RVG-Exos crossed BBB and successfully delivered siRNA to brain **(Alvarez-Erviti et al., 2011)**.

Besides Exo implementation in gene and drug delivery, Exos have been extensively studied for their use in immunotherapy. Exos have been employed in cancer immunotherapy (cancer vaccine) via loading Exos with tumor peptide or antigen to elicit immunostimualtory effects against tumor growth. These Exos have shown a remarkable success in immune stimulation with better stability and biocompatibility, compared to conventional non-cell and cell based strategies **(Bell et al., 2016)**. Dendritic cell-derived Exos (DEX) and tumor cell-derived Exos (TEX) are the common examples for Exo implementation in cancer immunotherapy **(Chaput et al., 2005; Tan et al., 2010)**. Exos secreted by immature dendritic cells (DCs) loaded with tumor peptide have predominant ability to suppress tumor growth, compared to DCs **(Zitvogel et al., 1998)**. The tumor suppression by peptide-loaded DEX occurred by activating cytotoxic T lymphocytes via transferring immunostimualtory peptides to DCs **(Andre et al., 2004)** or via combining these DEX with Toll-like receptor 3 and 9 ligands **(Chaput et al., 2004)** or immunopotentiating drug (cyclophosphamide) **(Taieb et al., 2006)**. Similarly, in spite of the role of TEX in tumor progress and metastasis, TEX have the ability to activate cytotoxic T lymphocytes via presenting tumor antigens to DCs **(Wolfers et al., 2001; Tickner et al., 2014; Whiteside, 2016)**. Accordingly TEX can be adopted in cancer immunotherapy. It is noteworthy that

Exos have been investigated in clinical trials for cancer therapy **(Tan et al., 2010; El Andaloussi et al., 2013; J. Wang et al., 2016a)**.

Despite of these promising implementations of Exos, several challenges and limitations embarrass this growing field **(Johnsen et al., 2014; Stremersch et al., 2016; Vader et al., 2016; Doeppner et al., 2017; Jiang and Gao, 2017; Lu et al., 2017)**, such as;

1) The low yield of Exos, thus finding scalable isolation approach is of utmost importance and challenging.
2) Lacking complete and sufficient understanding of Exo biogenesis, secretion and uptake.
3) Their poor pharmacokinetics and biodistribution, particularly poor tumor targeting. Exos have a short half-life with prominent uptake by mononuclear phagocyte system (liver and spleen) in spite of their endogenous origin and nano size.
4) Low loading efficiency of Exos using the current loading techniques such as transfection, incubation, electroporation and sonication. Thereby, a further modification in these methods or developing new ones is of utmost necessity.
5) Finding a preferential type of donor cell, particularly for clinical use, mesenchymal cells and immature dendritic cells are the common candidates, but that growing field requires more versatility in the number of available donor cells.

To address these hurdles, dedicated efforts of researches have been devoted. For example, to increase the quantity of the collected Exos (EVs), various strategies have been studied **(Narayanan et al., 2013; Riches et al., 2014; J. Li et al., 2015; Atienzar-Aroca et al., 2016; Patel et al., 2017; Vulpis et al., 2017)**. It was found

that the cell density of cell culture and Exo collection frequency has a great impact on the yield of Exos **(Patel et al., 2017)**. The decrease in cell density and multiple Exo collection per the same cultured cells result in an increase in the secretion of similar Exos **(Patel et al., 2017)**. Probably, Exo secretion is regulated by an unknown feedback mechanism due to the Exos already secreted and existed extracellularly **(Riches et al., 2014)** and thereby removing these secreted Exos by frequent collection will lead to enhance Exo release **(Patel et al., 2017)**. The incubation time is found to control the quantity of the isolated Exos as indicated by Narayanan et al. who indicate that the 5-day-incubation results in a higher Exo yield than 1- or 2-day-incubation **(Narayanan et al., 2013)**. Furthermore, cell cultured under a stress factor has been investigated to expand Exo secretion. Retinal pigment epithelium cells cultured under an oxidative stress produces higher quantities of Exos **(Atienzar-Aroca et al., 2016)**. Similarly, Genotoxic stress of anticancer agent, melphalan, enhances multiple myeloma cells to secrete Exos **(Vulpis et al., 2017)**. In addition, the characters of the culture medium have affected the extent of Exo (EV) secretion. Using serum-free medium enhances the release of Exos (EVs) of varying composition, compared to conventional culture medium **(J. Li et al., 2015)**.

Another hurdle is the uncertain uptake mechanism of Exo internalization by different recipient cells. To address such issue, potential uptake pathways of Exos have investigated. It has been shown that Exo internalization into recipient cells is an energy-dependent process and Exos can enter the recipient cells via direct membrane fusion and/or endocytosis **(Fig. 1.1) (Fitzner et al., 2011; Fruhbeis et al., 2013; Mulcahy et al., 2014; McKelvey et al., 2015; French et al., 2017)**. Endocytic pathways include clathrin-mediated endocytosis (CME), caveolin-dependent endocytosis (CDE), lipid raft-mediated endocytosis, macropinocytosis and

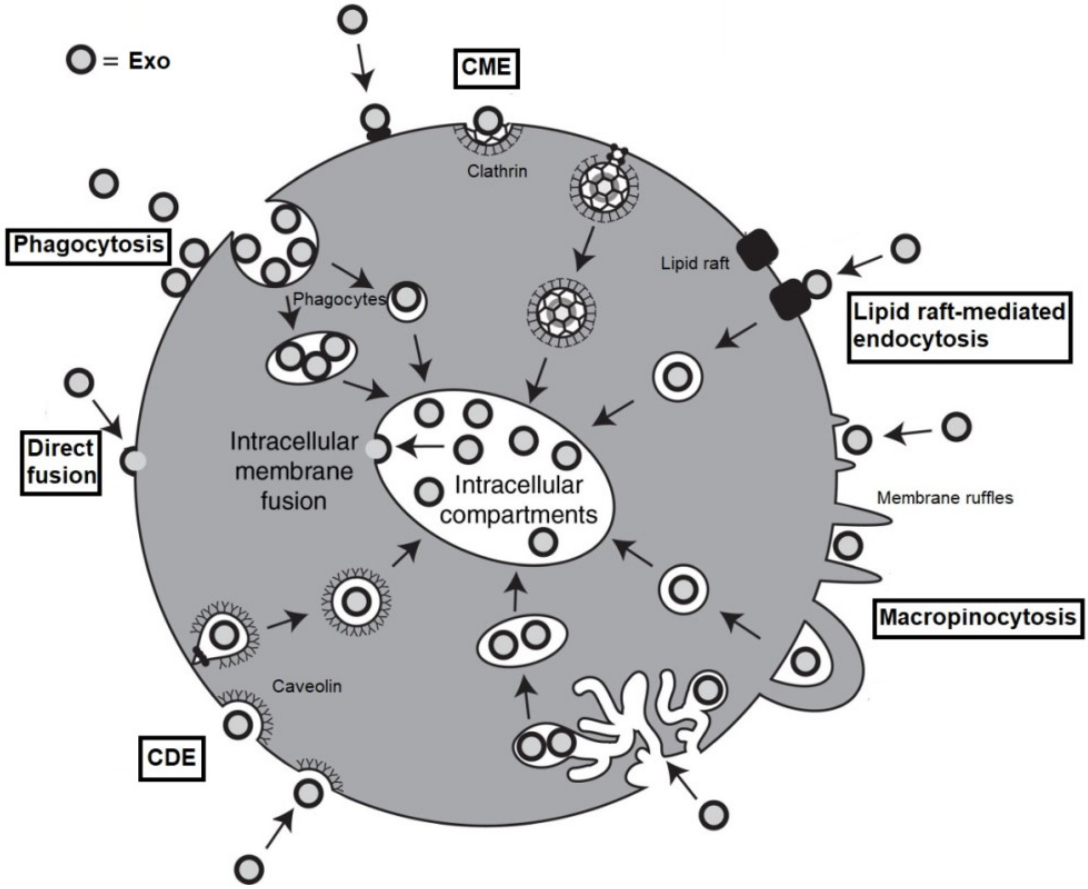

Figure. 1.1. Different pathways of Exo uptake

The figure shows potential uptake mechanisms of Exos and is reproduced from an article of **(Mulcahy et al., 2014)** which is an Open Access article distributed under the terms of the Creative Commons Attribution-Noncommercial 3.0 Unported License, permitting all non-commercial use, distribution, and reproduction in any medium, provided the original work is properly cited. License URL: https://www.tandfonline.com/action/showCopyRight?scroll=top&doi=10.3402%2Fjev.v3.24641

phagocytosis **(Conner and Schmid, 2003; Doherty and McMahon, 2009; Svensson et al., 2013; T. Tian et al., 2014a)**. However, no consensus is pointed for the type and the number of pathways driving Exo uptake and whether other factors are involved in Exo uptake such as the composition of Exos, donor cells and recipient cells.

Biodistribution and pharmacokinetics of Exos are critical parameters for developing an efficient Exo-based DDS for different disease, especially cancer. Intravenously administered Exos have a short half-life because Exos are rapidly cleared from blood circulation via mononuclear phagocyte system (MPS) **(Takahashi et al., 2013; Lai et al., 2014; T. Smyth et al., 2015)**. Unmodified Exos have a poor tendency to target tumor cells after intravenous injection into the blood circulation of tumor-bearing mice **(T. Smyth et al., 2015)**. Accordingly, Exo engineering has been evolved to overcome such short circulation time and poor tumor targetability **(Vader et al., 2016; Barile and Vassalli, 2017)**.

Taken together, the field of Exos as drug delivery systems is increasingly growing depending on the intriguing characteristics of Exos such as the presence of surface proteins, cell tropism, innate ability in transferring proteins and mRNAs between cells, endogenous origin, *in vivo* stability and nano size. Despite the expected predominance of cancer derived Exos in targeting tumor, many limitations for this promising filed are exist such as the low yield, loss of consensus on the mechanism driving Exo internalization into cells and poor tumor targeting. The objective of this thesis, therefore, was to overcome such limitations via introducing a novel strategy to expand Exo yield from cancer cells using co-incubation with liposomes, studying different uptake pathways of Exos and PEGylation of autologous Exos to increase their accumulation in tumor tissue.

2.1. Background

Exo enrichment is a challenging task limited by many factors such as the poor purity and small quantity of isolated Exos and the low Exo secretion from donor cells. Thereby, many isolation methods are currently developed overcome such limitations. The first accepted method was ultracentrifugation followed by purification with a sucrose gradient **(Théry et al., 2006)**. Ultracentrifugation, however, has the disadvantage of being a time-consuming process that can lead to the degradation of biomolecules, which in turn, can result in a lowering of the purity of Exos **(Van Deun et al., 2014; Zlotogorski-Hurvitz et al., 2015)**. Thus, many polymeric reagents have been developed to isolate Exos via precipitation, which is a process that is somewhat superior to ultracentrifugation in terms of purity and yield of Exos **(Van Deun et al., 2014)**. Nonetheless, almost all the currently applied methods failed to efficiently enrich Exos in large quantities, probably due to the low production level of Exos by donor cells. Accordingly, a novel approach to substantially augment the production of Exos is urgently needed to ensure the widespread utilization of Exos in basic research avenues including the drug delivery field.

Liposomes have been widely used as delivery carriers for anticancer agents and nucleic acids **(Huang, 2008; Zhang et al., 2012; Torchilin, 2014)**. Liposomes are known to interact with the cell surface in a physicochemical property-dependent manner, which results in cell stimulation. Elsabahy and Wooley **(Elsabahy and Wooley, 2013)** reported that nanomaterials could induce the production of cytokines in a variety of cells, particularly immune cells, and thus the level of cytokines could be used as a tool to evaluate the interactions between nanoparticles and cells, as in the process of immunotoxicity. In a similar manner, DOTAP cationic liposomes have been used to induce the expression of co-stimulatory CD80 and CD86 on dendritic cell

surfaces, which started an immune response **(Cui et al., 2005)**. Furthermore, lowering the positive charge on the surface of cationic nanoparticles via partial histamine modification has been used to diminish their immunotoxic response via a lowering of their interaction with cells **(Shrestha et al., 2012)**. In addition, the lipid composition of liposomes frequently changes and their surface properties can be altered by many modification options such as PEGylation and the addition of cationic lipids. Accordingly, I assume that co-incubation with liposomes and changing their physicochemical properties may impact Exo secretion from cells, and consequently affect the yield of Exo collection.

In this chapter, therefore, I investigated the response of tumor cells to different liposome preparations in terms of Exo secretion from those cells. It was found that co-incubation with non-PEGylated bare liposomes increased Exo secretion from the tumor cells I used in both a lipid-dose and a lipid-composition-dependent manner. Interestingly, PEGylation to the liposomes suppressed the secretion of Exos from the cells I used.

2.2. Materials and methods

2.2.1. Materials and antibodies

Hydrogenated soy phosphatidylcholine (HSPC), 1,2-dioleoyl-*sn*-glycero-3-phosphoethanolamine (DOPE), 1,2-dioleoyl-3-trimethylammonium propane chloride salt (DOTAP), and 1,2-distearoylsn-glycero-3-phosphoethanolamine-n-[methoxy (polyethyleneglycol)-2000] ($mPEG_{2000}$-DSPE) were generously donated by NOF (Tokyo, Japan). Cholesterol (CHOL) was purchased from Wako Pure Chemical (Osaka, Japan). O,O′-ditetradecanoyl-N-(alpha-trimethyl ammonio acetyl) diethanolamine chloride (DC-6-14) was purchased from Sogo Pharmaceutical (Tokyo, Japan). 3ß-[N-(N',N'-dimethylaminoethane)-carbamoyl] cholesterol hydrochloride (DC-Chol) was purchased from Avanti Polar Lipids (LA, US). Anti-TSG101 (ab30871) and HRP conjugated goat anti-rabbit IgG (immunoglobulin G) H&L (ab6721) were purchased from Abcam (Cambridge, UK). Anti-CD63 (sc-15363) antibody and anti-CD81 (sc-9158) were purchased from Santa Cruz Biotechnology (CA, US). PKH67 Green Fluorescent Cell Linker kit was purchased from Sigma Aldrich (Missuori, US). Exo-depleted fetal bovine serum (exo-FBS) was purchased from System Biosciences (CA, US). Normal fetal bovine serum (FBS) was purchased from Mediatech (CA, US). All other reagents were of analytical grade.

2.2.2. Cell lines and cell culture

Four cancer cell lines were purchased from the Cell Resource Center for Biomedical Research (RIKEN RBC CELL BANK, Saitama, Japan): the Colon 26 (C26) murine colorectal cancer cell line, the B16BL6 murine melanoma cell line, the MKN45 human gastric cancer cell line, and the DLD-1 human colorectal cancer cell line. They were employed as models for cancer cell lines in this study. They were maintained in RPMI1640 (Wako Pure Chemical, Osaka, Japan) supplemented with 10%

Exo-depleted FBS (System Biosciences, CA, US), 100 IU/ml penicillin, and 100 µg/ml streptomycin (MP Biomedicals, CA, US) until reaching 80-90% confluency. All incubation processes were carried out under 5% CO_2 at 37 °C.

2.2.3. Preparation of liposomes

Four types of HSPC-based liposomes and six types of DOPE-based liposomes were prepared by the thin-film hydration method as previously described **(Ishida et al., 2005)**. The lipid composition/molar ratio of the prepared liposomes is described in **Table 1**. In brief, the lipids were dissolved in chloroform and then lipid film was produced by removing the organic solvent via a rotary evaporator at 37 °C under reduced pressure at 40 hPa for 1 h. The resultant lipid film was then hydrated using HEPES buffer (250 mM HEPES, 139 mM NaCl, adjusted to pH 7.4) at 65 °C with shaking for 2 h. The resultant large multilamellar vesicles were then extruded through a polycarbonate membrane with pore sizes of 400, 200 and 100 nm using an extrusion device (Lipex Biomembranes Inc., VC, Canada). The diameters and zeta-potentials of prepared liposomes were determined in PBS at 25 °C using a Zetasizer Nano ZS (Malvern Instruments Ltd., WR, UK) **(Table 2.1)**. Colorimetric assay was used to measure the phospholipid content of the prepared liposomes **(Bartlett, 1959)**.

2.2.4. Collection of Exos

Cancer cells were cultured in Exo-depleted conditioned medium for the indicated times, and then the cell culture medium was collected for Exo enrichment. To collect Exos secreted in response to liposome stimulation, the cancer cells were incubated for the indicated times in the presence of different liposome preparations of different lipid concentrations in Exo-depleted conditioned medium, and then the cell culture medium was collected for Exo isolation. Following collection of the culture

medium, cells were harvested for cell viability determination using a Countess II automated cell counter (Thermo Fisher Science Inc.,

	Composition (molar ratios)	Size (d.nm)	Zeta-potential (mV)
NL	**HSPC/CHOL (2/1)**	**130 ± 1.72**	**- 0.95 ± 0.62**
PEGylated NL	**HSPC/CHOL/mPEG$_{2000}$-DSPE (2/1/0.1)**	**120 ± 3.67**	**- 0.59 ± 0.05**
CL1	**HSPC/CHOL/DC-6-14 (2/1/0.2)**	**121 ± 3.11**	**+ 9.22 ± 1.63**
PEGylated CL1	**HSPC/CHOL/DC-6-14/mPEG$_{2000}$-DSPE (2/1/0.2/0.1)**	**118 ± 0.80**	**- 0.51 ± 0.14**
CL2	**DOPE/DC-6-14 (2/1)**	**137 ± 2.45**	**+ 22.20 ± 1.49**
PEGylated CL2	**DOPE/DC-6-14/mPEG$_{2000}$-DSPE (2/1/0.1)**	**113 ± 1.15**	**+ 1.54 ± 0.16**
CL3	**DOPE/DOTAP (2/1)**	**154 ± 9.56**	**+ 21.37 ± 1.45**
PEGylated CL3	**DOPE/ DOTAP /mPEG$_{2000}$-DSPE (2/1/0.1)**	**98 ± 0.18**	**+ 0.36 ± 1.01**
CL4	**DOPE/DC-Chol (2/1)**	**177 ± 3.74**	**+ 17.5 ± 0.42**
PEGylated CL4	**DOPE/ DC-Chol /mPEG$_{2000}$-DSPE (2/1/0.1)**	**118 ± 3.74**	**+ 0.45 ± 0.19**

NL: Neutral bare liposomes, CL: Cationic bare liposomes

Table 2.1. Lipid composition and physicochemical properties of prepared liposomes

MA, US) by staining cells with trypan blue **(Yao et al., 2015)**. To remove cell debris in addition to the apoptotic bodies and microvesicles, the collected culture medium was exposed to differential centrifugations at 4 ^{o}C (200 x g for 10 min, 2000 x g for 20 min and 12,500 x g for 30 min) **(Théry et al., 2006; Van Deun et al., 2014; Zlotogorski-Hurvitz et al., 2015)**. Then, Exos were enriched from the supernatant using either of the following two methods: ultracentrifugation (100,000 x g and 70 min) or an Exoquick-TC^{TM} precipitation reagent (System Biosciences, CA, US) according to the manufacturer's recommended protocol **(Théry et al., 2006; Van Deun et al., 2014; Zlotogorski-Hurvitz et al., 2015; Yim et al., 2016)**. For the latter method, the reagent was added to the supernatant in a 1:5 ratio and then mixed well. The mixture was let stand at 4 °C for 24 h. The supernatant was then completely discarded after two sequential centrifugation steps at 1,500 x g for 30 and 5 min. The Exo pellet was dispersed in PBS for further analysis and experiments. The liposomes in the incubation medium did not influence in the recovery ratio of Exos under the experimental condition in this study. To confirm that the Exo samples contained no remains of the liposomes used in stimulation, Exo-depleted conditioned medium was incubated under similar experimental conditions in the presence of different liposome concentrations followed by precipitation using sequential centrifugations with ultracentrifugation or Exoquick-TC^{TM}. Then, the collected samples of liposome contaminants (without Exos) were analyzed in the same manner as the Exo samples.

2.2.5. Characterization and analysis of collected Exos

Bio-Rad DC® protein assay (Bio-Rad Laboratories Inc., CA, US) was used to determine the protein concentration of the Exos and liposome-bound proteins (liposome contaminants) according to the manufacturer's recommended protocol. A linear standard curve with bovine serum albumin (BSA) was used to calculate the

protein concentration. To ensure a precise evaluation of Exo yield, the amount of proteins bound to the liposomes, which might have contaminated the collected Exo samples, was always subtracted from the final protein amount in the Exo sample. The amount of protein in the Exo samples was expressed as μg/10^6 viable cells or as μg/ml.

To verify that the collected samples contain the specific EV type, Exos, Exo marker proteins (TSG101, CD63 or CD81) in the collected samples were identified by Western blot analysis. Briefly, protein samples were mixed with 2x sample buffer (0.1 M Tris, 4% SDS, 12% 2-mercaptoethanol, 20% glycerol, slight amount of bromophenol blue) at a ratio of 1:1 (v/v), and then heated at 95 °C for 5 min. Proteins in the samples were electrophoretically separated on 5-20% gradient gels (epagele-PAGEL; ATTO, Tokyo, Japan) at 25 mA per each gel for 70 min, as previously described **(Kawanishi et al., 2015)**. Each lane was loaded with 60 μg of protein. MagicMark™ XP Western Protein Standard (20-220 kDa, Thermo Fischer Inc., MA, US) was employed as a molecular weight standard. The separated proteins were blotted to a nitrocellulose membrane by electrophoresis at 12 V for 30 min using a semi-dry blotting system (ATTO, Tokyo, Japan). Then, for blocking, the membrane was incubated at 37 °C for 1 hour in the blocking buffer 5% BSA in Tris-buffered saline with 0.05% Tween 20 (TBST 0.05%). The blocked membranes were further incubated with different primary antibodies in 2% BSA (in TBST 0.05%) in a 1:1,000 (v/v) concentration for Anti-TSG101 antibody and a 1:40 (v/v) concentration for anti-CD63 and anti-CD81 antibodies at 4 °C overnight. After that, the membranes were treated with HRP conjugated goat anti-rabbit IgG H&L antibody in TBST 0.05% with a dilution (1:20,000) at 37 °C for 1 h. Finally, membrane visualization was carried out by incubating the membrane with Amersham™ ECL™ Prime Western Blotting

Detection Reagent (Sigma Aldrich, Missouri, US) at room temperature for 5 min followed by imaging using image quant LAS 4000 (GE Healthcare Life Sciences, MA, US).

2.2.6. Evaluation of the *in vitro* cellular uptake of collected Exos

To assess the cellular uptake of collected liposomes, B16BL6 cells, which exhibited the highest Exo yield among all tested cancer cell lines, was incubated for 48 h under both normal (exo-N) and stimulation conditions with 1 mM CL1 (exo-S1) or 0.05 mM CL3 (exo-S2). These two concentrations of CL1 and CL3 were selected as examples for the stimulating action of solid and fluid liposomes with a sublethal effect on cell viability. Exos were harvested from B16BL6 using ultracentrifugation at 100,000 x g for 70 min after the removal of cell debris, apoptotic bodies and microvesicles, as previously mentioned **(Théry et al., 2006; Van Deun et al., 2014; Zlotogorski-Hurvitz et al., 2015)**. The harvested Exos from B16BL6 were evaluated for their cellular uptake by either the autologous cell line B16BL6 or the allogeneic cell line C26. Exos were labeled using green fluorescent dye, PKH67 (Sigma Aldrich, Missuori, US), according to the manufacturer's protocol with minor modifications **(Morelli et al., 2004; Parolini et al., 2009; Ekstrom et al., 2012)**. Briefly, a suspension containing the same amount of Exos was washed once with PBS by ultracentrifugation at 100,000 x g for 70 min. The Exo pellets were re-suspended in diluent C supplied in the package (Sigma Aldrich) and then mixed with an equal volume of the 2x dye solution in diluent C (2 x 10-6 M) for 5 min. The staining was stopped by the addition of an equal volume of Exo-depleted FBS. The stained Exos were recovered as pellets by ultracentrifugation at 100,000 x g for 70 min. The pellets were then re-suspended in an equal volume of conditioned culture medium. Exo uptake was examined via flow cytometry (Gallios, Beckman Coulter, CA, US) and

confocal laser scanning microscopy (LSM 700, ZEISS) as described below. The liposome was incubated in Exo-depleted conditioned medium in the absence of cells. The collected supernatant was sequentially centrifuged as described above to obtain liposome contaminant that contained liposome-bound proteins. The liposome contaminants were stained and their cellular uptake was evaluated as described below.

2.2.6.1. Flow cytometry

Target cancer cells (B16BL6 or C26) were cultured at 1.5 x 10^5 cells in 2 ml of culture medium using a 6-well plate followed by incubation for 24 h. Then, labeled Exos and/or liposome contaminants were incubated with cancer cells in Exo-depleted conditioned medium at a final protein concentration of 3 μg/ml of Exo sample or its equivalent of liposome contaminants. After 24 h post-incubation, the cancer cells were harvested, washed twice with PBS, and then examined by flow cytometry. The data were analyzed using Kaluza 1.2 software (Beckman Coulter, CA, US) **(Morelli et al., 2004; Ekstrom et al., 2012)**.

2.2.6.2. Confocal laser scanning microscopy:

Target cancer cells (B16BL6 or C26) were precultured for 24 h at a density of 3 x 10^4 cells in 200 μl of the Exo-depleted conditioned medium using Lab-Tek II chamber slides (Thermo Fischer Inc., MA, US). Labeled Exos and/or liposome contaminants were added into each well at a final protein concentration of 3 μg/ml of Exo sample or its equivalent of liposome contaminants. The cells were then incubated for a further 24 h. After aspiration of the culture medium, adhered cells were washed with PBS and then incubated for 5 min in the presence of Hoechst 33342 DNA dye (1.78 μM) (Ana Spec Inc., CA, US). After aspiration, cells were washed twice with PBS and then let stand for 30 min to dry. The dried cells were fixed with Fluoromount/Plus (Diagnostic Biosystems, CA, US). Slides were examined at 63x

magnification via confocal laser scanning microscopy. The scanned images were processed using LSM-ZEN2012 software (ZEISS) **(Morelli et al., 2004; Parolini et al., 2009; Ekstrom et al., 2012)**.

2.2.7. Statistical analysis

All values were expressed as mean ± SD. Statistical analysis was performed via one way ANOVA tests (Tukey's and Dunnett's multiple comparisons tests) using Graphpad Prism 6.01 software (GraphPad Software Inc., CA, US). The level of significance was set at $p<0.05$.

2.3. Results

2.3.1. Effect of incubation time and type of cancer cell line on Exo secretion

To trace the effect of incubation time on Exo secretion from cancer cell lines, the four types of cancer cells, namely C26, B16BL6, MKN45 and DLD-1, were cultured without co-incubation with liposomes for 24, 48 and 72 h, and the Exos were then collected by Exoquick-TC^{TM}. Exo protein concentration was used as an indication of Exo yield. **Fig. 2.1** shows that Exo secretion was detected in all cell lines and that the Exo yield was increased with incubation time in all cell lines except for DLD-1. Exo release after 72 h was in the following descending order: B16BL6 cells followed by DLD-1 then C26 and finally MKN45 by 786.72 ± 69.92, 438.79 ± 27.66, 393.05 ± 33.24, and 376.10 ± 72.96 μg/10^6 viable cells, respectively. These results manifest that all tested cancer cell lines can secret Exos in both incubation time- and cancer cell-type-dependent manners with the highest level of Exos secreted by B16BL6 cells following 72 h of incubation time.

2.3.2. Evaluation of potential liposome contaminants

Incubation of cells with bare liposomes was investigated a potential strategy to enhance the yield of Exos collected by either sequential centrifugations, the method widely used to obtain Exos **(Théry et al., 2006)**, or by Exoquick-TC^{TM} **(Yim et al., 2016)**, protein levels were taken as an indicator for Exo yield. It is well known that liposomes are easily interacted with serum proteins **(Ishida et al., 2001**, **2002)** and the liposomes can then be precipitated by ultracentrifugation, which is similar to our experimental condition. Accordingly, I investigated the possibility that liposome-bound proteins were being contaminated in the collected Exo fraction. As shown in **Fig. 2.2**, the liposomes added into the Exo-depleted conditioned medium were precipitated together with serum proteins regardless of the collection method. To

exclude the contribution of liposome-bound proteins to the overall protein concentration in the assayed sample, the amount of liposome-bound protein was subtracted from the overall protein concentration of the collected Exos in all experiments conducted in this study. That contamination was only significantly detected with HSPC solid liposomes. While fluid liposomes showed no/low liposome contamination which could be omitted **(Fig. 2.2 B)**. The observed difference in the contamination level between fluid and solid liposomes might be related to their stability after incubation at 37 °C. After incubation, fluid liposomes will aggregate resulting in increasing their size, while solid liposomes will remain intact without a change in their nano-size. Thereby, during the sample purification via sequential centrifugation at 300, 2000 and 12,500 x g, fluid liposomes were easily removed while solid liposomes skipped these centrifugation steps and remained in the sample for co-isolation with Exos at 100,000 x g. Thus, it was necessary to present the contamination happened with HSPC liposomes. To confirm the detected no/low contamination with fluid liposomes, nanoparticle tracking analysis (NTA) was employed. The results indicated the presence of tiny amounts of fluorescent (DiI) labeled fluid liposomes (CL3) in the collected samples compared to the added amount **(Figs. 2.3 A and B)**. **Fig. 2.2 A** also showed that the contamination was higher with Exoquick-TC^{TM} than ultracentrifugation. This is inconsistent with the literature which indicated that the protein contamination is higher with ultracentrifugation due to the degradation of large proteins by the high speed centrifugation and then precipitation with the collected Exo sample **(Van Deun et al., 2014; Zlotogorski-Hurvitz et al., 2015)**. According to our current knowledge, the coexistence of Exos and liposomes is novel to be investigated. Thus, other methods for Exo analysis like

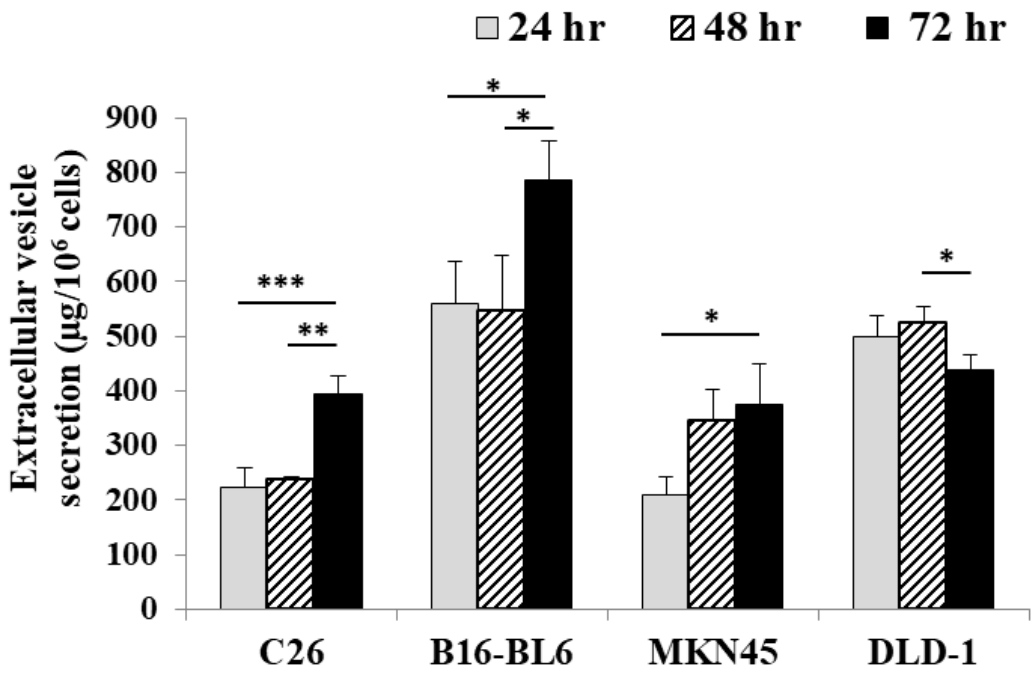

Figure 2.1. Relationship between incubation time and yield of Exos from four different cancer cell lines.

The secreted Exos were collected by Exoquick-TC™ after incubation of different cancer cell lines for the indicated times in Exo-depleted culture medium. The protein amount in the collected fraction was determined via Bio-Rad DC® protein assay. Data are represented as the mean ± SD (n=3). An one way ANOVA test (Tukey`s test) was applied for each type of cancer cell. * $p < 0.05$, ** $p < 0.01$ and *** $p < 0.001$.

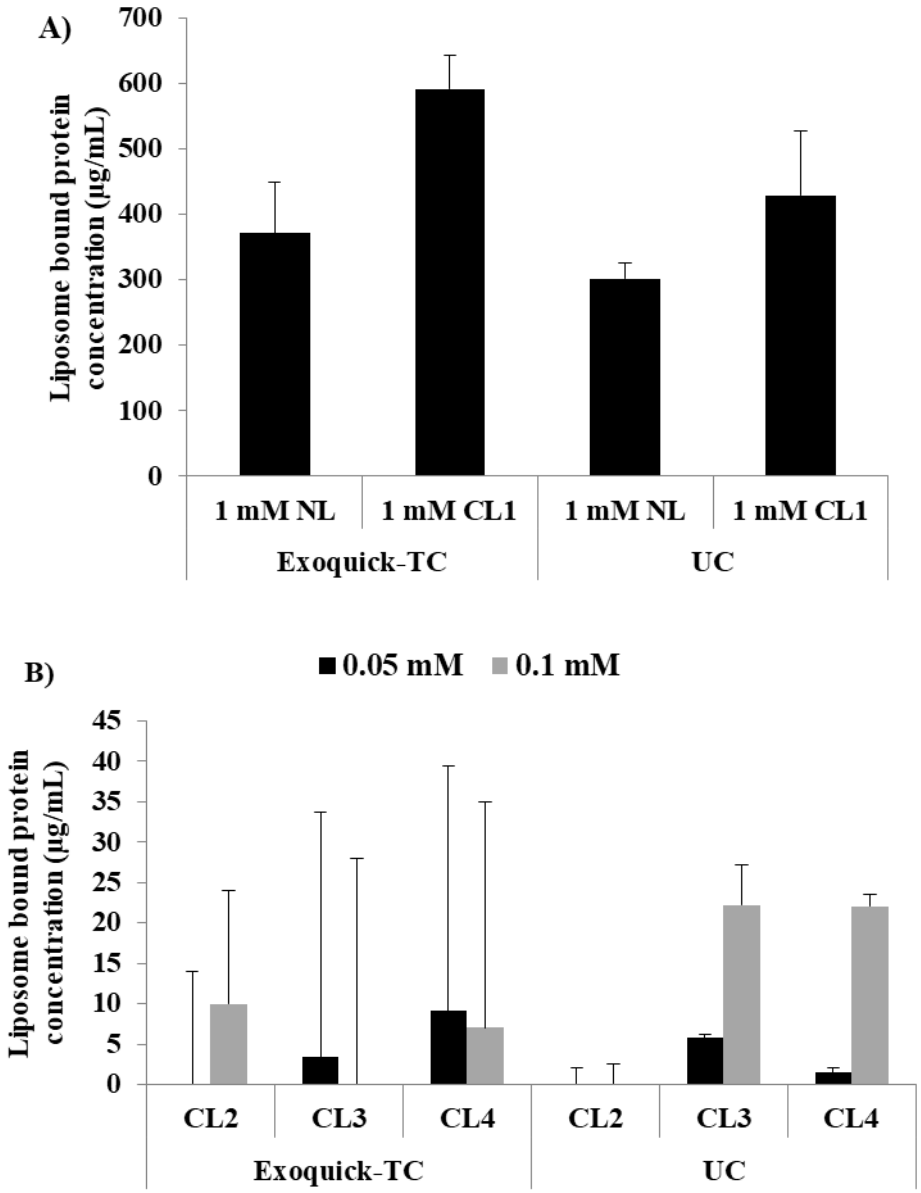

Figure 2.2. Contaminates of liposome-bound proteins for different liposome preparations using Exoquick-TC™ or ultracentrifugation.

Bio-Rad DC® protein assay was used to evaluate the protein amount the potential contaminants of liposome-bound proteins for (A) HSPC liposomes and (B) DOPE cationic liposomes using Exoquick-TC™ or ultracentrifugation (UC). Data are represented as the mean ± SD (n=3).

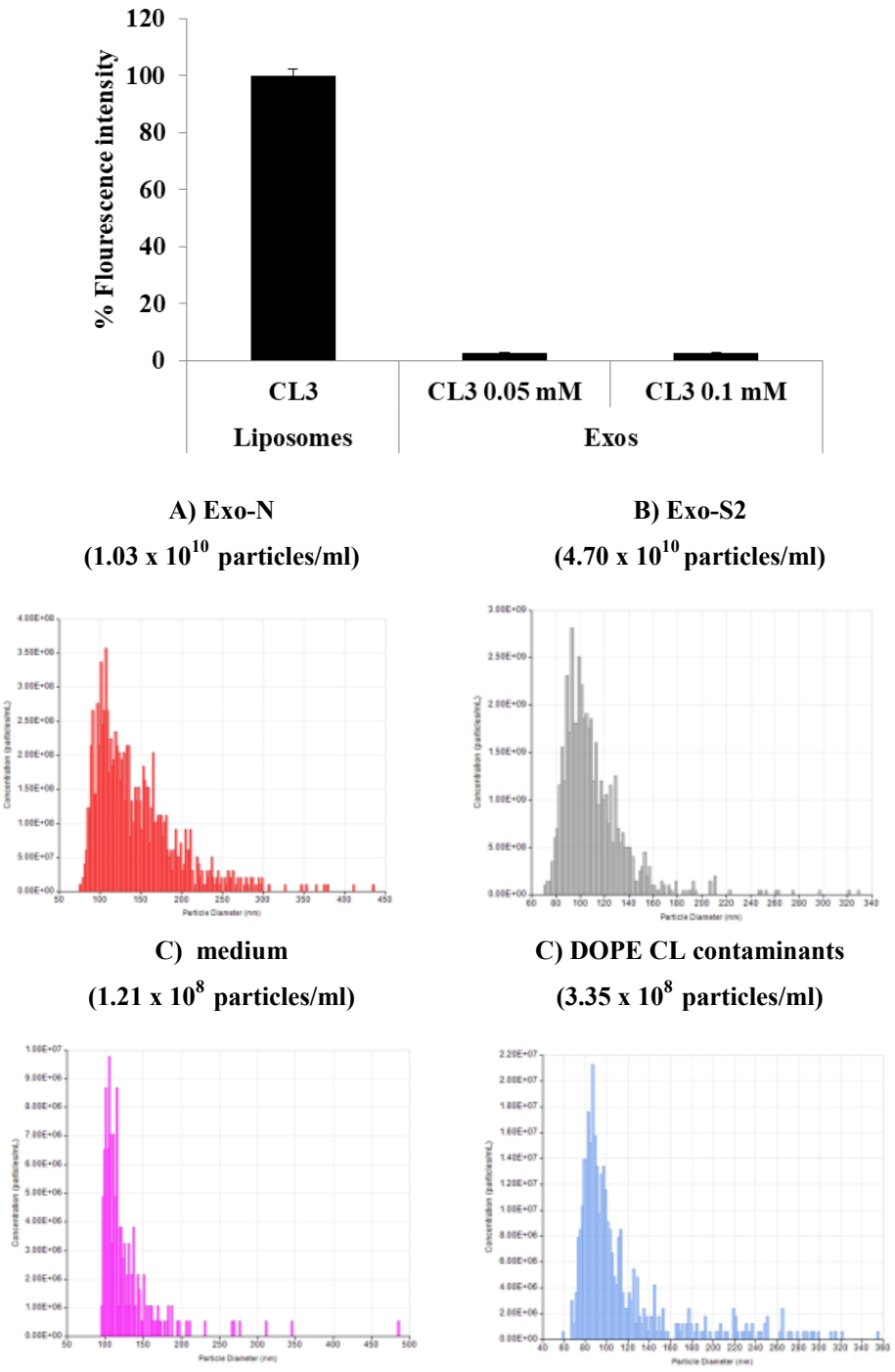

Figure 2.3. Contaminates of liposome-bound proteins for CL3 using ultracentrifugation.

The amount of CL3 contaminates were evaluated via (A) measuring the fluorescence intensity of DiI contaminates using a plate reader or (B) counting the particle number of these contaminates using nanoparticle tracking analysis (NTA).

transmission electron microscopy (TEM), dynamic light scattering (DLS) and nanoparticle tracking analysis (NTA) were unfortunately inconclusive to distinguish between Exos and liposomes due to the similarity in their shape and size. Moreover, liposomes were already used as a model for Exos in another study by Lane, et al. **(Lane et al., 2015)**. Nevertheless, these results manifest that Exos were efficiently obtained by either sequential centrifugations or Exoquick-TC^{TM}.

2.3.3. Effect of different HSPC-based liposome preparations on Exo secretion

To further investigate the stimulatory effect of liposomes, the HSPC-based liposomes listed in **Table 2.1** were incubated with different cancer cell lines for 48 h. As shown in **Fig. 2.4**, Exo secretions from all cell lines were increased with increasing phospholipid concentration (dose) of either neutral or cationic bare liposomes (NL or CL1). Cationic bare liposomes (CL1) showed stronger stimulant activity on Exo secretion than neutral bare liposomes (NL) under the same experimental conditions. Among the tested cell lines, B16BL6 seems to be the most responsive cell line for liposomal stimulation in terms of Exo secretion followed by MKN45, DLD-1 and finally C26. Surprisingly, neither PEGylated NL nor PEGylated CL1 showed any stimulatory effect on Exo secretion, but these rather inhibited essential Exo secretion in a dose-dependent manner in some cell lines. This tendency was confirmed by the Exo collection with ultracentrifugation **(Fig. 2.5)**. Taken together, these results showed that bare liposomes have the ability to induce Exo secretion and that a cationic surface charge further can increase the stimulatory effect of bare liposomes. On the other hand, it is likely that the PEGylation of these bare liposomes may diminish their stimulatory effect.

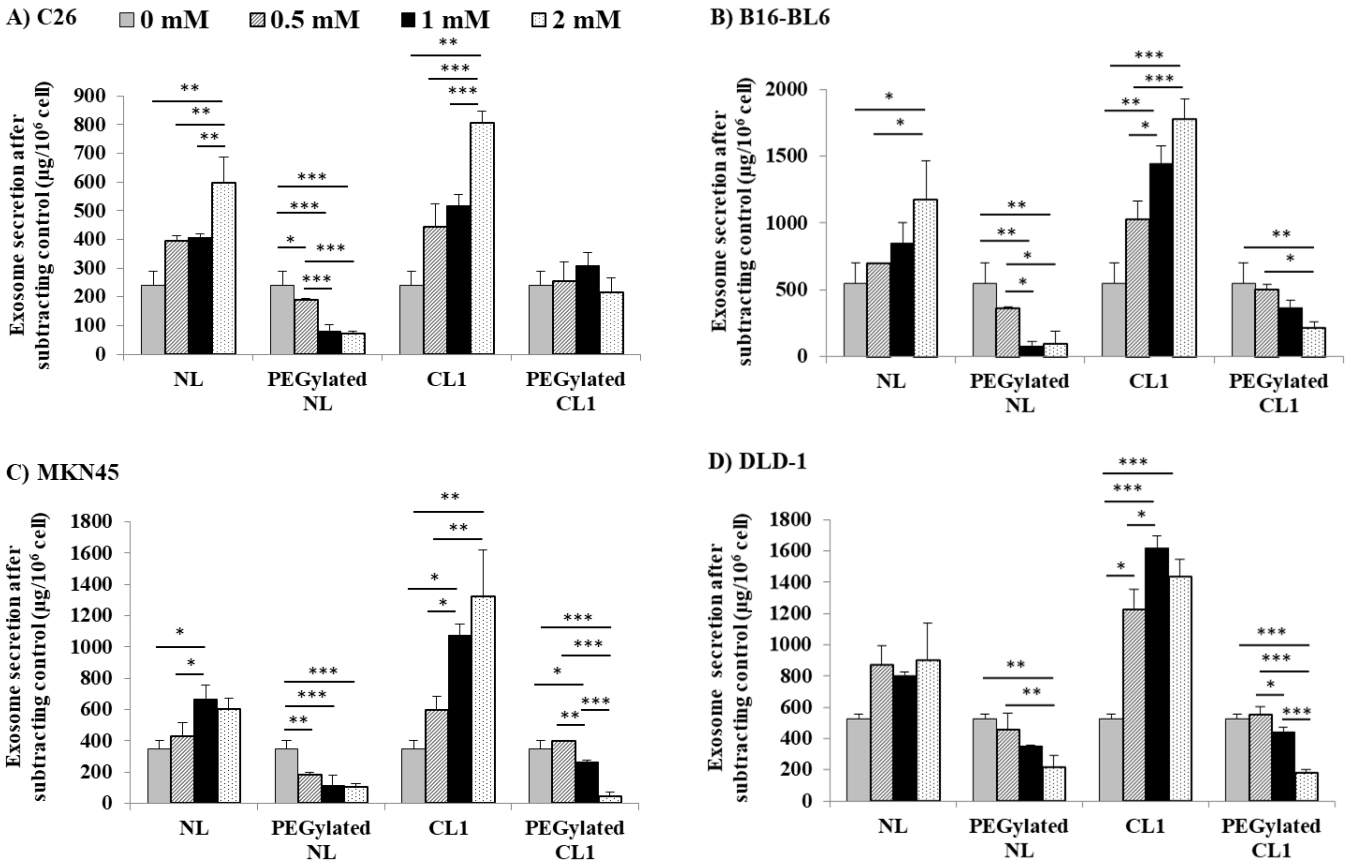

Figure 2.4. The effect of incubation with different liposome preparations on Exo secretion f

The secreted Exos were collected by Exoquick-TCTM after incubation of the four cancer cell lines, C26, B16BL6, MKN45 and DLD-1, for 48 h in the presence of different concentrations of different HSPC-liposome formulations. The protein amount in the collected fraction was determined via Bio-Rad DC® protein assay. Data are represented as the mean ± SD (n=3). An one way ANOVA test (Tukey`s test) was applied for each liposome formulation within each cancer cell .line. * $p < 0.05$, ** $p < 0.01$ and *** $p < 0.001$

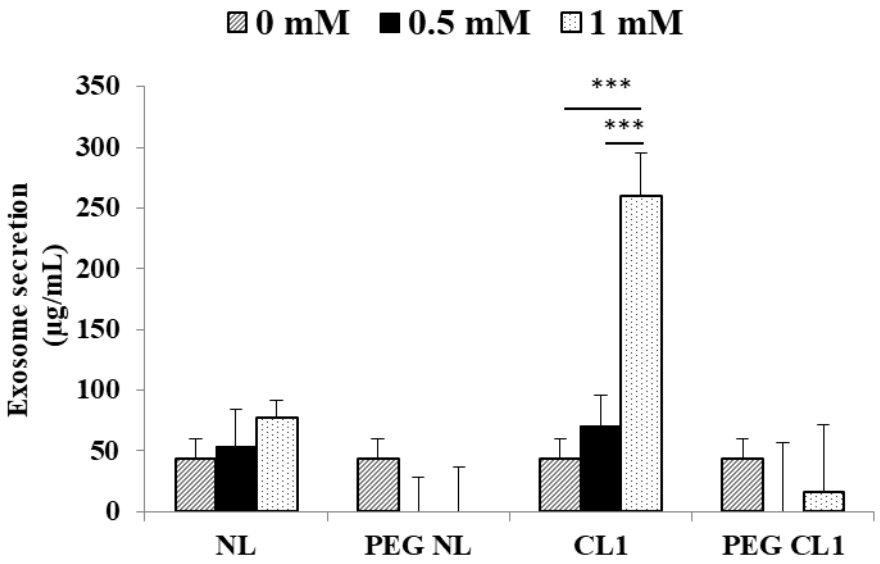

Figure 2.5. The effect of incubation with different HSPC-based liposome preparations on Exo secretion from the B16-BL6 cancer cell line using ultracentrifugation.

The Exos secreted from B16-BL6 were collected by ultracentrifugation. The protein amount in the collected fraction was determined via Bio-Rad DC® protein assay. Data are represented as the mean ± SD (n=3). An one way ANOVA test (Tukey`s test) was applied for each liposome formulation. *** $p < 0.001$.

2.3.4. Effect of cationic lipid type in cationic liposomes (CL) on Exo secretion

To gain further insight into the effect of the type of cationic lipids in the CLs on Exo secretion, C26 cells were selected due to having the lowest Exo yield, which required greater stimulation via powerful cationic lipid. C26 cells were incubated for 48 h in the presence of various CL preparations (CL2, CL3 and CL4), as listed in **Table 2.1**. All the tested DOPE-based CLs caused bell-shaped stimulation on Exo secretion in response to liposomal dose **(Fig. 2.6 A)**. DOPE-based cationic liposomes, tested at just 0.06 mM, showed higher stimulation activity on C26 (1.55-, 2.49- and 1.34- fold increases for CL2, CL3 and CL4, respectively) **(Fig. 2.7)** compared with HSPC-based cationic liposome (0.5 mM, CL1) **(Fig. 2.4 A)**. Such stimulatory effect of DOPE-based cationic liposomes was mediated in a liposomal dose-dependent manner. At a lower liposomal dose, DOPE-based cationic liposomes could efficiently trigger Exo secretion without significantly affecting cell viability **(Fig. 2.6)**. On the other hand, at a higher liposomal dose, such stimulatory effect was substantially decreased **(Fig. 2.6 A)** presumably via decreasing cell viability **(Fig. 2.6 B)**. The highest increase in Exo yield harvested at 0.1 mM was from CL3 followed by CL2 with 3.17- and 2.63-fold increases, respectively, compared with untreated cells. CL4 produced the lowest increase in Exo secretion (only 1.39-fold), which could have been due to a lowered level of membrane fluidity caused by an increase in the cholesterol content from DC-Chol in the liposomal membrane. Stimulation/inhibition observed in HSPC-based liposomes was also observed in DOPE-based liposomes **(Fig. 2.8)**. The dose-dependent stimulatory activity of cationic DOPE-based liposomes was inhibited by PEGylation as shown in **Fig. 2.8 A** (Exoquick-TC^{TM}) and **Fig. 2.8 B** (ultracentrifugation method). These results showed that the stimulation of Exo secretion is affected by liposome lipid composition especially cationic lipid types in

tandem with phospholipid types and cholesterol content. Furthermore, NTA also indicated the ability of CL3 to enhance the yield of Exo collected by ultracentrifugation **(Fig. 2.3 B)**. To confirm the ability of fluid liposomes in enhancing Exo secretion without any possibility of liposome interference, a pulse experiment was conducted via a brief incubation of C26 with fluid liposomes (CL3) for 3 h and then the incubation continued to 48 h after replacing the culture medium with fresh one. **Fig. 2.9** showed that pulse incubation with CL3 also enhanced Exo secretion, compared to untreated cells. Thereby, fluid cationic liposomes are an excellent candidate for enhancing Exo yield via liposomal stimulation.

2.3.5. Characterization of Exos collected by ultracentrifugation or Exoquick-TC™

Proteins were obviously detected in the obtained Exos regardless of the collection method**.** Exoquick-TC™ was likely to recover a large amount of Exos compared with sequential centrifugations. Incubation of cells with cationic bare liposomes (CL) increased the protein amount in the collected Exos regardless of the collection method**.** Fluid CL appeared to increase the production of Exos much more than solid CL. However, it is not clear whether the samples specifically contain the subtype of EVs, called Exos. Accordingly, to verify the existence of Exos in the collected samples, the presence/absence of major Exo markers, such as (CD63, CD81 and TSG101) **(Lee et al., 2012; Carrière et al., 2016)**, in the collected samples was scrutinized using the corresponding antibodies **(Fig. 3.10)**. All the examined markers were detected in all the collected samples incubated in the presence or absence of liposomes. None of these markers was detected in the liposome contaminants.

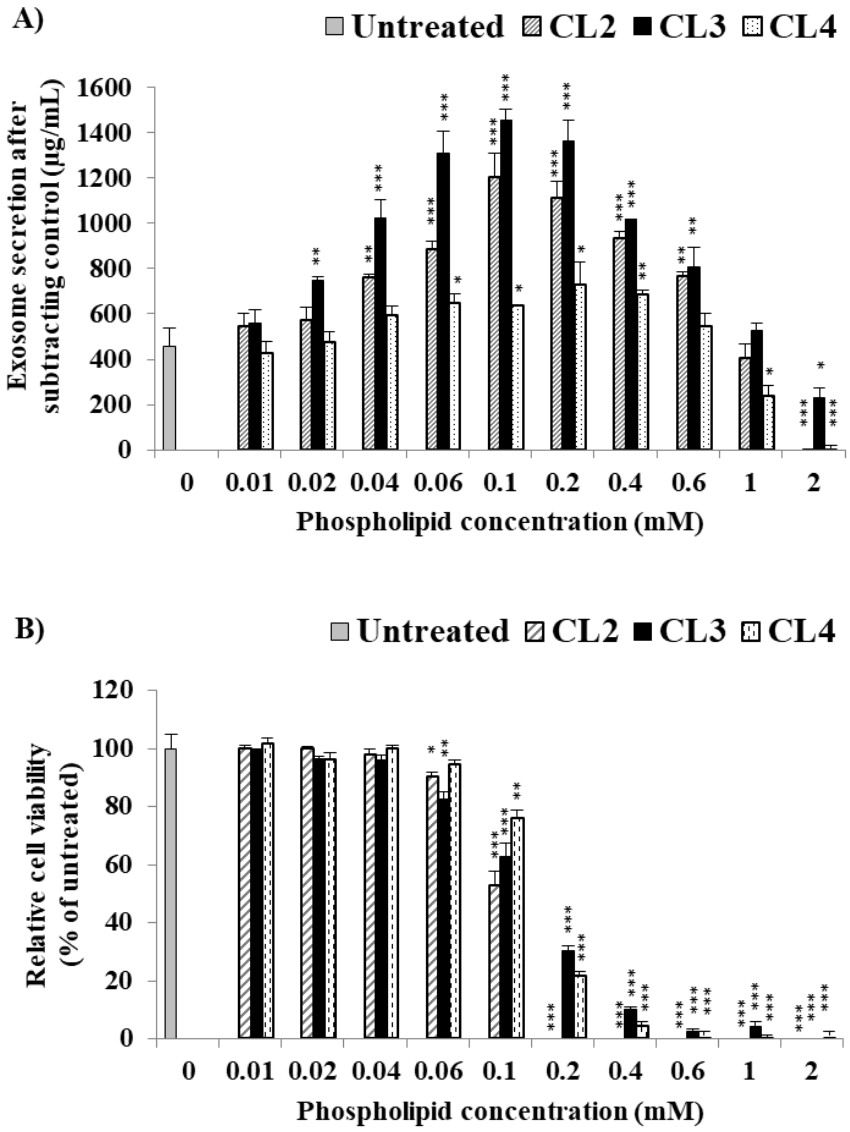

Figure 2.6. Effect of different cationic liposomes on Exo secretion (expressed as µg/mL) and cell viability.

The secreted Exos were collected by Exoquick-TC™ after incubation of C26 cancer cells for 48 h in the presence of different concentrations of different DOPE-cationic liposome formulations. The protein amount (A) in the collected fraction was determined via Bio-Rad DC® protein assay. Cell viability (B) of the harvested C26 cancer cells was evaluated via a Countess II automated cell counter by staining the cells with trypan blue after collecting the culture medium for Exo enrichment. Data are represented as the mean ± SD (n=3). An one way ANOVA test (Dunnett`s test) was applied by comparing each phospholipid concentration with the control (untreated). * $p < 0.05$, ** $p < 0.01$ and *** $p < 0.001$.

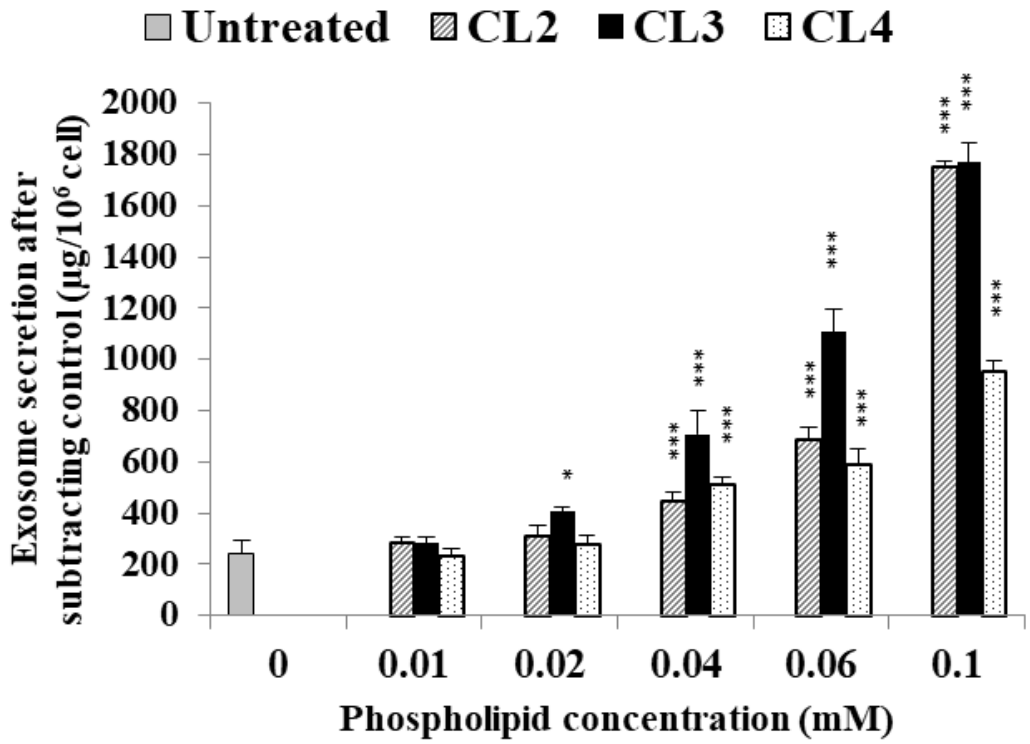

Figure 2.7. Effect of different types of cationic DOPE-based liposomes on Exo secretion (expressed as µg/10^6 cell) from the C26 cancer cell line.

The Exos secreted from C26 were collected by Exoquick-TC™. The protein amount in the collected fraction was determined via Bio-Rad DC® protein assay. Data are represented as the mean ± SD (n=3). An one way ANOVA test (Dunnett`s test) was applied by comparing each phospholipid concentration with the control (Untreated). * $p < 0.01$ and *** $p < 0.001$.

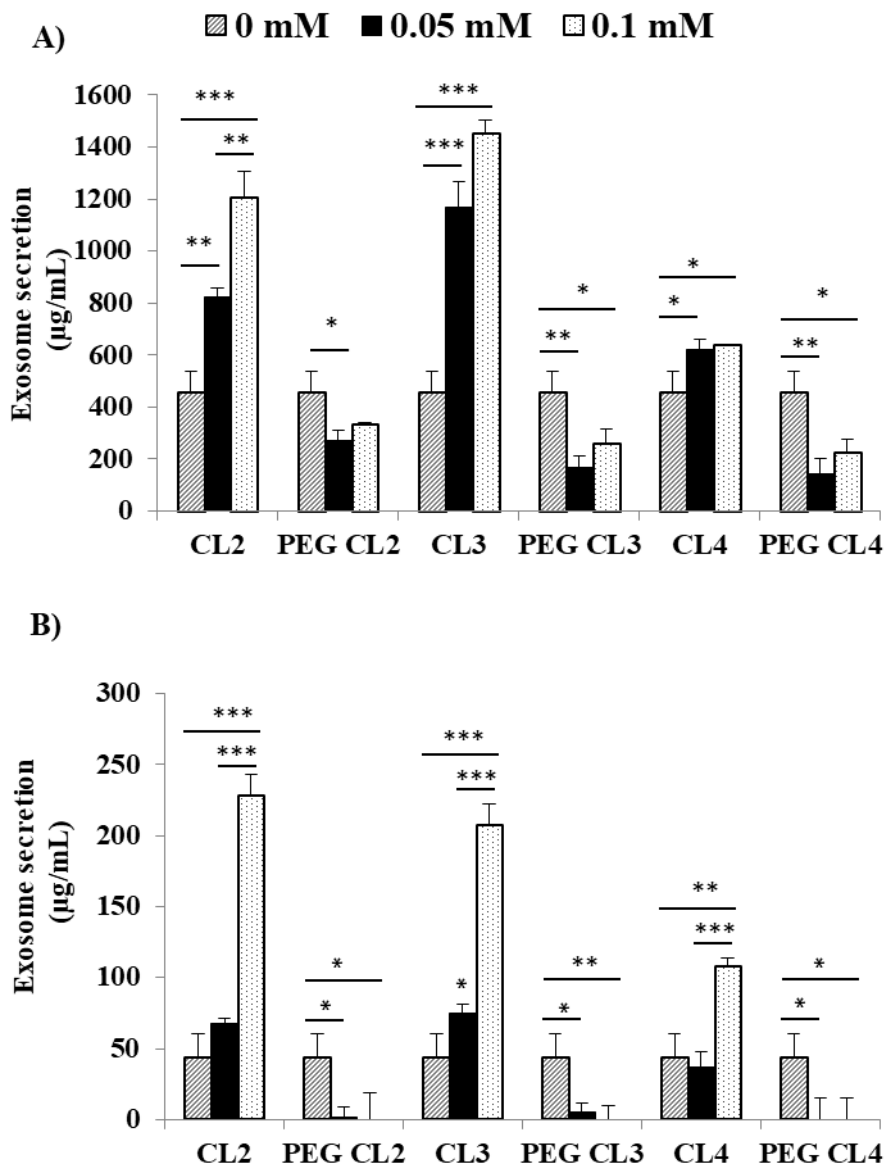

Figure 2.8. Effect of different types of cationic DOPE-based liposomes (including PEGylated liposomes) on Exo secretion from (A) C26 using Exoquick-TC™ and (B) B16-BL6 using ultracentrifugation.

The secreted Exos were collected after incubation of cancer cell lines for 48 h. in the presence of different concentrations of PEGylated and non-PEGylated DOPE-cationic liposomes. The protein amount in the collected fraction was determined with Bio-Rad DC® protein assay. Data are represented as the mean ± SD (n=3). An one way ANOVA test (Tukey`s test) was applied for each liposome formulation. * $p < 0.05$, ** $p < 0.01$ and *** $p < 0.001$.

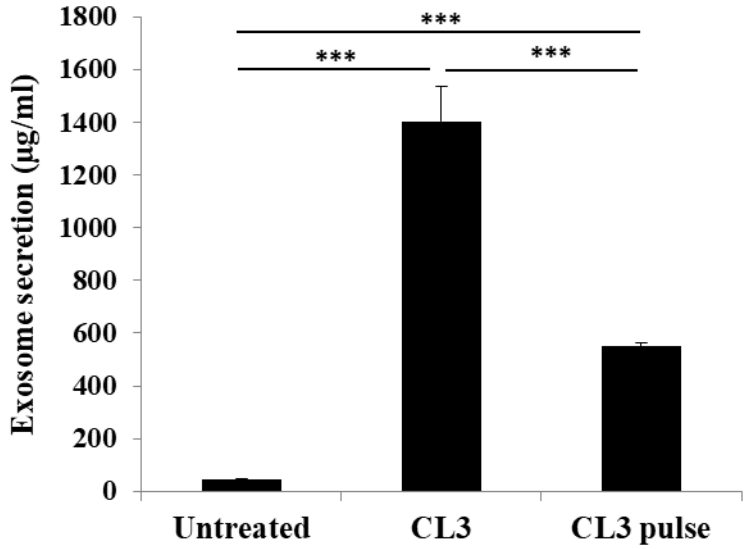

Figure 2.9. Pulse experiment for stimulating Exo secretion via short incubation with CL3.

Cells were incubated in the presence of 0.1 mM CL3 for 3 h (short liposome co-incubation). After 3 h incubation, the culture medium was replaced with fresh medium and cells were further incubated to 48 h. Then, the medium was collected for Exo isolation via ultracentrifugation.

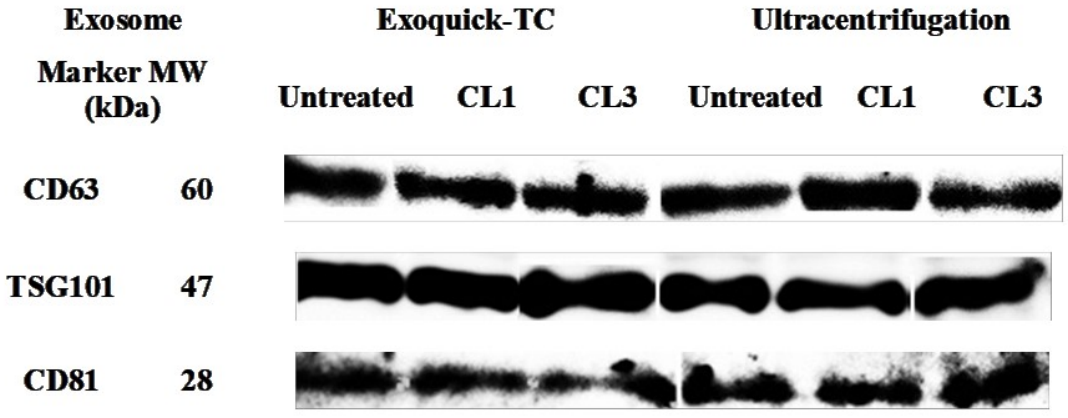

Figure 2.10. Characterization of Exos collected by Exoquick-TC™ or ultracentrifugation.

Identification of Exo markers in the collected samples was conducted via Western blotting.

2.3.6. *In vitro* cellular uptake of harvested Exos

The role of Exos in cell-cell communication is very important, particularly in the disease status of cells. Thus, Exo-based drug delivery is currently the focus of many studies particularly in cancer therapy **(Lakhal and Wood, 2011; Tan et al., 2013; Johnsen et al., 2014)**. Here, the cellular uptake of Exos collected was studied either under normal conditions (exo-N) or under stimulation with 1 mM CL1 (exo-S1) and 0.05 mM CL3 (exo-S2). In addition, the cross-reactivity of Exos harvested from an autologous tumor cell line (B16BL6) towards another tumor cell line (C26) was investigated.

Control Exos (exo-N) were taken up by the autologous cells (B16BL6) as well as by other cells (C26) **(Figs. 2.11 A and B)**. The exo-S2 was also taken up by both cell lines (B16BL6 and C26) **(Figs. 2.11 A and B)**. Interestingly, there was little uptake of exo-S1 by the cancer cells **(Figs. 2.11 A and B)**. Compared with exo-N, exo-S2 was taken up by a higher percentage in both cancer cells **(Fig. 2.11B)**. Notably, the uptake level of both exo-N and exo-S2 by autologous cells (B16BL6) was higher than that by the C26 cells. Protein-bound liposome prepared with Exo-depleted conditioned medium showed very weak uptake signals with flow cytometry (negligible). The value was subtracted from the corresponding Exo sample. These observations were further emphasized when the Exos inside target cells were visualized under LSM **(Fig. 2.12)**. LSM images showed that green-labeled exo-N and exo-S2 were significantly internalized by the autologous cells (B16BL6) as well as by other cancer cells (C26), while little faint green aggregations were detected in the case of exo-S1 **(Fig. 2.12)**. The uptake of liposome associated with serum proteins from Exo-depleted conditioned medium was weak and negligible. It is likely that Exo uptake depends on the type of target cancer cell besides the type of liposomes used in stimulating Exo release.

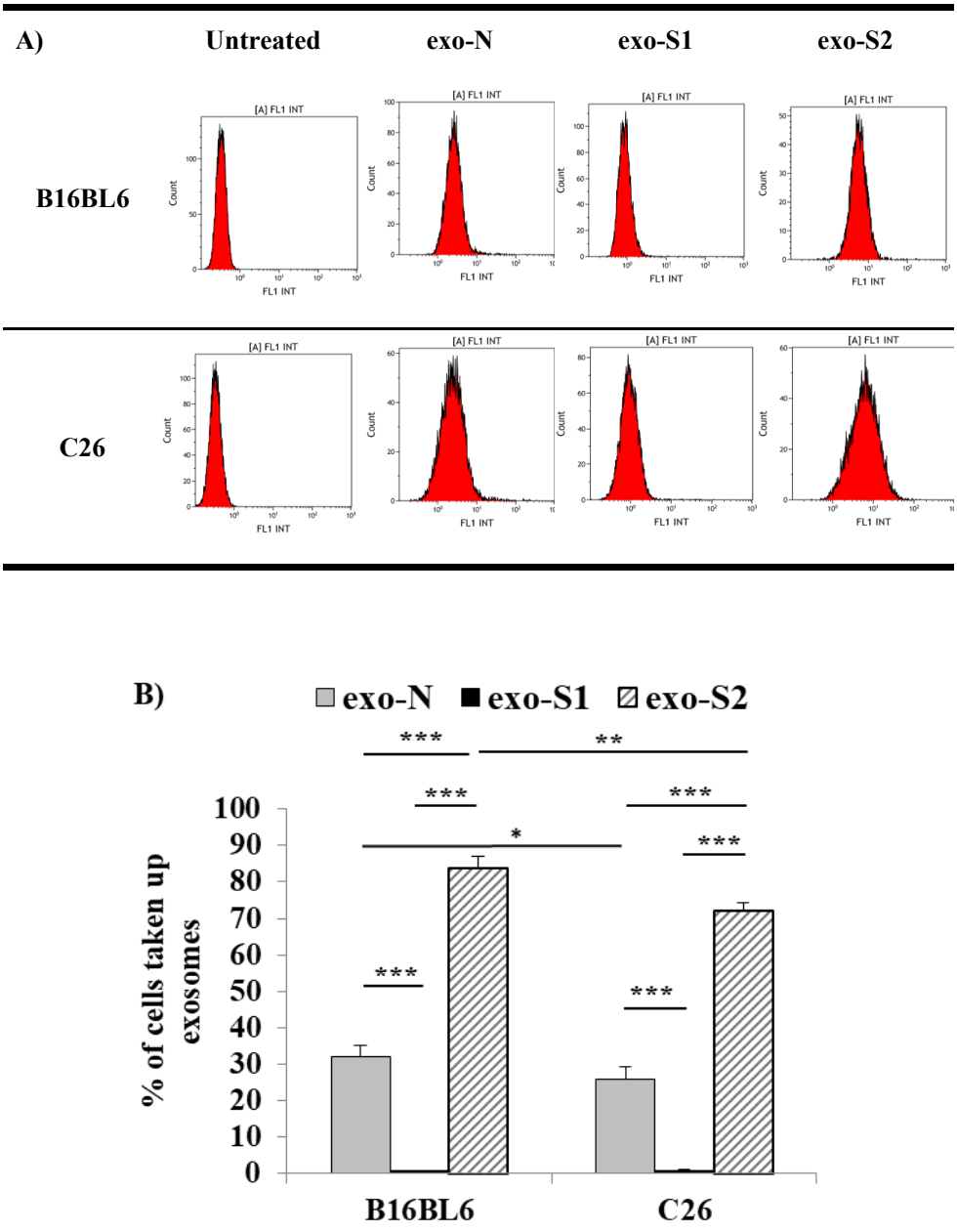

Figure 2.11. Flow cytometry analysis of Exo internalization.

The percentage of cells taken up Exos was evaluated by flow cytometry after incubation of PKH67-labeled Exos collected by ultracentrifugation from B16BL6, for 24 h with autologous cancer cells (B16BL6) and other cells (C26). Data are represented as one set (A, B) and the mean ± SD (n=3) after subtracting the background (C). An one way ANOVA test (Tukey`s test) was applied within each type of cancer cell and also between the two types of cancer cells. * $p < 0.05$, ** $p < 0.01$ and *** $p < 0.001$.

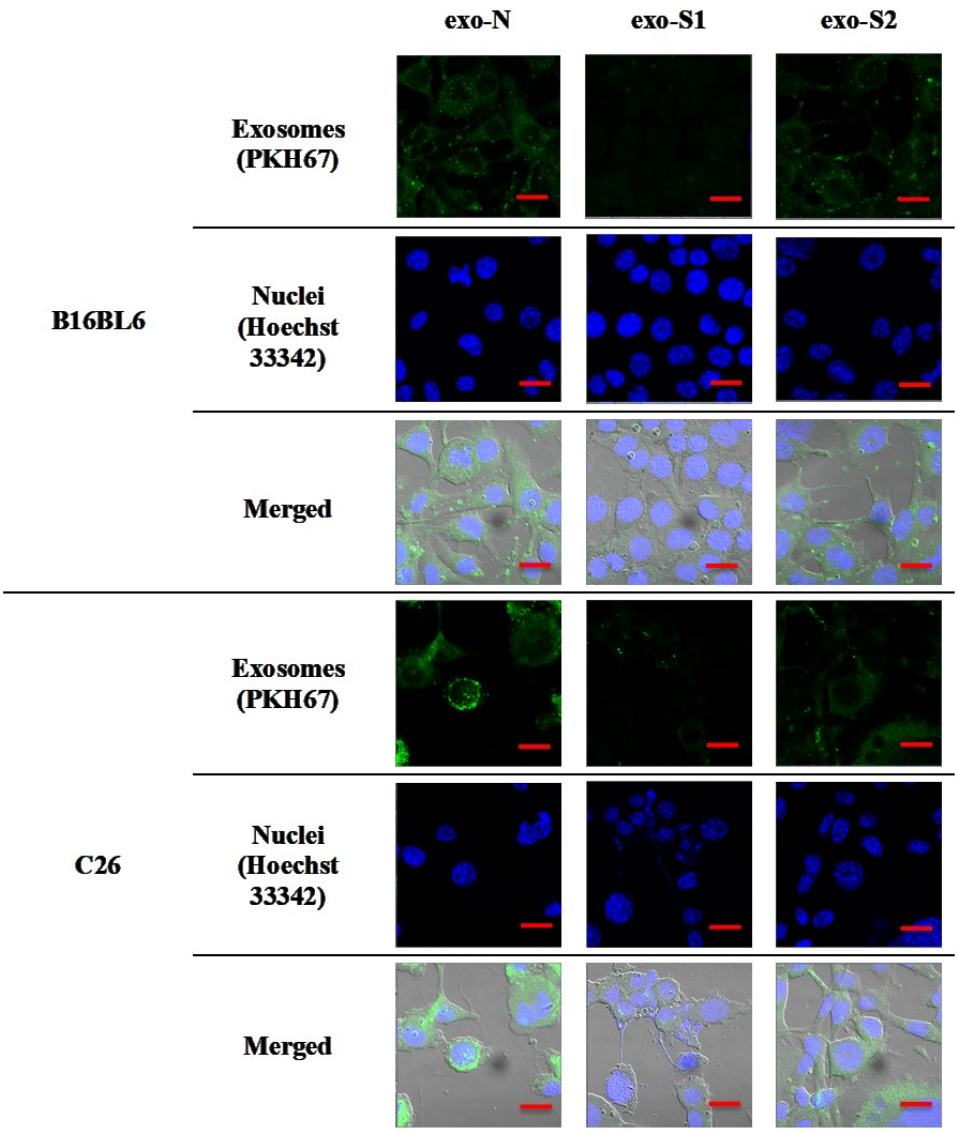

Figure 2.12. Confocal laser scanning microscopy for tracking Exo internalization.

The uptake of Exos by cancer cells was imaged by a confocal laser scanning microscope after incubation of PKH67-labeled Exos collected by ultracentrifugation from B16BL6 cells, for 24 h with autologous cancer cells (B16BL6) and other cells (C26). All images represent one set of triplicates. Exos were labeled with PHK67 (green), and the DNA core was stained with Hoechst 33342 (blue). Scale bar indicates 20 μm.

2.4. Discussion

Many studies have reported different stimulation models for Exo secretion from cells via manipulation of the cells, their receptors, the plasma membrane, or even intracellular electrolytes **(Savina et al., 2005; Lachenal et al., 2011; Raposo and Stoorvogel, 2013)**. These studies monitored only the stimulation action as a result of a specific condition or biological process. In the present study, it was demonstrated that *in vitro* incubation of bare liposomes with cancer cells enhances Exo secretion from different types of cancer cells, resulting in an increased yield of Exos **(Figs. 3.2 and 3.3)**. In particular, fluid cationic bare liposomes produced the greatest increase in Exo secretion at the optimum dose with less cytotoxicity **(Figs. 3.4, 3.5 and 3.6)**. Thus, liposome-mediated stimulation of cancer cells could be a promising method to enrich Exo yield. Such an increased yield of Exos supports the expansion of basic research regarding Exo analysis and their application as drug delivery vehicles. Interestingly, PEGylation to the bare liposomes inhibited Exo secretion **(Figs. 3.2 and 3.6)**. The suppressive effect of PEGylation might be considered a new benefit for using PEGylated liposomes in treating tumors, because it has been reported that Exos play a controversial role in tumor progress by stimulating/suppressing the immune system **(Théry et al., 2002; Hedlund et al., 2011)**. Therefore, PEGylated liposomes may subside the bimodal role of Exos, particularly in tumor metastasis. These observations suggest that our approach may be a new strategy to stimulate/inhibit the secretion of Exos derived from cancer cells if the physicochemical properties of liposomes can be correctly manipulated.

The underlying mechanism behind increased Exo secretion via stimulation of liposomes remains uncertain. Raposo and Stoorvogel reported some different mechanisms for Exo release in a response to stimulation **(Raposo and Stoorvogel, 2013)**. For instance, the increased secretion of Exos was triggered by stimulating p53 in

tumor cells under stress conditions **(Lespagnol et al., 2008)**, via the activation of purinergic receptors, by changes in intracellular Ca^{2+} levels or by causing a depolarization of the cell membrane, which occurs by positively charged ions such as K^{+} **(Savina et al., 2005; Lachenal et al., 2011; Raposo and Stoorvogel, 2013)**. The stimulatory effect of neutral bare liposomes (NL) and cationic bare liposomes (CL), observed in this study, might have been caused by these mechanisms.

The observed strong stimulation caused by CL rather than NL **(Figs. 3.2, 3.3, 3.4, 3.5 and 3.6)**, is notably related to the cationic lipid in CL. Many studies have reported that CLs induce cytotoxicity in a dose-dependent manner **(Elsabahy and Wooley, 2013; Chou et al., 2014)**. Therefore, the stimulatory effect of CL might reflect its cytotoxicity; more stress due to CL is applied to cancer cells, which may produce more Exos as a defensive mechanism **(Zhou et al., 2013)**. The higher stimulatory effects of CL2 and CL3 are probably due to their higher interaction with tumor cells via not only surface cationic charge but also membrane fluidity **(Socaciu et al., 2000; Kočišová et al., 2013)** as well as to subsequent cell damage **(Chou et al., 2014)**. It appears that membrane fluidity of liposomes also contributes to enhanced Exo secretion because both CL2 and CL3 produced Exos at a higher rate compared with CL4, which contains cholesterol (DC-Chol) that creates a solid-phase membrane.

Interestingly, PEGylation to the surface of liposome suppressed secretion of Exos from the cells **(Figs. 3.2 and 3.6)**. The PEG conformation has a great effect on liposome-cell interactions; the mushroom structure of PEG on the surface of liposomes reduces nanoparticle-cell interactions, rather than the brush structure **(Hu et al., 2007)**. In addition, the negative surface charge of PEGylated liposomes **(Table 1)** reduces or prevents the interaction between liposomes and cells due to electronic repulsion between these nanoparticles and negatively charged cell membranes **(Hu et**

al., 2007). However, these factors cannot account for the suppression of the Exo secretion by PEGylation that was observed in the present study. Uz et al. recently found that the PEGylation of gold nanoparticles altered the cell cycle and caused DNA damage without apoptosis, which effectively disrupted cell division and replication. They showed that the effect was dependent on PEG grafting density and concentration; at a particular PEG grafting density (~0.65 chains/nm^2), none of these severe damages were observed **(Uz et al., 2016)**. Literature studies have documented how the nanoparticles, which show no toxic effects according to classic toxicity test results, may severely disrupt cell-cycle steps, and cause DNA damage or apoptosis. Accordingly, the PEGylated liposomes in this study might have stimulated cells via liposome-cell collisions, which could have resulted in a suppression of Exo secretion. The mechanism behind this reaction will require further study.

The uptake of Exos depends on many factors such as innate uptake ability of target cancer cell, characters of collected Exos and the interaction between Exos and target cancer including adhesion, fitting surface antigen and fusion. Many studies have already reported that any change in Exo characters significantly affects their cellular uptake **(Christianson et al., 2013; Inder et al., 2014; T. J. Smyth et al., 2014)**, which is consistent with our current observation (**Fig. 11**). The cellular uptake of Exos obtained under normal and stimulated conditions extensively differed in a response to liposome type used in stimulation. The highest percentage of Exo internalization was observed for exo-S2 followed by exo-N, while exo-S1 showed no detectable cellular uptake (**Fig. 11**). This might have been related to changes in the surface proteins of Exos **(Mulcahy et al., 2014; McKelvey et al., 2015)**, which are responsible for cellular targeting and uptake. The similarities of the exosomal surface

proteins with autologous cells may explain the higher ability of B16BL6 to take up Exos compared with the C26 cancer cell line.

3.1. Background

In the chapter II, I reported that the incubation of cancer cells with liposome formulations of different physiochemical properties enhanced Exo secretion and increased Exo yield by conventional separation methods. Fluid DOPE-based cationic liposomes were more effective than solid HSPC-based liposome in increasing yield. In addition, the collected Exos showed different uptake propensities depending on the properties of the liposome preparations used for incubation. Uninduced Exos and Exos induced by fluid cationic liposomes had higher uptake by autologous Exos than Exos induced by solid cationic liposomes. Further experiments are needed to understand the mechanisms behind these observations.

The mechanisms of interaction of Exos with cells and how this influences their uptake by recipient cells is not well understood, even the basic question of whether Exo uptake occurs through endocytosis or direct membrane fusion. Clarifying the mechanism of Exo uptake is the key to their development as DDS. Many reports have demonstrated that Exo uptake by target cells is driven heterogeneously via various mechanisms, depending on the nature of the Exo surface membrane proteins available to interact with the membrane receptors of target cells **(Morelli et al., 2004; Glebov et al., 2006; Feng et al., 2010; T. Tian et al., 2010; Montecalvo et al., 2012; Mulcahy et al., 2014)**. One class of Exo surface proteins is the tetraspanins, which are thought to be Exo markers with a role in the adhesion of Exos to recipient cells, facilitating Exo uptake **(French et al., 2017)**. For instance, CD9 and CD81 participate in attachment and uptake of Exos by dendritic cells **(Morelli et al., 2004)**. Flotillin-1, a plasma membrane microdomain, is another exosomal surface protein that controls the clathrin independent endocytosis pathway in cells **(Glebov et al., 2006; Meister and Tikkanen, 2014)**. In addition, EGF is another exosomal surface protein with a

predominant role in the uptake process via EGFR-mediated endocytosis **(Liu et al., 2011)**. Similarly, Annexin-A2 mediates endocytic entry to cells **(S. Wang et al., 2016b)**. Other plausible mechanism for Exo uptake may be clathrin-dependent endocytosis, lipid raft-mediated endocytosis, phagocytosis and/or macropinocytosis **(Morelli et al., 2004; Feng et al., 2010; T. Tian et al., 2010; Montecalvo et al., 2012)**.

In this chapter, I expanded the research shown in the chapter II to reveal the importance and role of Exo proteins in the uptake of Exos induced by liposomes with varying physiochemical properties. In addition, I have studied the uptake mechanisms of Exos by different cancer cell lines, induced by changing liposome properties. The results indicate that the induced Exos display different expression of surface proteins and different endocytosis pathways, which might reflect the amount and selectivity of Exo uptake.

3.2. Materials and methods

3.2.1. Materials and antibodies

Sucrose was purchased from Wako Pure Chemical (Osaka, Japan). Cytochalasin D, chlorpromazine (CPZ), amiloride hydrochloride hydrate and filipin complex were purchased from Sigma Aldrich (MO, US). All antibodies (Abs) were purchased from Abcam (Cambridge, UK), including anti-CD9 (RabMab, ab92726), anti-annexin-A2 (ab41803), anti-flotillin-1 (ab41927) and anti-EGF (ab9695). The reagents, HSPC, DOPE, (DOTAP), cholesterol, DC-6-14, anti-TSG101 (ab30871), HRP conjugated goat anti-rabbit IgG H&L (ab6721), PKH67 Green Fluorescent Cell Linker kit, exo-FBS and FBS , are previously described in the chapter II. All other reagents were of analytical grade.

3.2.2. Cell lines and cell culture

C26 and B16BL6 were supplied, maintained and cultured as previously described in the chapter II.

3.2.3. Preparation of liposomes

Two types of cationic liposomes, solid (HSPC-based liposomes) and fluid (DOPE-based liposomes), were prepared as previously described in the chapter II.

3.2.4. Collection of Exos

Exos, exo-N, exo-S1 and exo-S2, were collected from murine melanoma as previously described in the chapter II with an additional purification step, gradient ultracentrifugation, which was conducted using 0.3-2.5 M sucrose to alleviate the possibility of contamination by liposomes.

3.2.5. Shotgun analysis of Exo proteins

Shotgun analysis was conducted as described previously **(Kawanishi et al., 2015)**. Briefly, six μg protein from Exo samples was treated with buffer A (8 M urea,

2 mM EDTA, 250 mM Tris-HCl, pH 8.5) containing 10 mM 1,4-dithiothreitol (DTT) for 2 h at 37°C, followed by incubation with buffer A containing 25 mM iodoacetamide for 1 h at room temperature to conduct carbamidmethylation of the thiol group. The reaction product was mixed with 1/20 amount of trypsin solution (w/w) and incubated overnight at 37°C. The resultant peptide mixture was passed through a ZipTip µ-C18 (Millipore) for desalting, and 0.4 µg of that was subjected to nanoLC-MS/MS analysis.

For nanoLC-MS/MS analysis, the digested peptides were separated on an Acclaim PepMap RSLC Nano Column (75 µm x 150 mm, 2 µm, C18, Thermo Fisher Scientific Inc., MA, US) operated at a flow rate of 300 nL/min using UltiMate 3000 RSLCnano System (Thermo Fisher Scientific Inc., MA, US). Phase A was 0.1% formic acid, and phase B was 80% acetonitrile containing 0.08% formic acid. After an isocratic step at 4% B for 10 min, B was linearly increased to 55% within 204 min followed by increase to 90% within 10 min. After 4 min washing, B was decreased back to 4% within 1 min. Mass spectrometry (MS) was performed using Orbitrap Elite (Thermo Fisher Scientific Inc., MA, US) operated in positive ion mode (Nanoflow-LC ESI). Capillary voltage was set at 1.7 kV. The mass data was analyzed using Mascot (Matrix Science Inc., MA, US).

3.2.6. SDS PAGE electrophoresis and Western blotting analysis

Exo samples were separated on 5-20% gradient gels (epagele-PAGEL; ATTO, Tokyo, Japan) as previously described in chapter II for SDS PAGE electrophoresis and Western blotting analysis **(Kawanishi et al., 2015)**. After sample preparation, each lane was loaded with 20 µl of sample containing 15 µg and 60 µg for SDS PAGE and Western blot, respectively and electrophoresis was run. For simple SDS PAGE visualization, Precision Plus Protein All Blue Standard (10-250 kDa, Bio-Rad

Laboratories Inc., CA, US) was used as a standard, and the gel was stained with Coomassie brilliant blue dye (0.05%). For Western blotting, the procedures were as previously described in chapter II. After membrane blocking, the membrane was incubated with a 1:1,000 dilution of different primary Abs; anti-CD9, anti-annexin-A2, anti-flotillin-1 and anti-EGF in TBST 0.05% overnight at 4 °C. The membrane was washed and then incubated with the HRP conjugated goat anti-rabbit IgG H&L secondary antibody. The membrane was visualized and then imaged using image quant LAS 4000 (GE Healthcare Life Sciences). Exo marker, TSG101, was used as control (housekeeping) antigens.

3.2.7. Evaluation of the *in vitro* cellular uptake of collected Exos

The cellular uptake of different Exos derived from the donor B16BL6 melanoma cell line was evaluated in autologous B16BL6 cells and in the allogeneic colon cancer cell line C26 as previously described in chapter II. After 24 h incubation of cell seeding cells, PKH67-labeled Exos were added to the cultured cells to a final concentration of 2 µg Exo protein/mL. After a further 2-4 h incubation, cells were harvested and Exo uptake was evaluated via flow cytometry analysis using a Gallios flow cytometer (Beckman Coulter) and confocal laser scanning microscopy at 63x magnification using LSM 700 (ZEISS) **(Morelli et al., 2004; Parolini et al., 2009; Ekstrom et al., 2012; Holder et al., 2016)**.

To study the contribution of surface proteins to Exo uptake, the inhibitory effect of different Abs against major Exo surface proteins (anti-CD9, anti-annexin-A2, anti-flotillin-1 and anti-EGF Abs) on Exo uptake was evaluated. Prior to Exo incubation with the cultured cells, labeled Exos were mixed with the selected Abs in a ratio 1:1 µg Exo protein:µg Ab and then incubated at 4 ºC for 2 h. To study the Exo uptake mechanism, the inhibitory effect of different uptake inhibitors on Exo uptake

was evaluated, including cytochalasin D (0.5 -10 μM), CPZ (5-50 μM), amiloride hydrochloride (100- 1000 μM), filipin complex (1-10 μg/mL) and sucrose (0.45 M). Each uptake inhibitor blocks one or more uptake pathway **(Dutta and Donaldson, 2012; Mulcahy et al., 2014)**; cytochalasin D blocks phagocytosis, macropinocytosis and other endocytic pathways via disrupting actin polymerization **(Cooper, 1987; Sampath and Pollard, 1991; Fujimoto et al., 2000)**, CPZ inhibits clathrin-dependent endocytosis by interfering with the assembly of clathrin in plasma membrane **(L. H. Wang et al., 1993)**, sucrose non-specifically blocks clathrin-dependent endocytosis **(Carpentier et al., 1989)**, amiloride inhibits macropinocytosis by hindering Na^+/H^+ exchange **(Koivusalo et al., 2010)** and filipin inhibits lipid raft-mediated endocytosis via cholesterol sequestering action **(Auriac et al., 2010)**. First, the Countess II automated cell counter (Thermo Fisher Scientific Inc., MA, US) was adopted to evaluate cell viability after adding these inhibitors by staining cells with trypan blue dye. The uptake experiment was continued with inhibitor concentrations showing cell viability of not less than 80% **(Fig. 3.1)**. Prior to the incubation of labeled Exos with the cultured cells, they were pre-incubated for 30 min at 37°C for 4 h with different concentrations of inhibitors. To evaluate whether Exo internalization is energy-dependent, the incubation was also done at 4°C for 2 h.

3.2.8. Statistical analysis

All values were expressed as mean ± S.D. Statistical analysis was performed via an unpaired t test using Graphpad Prism 6.01 software (GraphPad Software Inc., CA, US). The level of significance was set at $p < 0.05$.

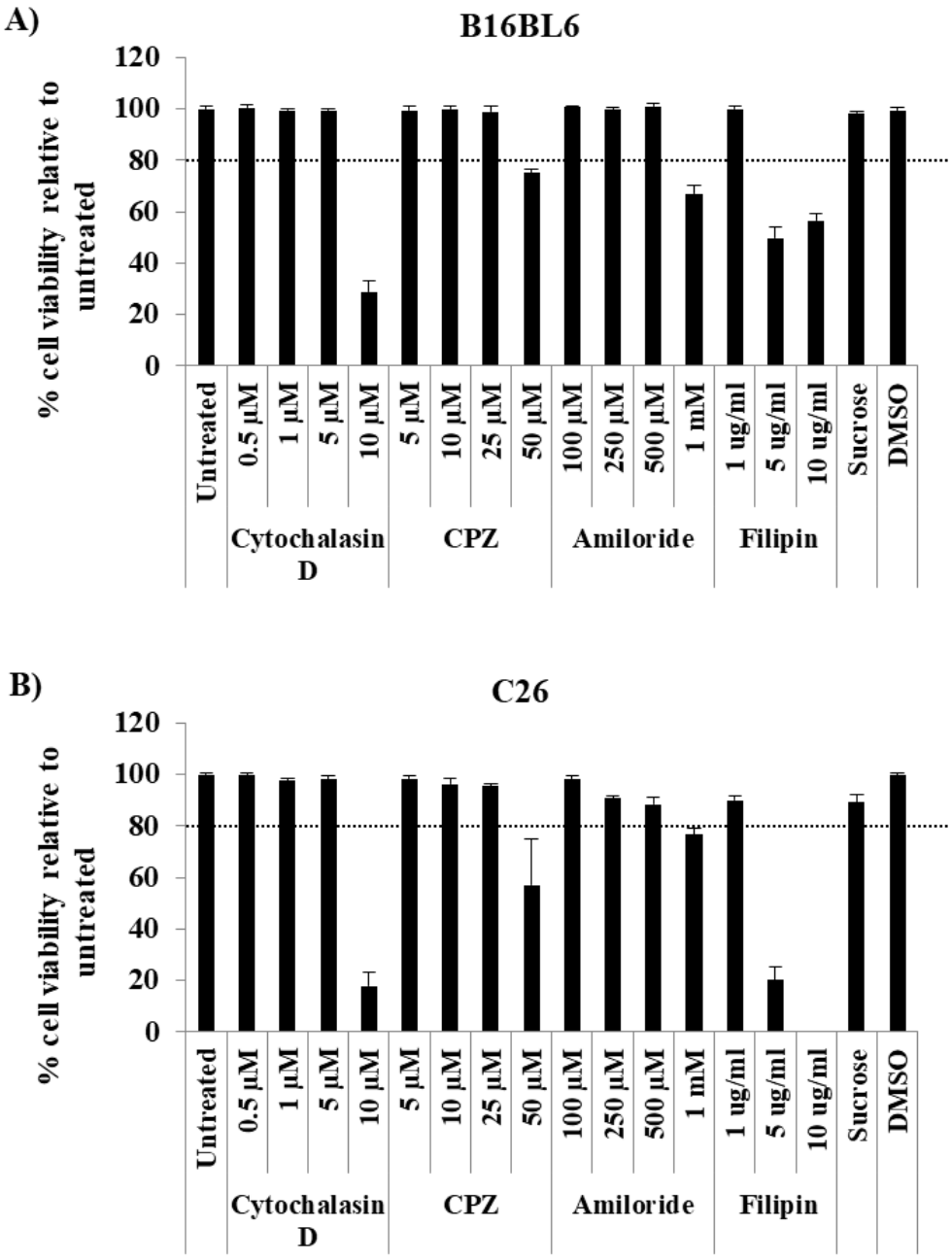

Figure 3.1. Effect of the uptake inhibitor concentration on cell viability of B16BL6 and C26.

B16BL6 (A) and C26 (B) cancer cell lines were incubated in presence of different concentrations of each uptake inhibitor and then cell viability was evaluated via a Countess II automated cell counter after staining cells with trypan blue dye. The cell viability was calculated as a relative percentage compared to untreated cells. All data represent the mean ± SD.

3.3. Results

3.3.1. *In vitro* cellular uptake study

The cellular uptake of Exos collected after 48 h incubations was studied under either normal conditions (exo-N) or after stimulation with 1 mM HSPC-based liposomes (exo-S1) and 0.05 mM DOPE-based liposomes (exo-S2). The uptake of exo-S1 was lower than that of exo-N and exo-S2 **(Figs. 2.11 and 2.12)**.

3.3.2. Analysis of Exo proteins

Many previous studies have reported the contribution of exosomal surface proteins to their cellular uptake, and have suggested their potential as drug delivery vehicles **(Mulcahy et al., 2014; Batrakova and Kim, 2015**, **2016)**. Accordingly, protein analysis of the collected Exos was conducted using three different techniques; shotgun analysis, SDS-PAGE and Western blotting. Shotgun analysis was performed to identify common exosomal markers **(Table 3.1)**. Detected proteins were divided into four categories; tetraspanins, heat shock proteins, enzymes and others. Several common exosomal markers such as CD63, CD81, HSP90 and TSG101 were shared by all collected Exos. However, several other proteins such as CD9, lactate dehydrogenase A (LDHA), flotillin-1, annexin-A2, epidermal growth factor (EGF), lysosomal membrane glycoprotein A (LAMP-2), niemann-pick disease type C1 (NPC1) and clathrin light chain were not detected in exo-S1. To further examine the differential expression of exosomal marker proteins, SDS-PAGE and Western blotting were carried out. SDS-PAGE demonstrated that all Exos samples shared most of main protein bands. But some proteins were missing in exo-S1 samples, especially in the tetraspanin region at 25 kDa **(Fig. 3.2)**. Exosomal proteins that might contribute to Exo uptake (CD9, annexin-A2, flotillin-1 and EGF) were then screened for by Western blotting analysis. As shown in **Fig. 3.3,** these proteins were detected at 25, 35

	exo-N	exo-S1	exo-S2
Proteins hits	404	258	552

	Protein name	Accession number	MW (KDa)	pI	Score (peptide matches)		
					exo-N	exo-S1	exo-S2
Tetraspanins	CD9	gi|388912	25.241	6.88	34	0	79
	CD63	gi|976238	25.479	6.69	42	35	99
	CD81 (Tapa-1 protein)	gi|8574076	25.797	5.54	421	394	453
	CD82	gi|148695678	22.373	7.98	114	68	93
	CD151 (SFA-1)	gi|2447007	28.257	7.44	89	62	73
Heat shock proteins	HSPA8 (HSP70.1)	gi|118490060	70.088	5.53	186	107	173
	HSP90 (Endoplasmin)	gi|119362	92.418	4.74	117	117	115
Enzymes	Lactate dehydrogenase A (LDHA)	gi|126048	36.475	7.74	79	0	26
	GAPDH	gi|120702	35.787	8.44	292	226	644
	Alpha enolase 1 (Eno-1)	gi|12832241	47.111	6.37	259	155	454
	Tyrosine 3-Monooxygenase/Tryptophan 5-Monooxygenase Activation Protein (YWHAE or Phopholipase A2)	gi|1304166	27.754	4.73	109	133	138
	L-lactate dehydrogenase B chain isoform Ldhbx	gi|938085832	37.325	5.85	119	92	82
	L-lactate dehydrogenase B chain isoform 2	gi|718551069	27.989		119	85	73
	Fructose-bisphosphate aldolase B	gi|15723268	39.548	8.52	48	79	52
	Phosphoglycerate kinase (PGK1)	gi|202423	44.508	7.53	108	75	345
	Chain A, Modified Glutathione S-Transferase (Pi) Complexed With S (P-Nitrobenzyl)glutathione	gi|4557944	23.471	7.85	107	164	147
Others	Flotillin-1	gi|2149604	47.484	6.71	50	0	86
	Annexin-A2	gi|113951	38.652	7.55	33	0	42
	Epidermal growth factor (EGF)	gi|49523319	122.888	6.79	39	0	24
	lysosomal membrane glycoprotein A (LAMP-2)	gi|293693	45.618	7.05	42	0	67
	NPC1	gi|2251242	142.795	5.52	42	0	64
	Clathrin (light chain)	gi|34785471	23.618	4.43	116	0	116
	TSG101	gi|3184260	44.096	6.28	153	121	184
	Eukaryotic translation elongation factor 1 alpha 1 (EEF1A1)	gi|13278546	50.082	9.1	187	85	255
	Programmed Cell Death 6 Interacting Protein (PDCD6IP)	gi|30048422	96.251	6.15	631	219	537
	Albumin (ALB)	gi|3647327	68.648	5.75	550	504	878
	Gamma actin	gi|6425087	43.572		264	162	451
	Cofilin-1 (CFL1)	gi|116849	18.548	8.22	175	48	142
	Ferritin heavy chain	gi|309233	21.086	5.62	53	41	50
	Alpha-4 integrin	gi|1173604	115.013	6.29	294	381	538
	Clathrin (heavy chain)	gi|51491845	191.435	5.48	327	96	1768
	Lactadherin (MFGE8)	gi|113865979	51.208	6.11	426	80	398

Table 3.1. Identification of Exo markers via shotgun analysis

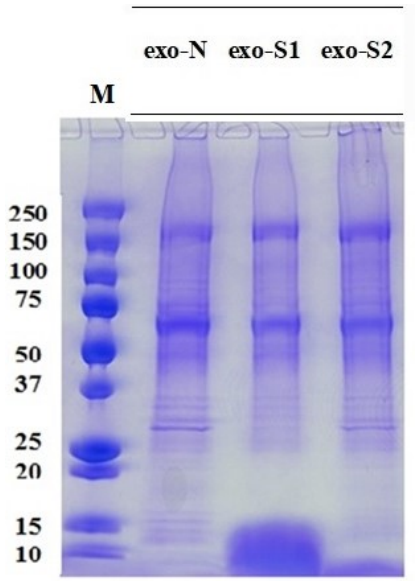

Figure 3.2. Analysis of Exo proteins by SDS PAGE

Exo proteins in each sample (exo-N, exo-S1 and exo-S2) were electrophoretically separated and then stained by Coomassie brilliant blue dye (0.05%). M, molecular weight marker.

Proteins (MW, kDa)		exo-N	exo-S1	exo-S2
CD9	**25**			
Annexin-A2	**35**			
Flotillin-1	**47**			
EGF cleaved form 1	**51**			
EGF cleaved form 2	**6**			
TSG101	**47**			

Figure 3.3. Identification of Exo marker proteins by Western blotting

Exo proteins in each sample (exo-N, exo-S1 and exo-S2) were electrophoretically separated and then blotted in presence of different Abs, including anti-CD9, anti-flotillin-1, anti-annexin-A2, anti-EGF and anti-TSG101. TSG101 was used as a reference (housekeeping) protein.

and 47 kDa corresponding to CD9, annexin-A2 and flotillin-1, respectively, in exo-N and exo-S2 (but not exo-S1) samples. In addition, in exo-N and exo-S2 samples, EGF showed bands at both 51 and 6 kDa, likely cleaved forms of pro-EGF (122.88 kDa). Interestingly, in exo-S1 samples, these proteins were absent or present at very low levels. It is worth noting that TSG101 (band at 47 kDa) was expressed equally in all Exos I tested confirming that equal amounts of Exos were loaded for electrophoretic separation. These results indicate that liposome stimulation caused changes in protein expression in derived Exos.

3.3.3. Contribution of Exo surface proteins to Exo uptake

The expression of EGF and flotillin-1 was higher in exo-N than exo-S2 samples, while annexin-A2 was higher in exo-S2. In addition, samples from both Exo types expressed CD9 to a similar degree. To get more insight into the role of certain proteins in uptake of Exos by cancer cells, samples of Exos displaying high protein expression (exo-N and exo-S2, **Fig. 2.11**) were selected for cellular uptake inhibition experiments. Briefly, labeled Exos were incubated with different Abs that would inhibit the interaction between surface proteins on Exos and their receptors on recipient cells, and then their uptake by donor B16BL6 and allogeneic C26 cancer cells was evaluated using flow cytometry and confocal laser scanning microscopy. In the exo-N sample (normal Exos), anti-CD9 Ab inhibited the uptake of Exos by B16BL6 cells by 24.1% **(Fig. 3.4A)**, while anti-flotillin-1 Ab inhibited the uptake of Exos by C26 cells by 26.7% **(Fig. 3.4B)**. These observations were confirmed using confocal laser scanning microscopy, where anti-CD9 Ab and anti-flotillin-1 Abs decreased the accumulation of exo-N (green) into B16BL6 and C26, respectively **(Fig. 3.5)**. In the exo-S2 samples, anti-CD9, anti-flotillin-1 and anti-EGF Abs inhibited the uptake of Exos by B16BL6 cells by 41.6%, 56.8% and 66.4%, respectively **(Fig.**

3.6A). Similarly, confocal microscopy showed the decrease in the internalization of exo-S2 (green) into B16BL6 **(Fig. 3.7)**. Interestingly, anti-flotillin-1 and anti-EGF Abs substantially restricted the uptake by C26 by 61.8% and 50.1%, respectively, while anti-CD9 Ab did not inhibit the uptake by C26 **(Fig. 3.6B)**. Confocal microscopy confirmed that anti-flotillin-1 and anti-EGF Abs inhibited the uptake of exo-S2 by C26 **(Fig. 3.7)**. These results suggest that different surface markers may be involved in the uptake of Exos by different cells.

3.3.4. Exo uptake mechanism

There have been a number of investigations into the mechanisms behind Exo uptake, in efforts to improve exosome-based drug delivery systems **(Mulcahy et al., 2014)**. Since exo-N and exo-S2 showed differences in protein expression **(Fig. 3.3)** and cellular uptake **(Figs. 3.4, 3.5, 3.6 and 3.7)**, the mechanism mediating their uptake was further investigated.

Uptake of exo-N by B16BL6 cells or C26 cells were strongly inhibited at 4°C, compared to normal conditions (37°C) **(Figs. 3.8 and 3.9)**. Similarly, uptake of exo-S2 by B16BL6 cells or C26 cells were strongly inhibited at 4°C, compared to normal conditions (37 °C) **(Figs. 3.8 and 3.9)**. These results suggest that the uptake of exo-N and exo-S2 by either B16BL6 cells or C26 cells was mediated by energy-dependent processes. The uptake mechanism was further studied using several chemical inhibitors. The uptake of exo-N by both B16BL6 cells and C26 cells was inhibited by cytochalasin D, CPZ and amiloride in a concentration-dependent manner **(Figs. 3.10A, 3.10B, 3.11 and 3.12)**. The uptake of exo-N by both cell lines was also inhibited in the presence of filipin and sucrose **(Figs. 3.10A, 3.10B, 3.11 and 3.12)**. These results indicate that exo-N were taken up by either B16BL6 cells or C26 cells via phagocytosis, clathrin-mediated endocytosis, lipid raft-mediated endocytosis and/or

macropinocytosis. In the uptake of exo-S2 by either B16BL6 cells or C26 cells, similar tendencies on inhibitory effect of various inhibitors were observed **(Figs. 3.13A, 3.13B, 3.14 and 3.15)**. The uptake by B16BL6 or C26 cells was inhibited by cytochalasin D, CPZ, amiloride, filipin and sucrose **(Figs. 3.13A, 3.13B, 3.14 and 3.15)**. These results indicate that the exo-S2 was also taken up by either B16BL6 cells or C26 cells via the same mechanisms as observed with exo-N. It is noteworthy that the impact of inhibitors on the uptake of both exo-N and exo-S2 was entirely stronger to B16BL6 cells than to C26 cells **(Figs. 3.10 and 3.13)**. This may suggest that B16BL6 cells highly interact with these Exos somehow via Exo specific surface protein and thus aggressively internalize them *in vitro*.

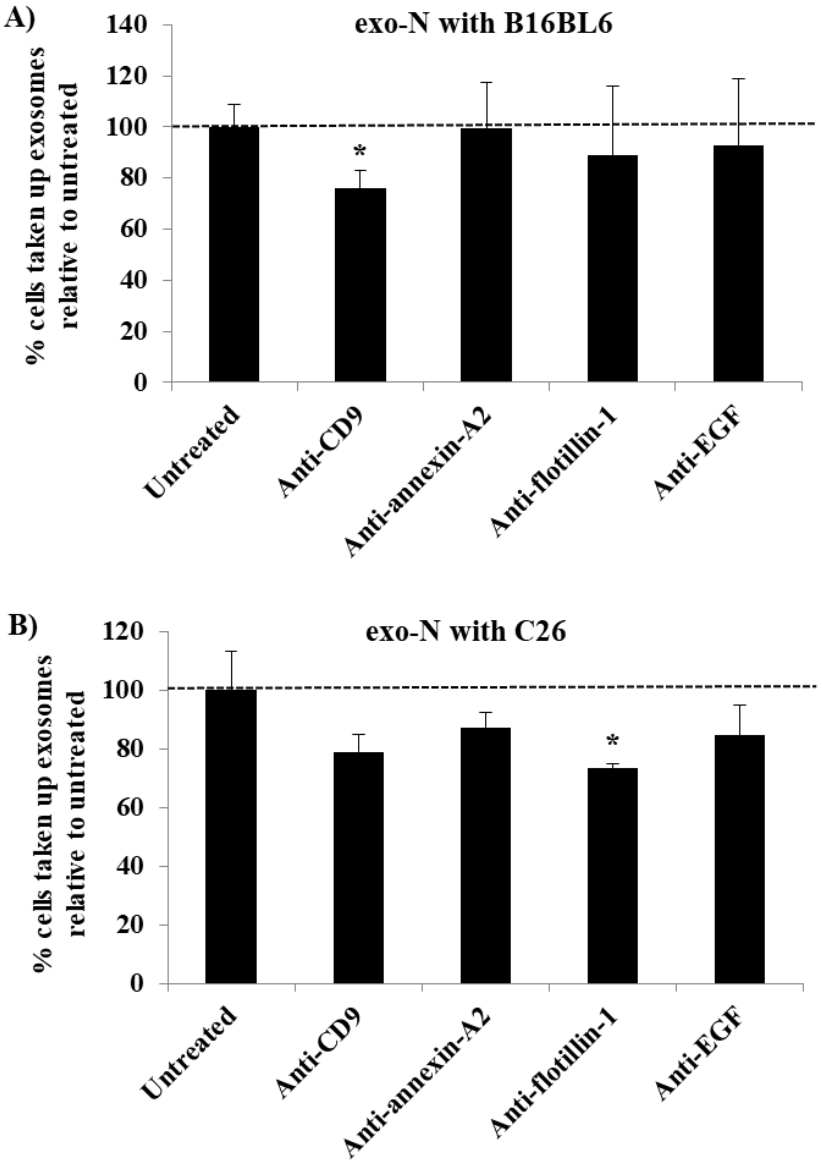

Figure 3.4. Identifying the role of certain marker proteins in the uptake of exo-N by donor cells B16BL6 and other allogeneic cells C26 via flow cytometry analysis.

Labeled exo-N were incubated with different Abs in a ratio 1:1 for 2 h at 4 °C and then added to different cancer cell lines, namely B16BL6 (A) and C26 (B). After 4 h incubation, cancer cells were harvested for analysis by flow cytometry. All data represent the mean ± SD of triplicates. An unpaired t test was applied for each value relative to untreated cancer cells, asterisks indicate different levels of significant difference; * $p < 0.05$.

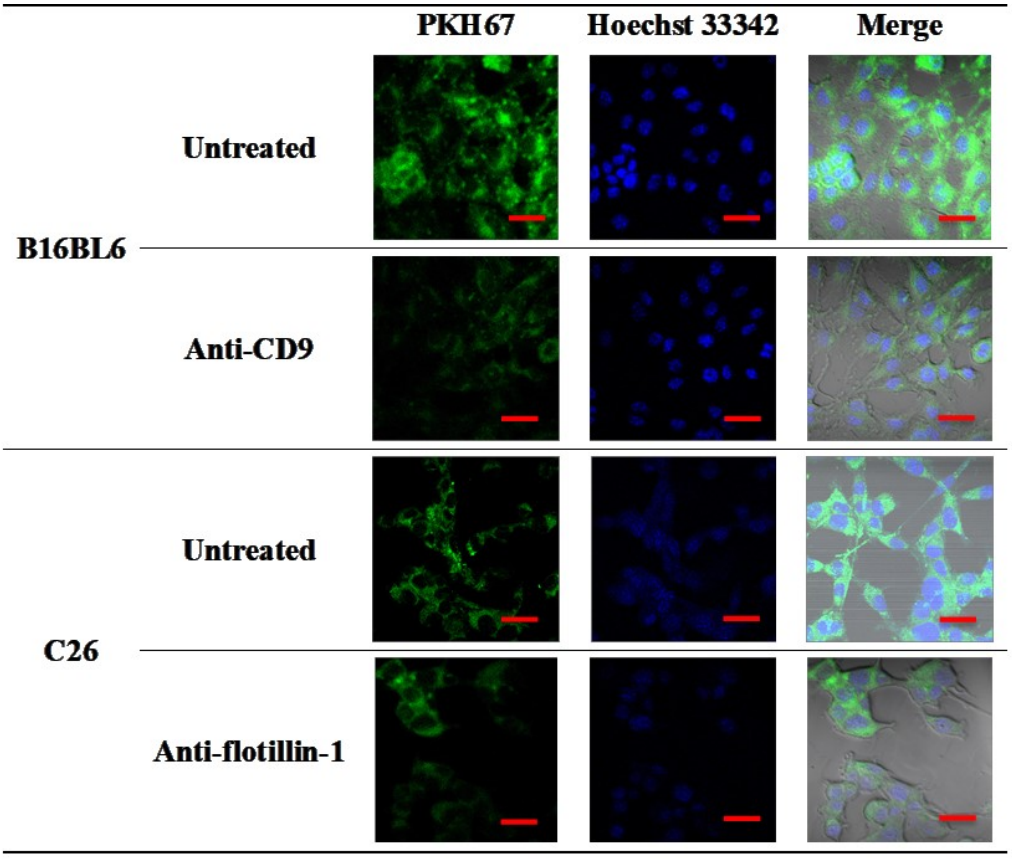

Figure 3.5. Identifying the role of certain marker proteins in the uptake of exo-N by donor cells B16BL6 and other allogeneic cells C26 via confocal laser scanning microscopy.

Labeled exo-N were incubated with different Abs in a ratio 1:1 for 2 h at 4 °C and then added to different cancer cell lines. After 4 h incubation, cancer cells were imaged by laser scanning confocal microscope after staining the DNA core with Hoechst 33342. All data represent one set of triplicates. Exos were labeled with PHK67 (green) and the DNA core was stained with Hoechst 33342 (blue). Scale bar indicates 20 μm.

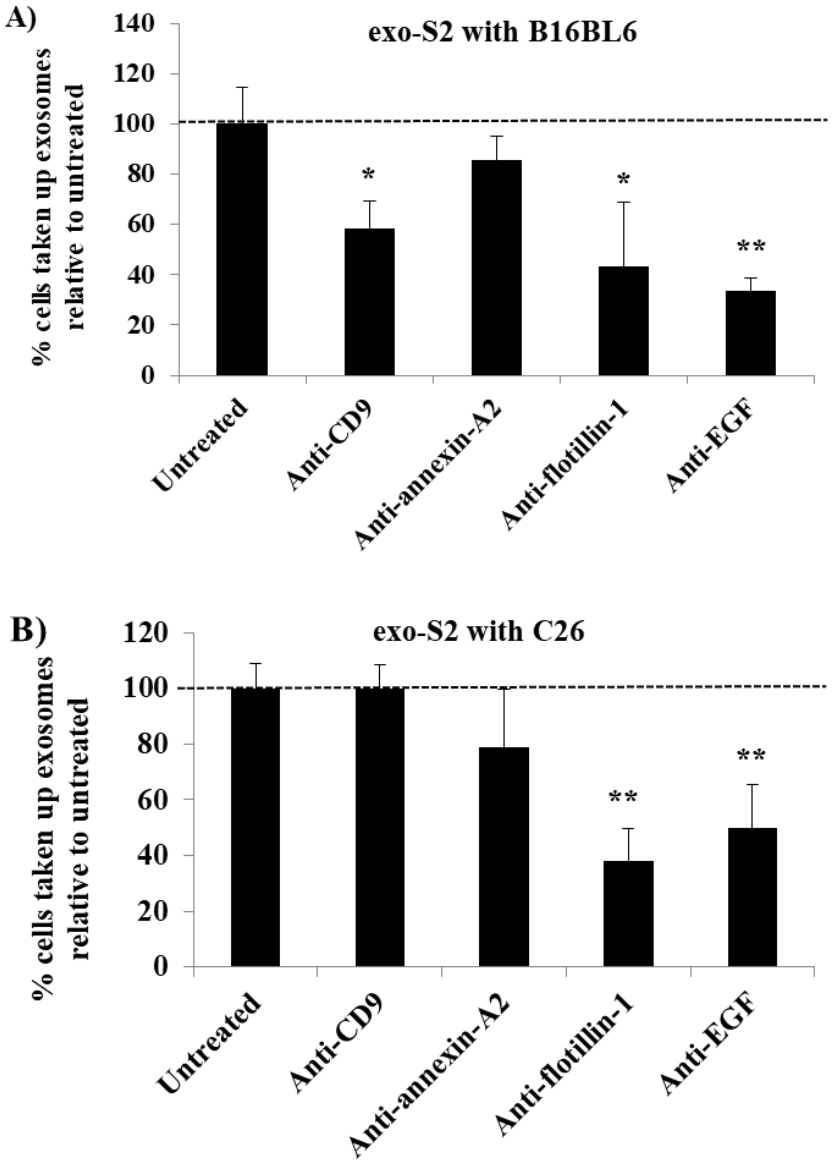

Figure 3.6. Identifying the role of certain marker proteins in the uptake of exo-S2 by donor cells B16BL6 and other allogeneic cells C26 via flow cytometry analysis.

Labeled exo-S2 were incubated with different Abs in a ratio 1:1 for 2 h at 4 °C and then added to different cancer cell lines, namely B16BL6 (A) and C26 (B). After 4 h incubation, cancer cells were harvested for analysis by flow cytometry. All data represent the mean ± SD of triplicates. An unpaired t test was applied for each value relative to untreated cancer cells, asterisks indicate different levels of significant difference; * $p < 0.05$ and ** $p < 0.01$.

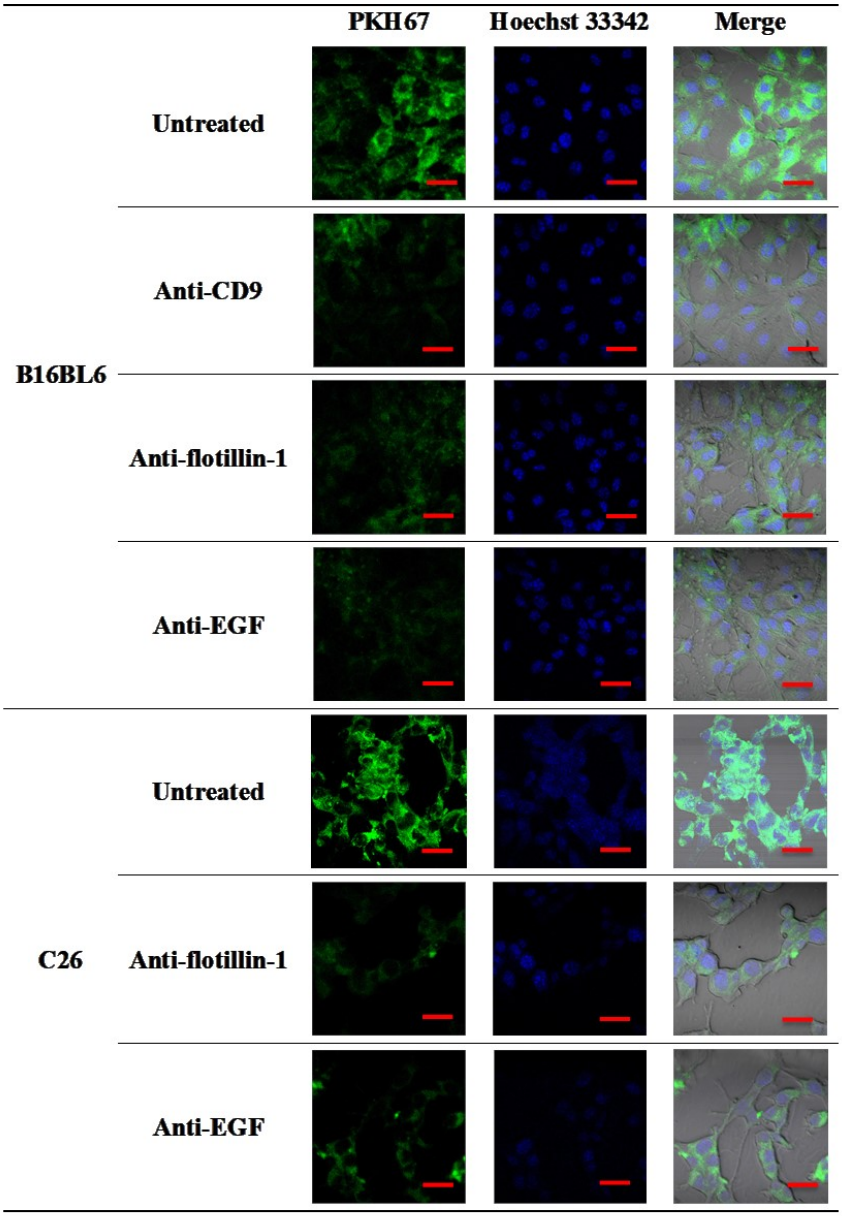

Figure 3.7. Identifying the role of certain marker proteins in the uptake of exo-S2 by donor cells B16BL6 and other allogeneic cells C26 via confocal laser scanning microscopy.

Labeled exo-S2 were incubated with different Abs in a ratio 1:1 for 2 h at 4 °C and then added to different cancer cell lines. After 4 h incubation, cancer cells were imaged by laser scanning confocal microscope after staining the DNA core with Hoechst 33342. All data represent one set of triplicates. Exos were labeled with PHK67 (green) and the DNA core was stained with Hoechst 33342 (blue). Scale bar indicates 20 μm.

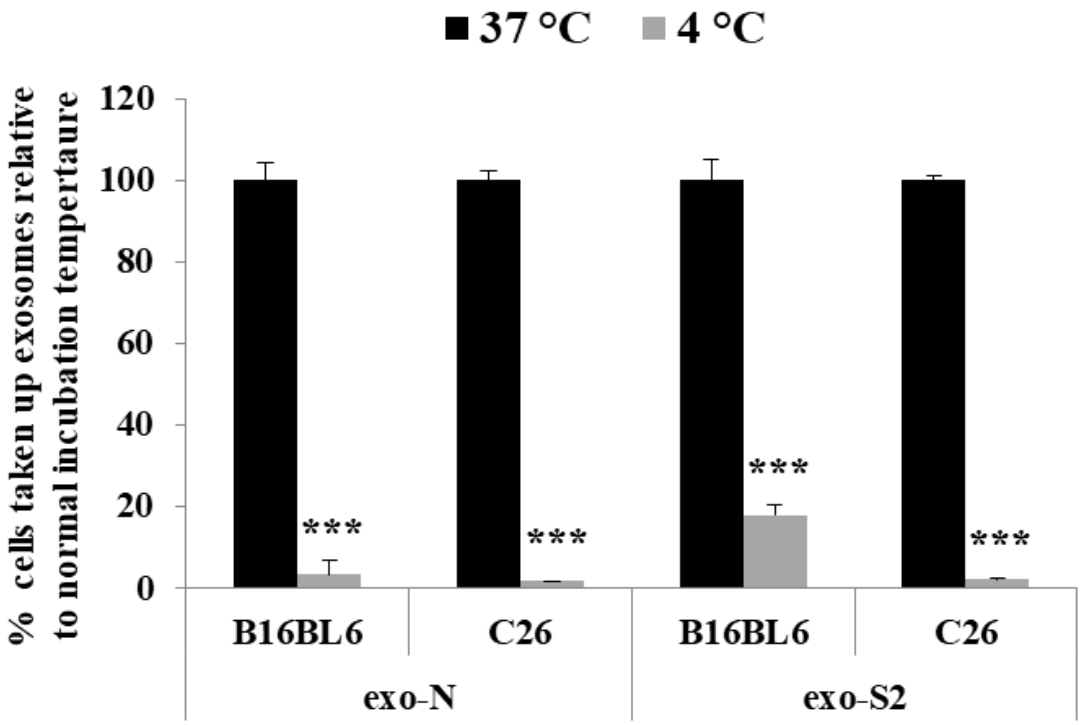

Figure 3.8. Identifying the effect of temperature on Exo uptake by donor cells (B16BL6) and allogeneic cells (C26) via flow cytometry analysis.

Labeled samples of exo-N and exo-S2 were incubated with different cancer cell lines at 4°C or 37°C. After 2 h incubation, cancer cells were harvested for analysis by flow cytometry. All data represent the mean ± SD of triplicates. An unpaired t test was applied for each value relative to untreated cancer cells (*** $p < 0.001$).

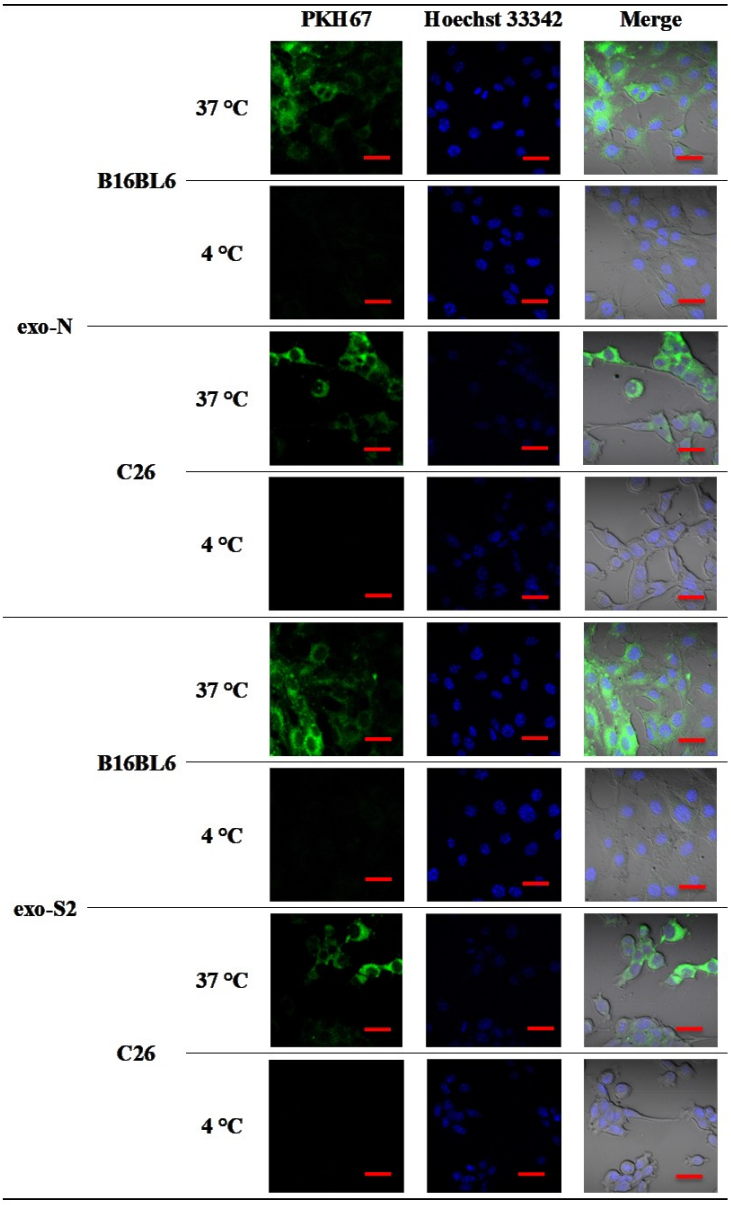

Figure 3.9. Identifying the effect of temperature on Exo uptake by donor cells (B16BL6) and allogeneic cells (C26) via confocal laser scanning microscopy.

Labeled samples of exo-N and exo-S2 were incubated with different cancer cell lines at 4°C or 37°C. After 2 h incubation, cancer cells were imaged by laser scanning confocal microscope after staining the DNA core with Hoechst 33342 (B). All data represent one set (B) of triplicates. Exos were labeled with PHK67 (green) and the DNA core was stained with Hoechst 33342 (blue). Scale bar indicates 20 μm.

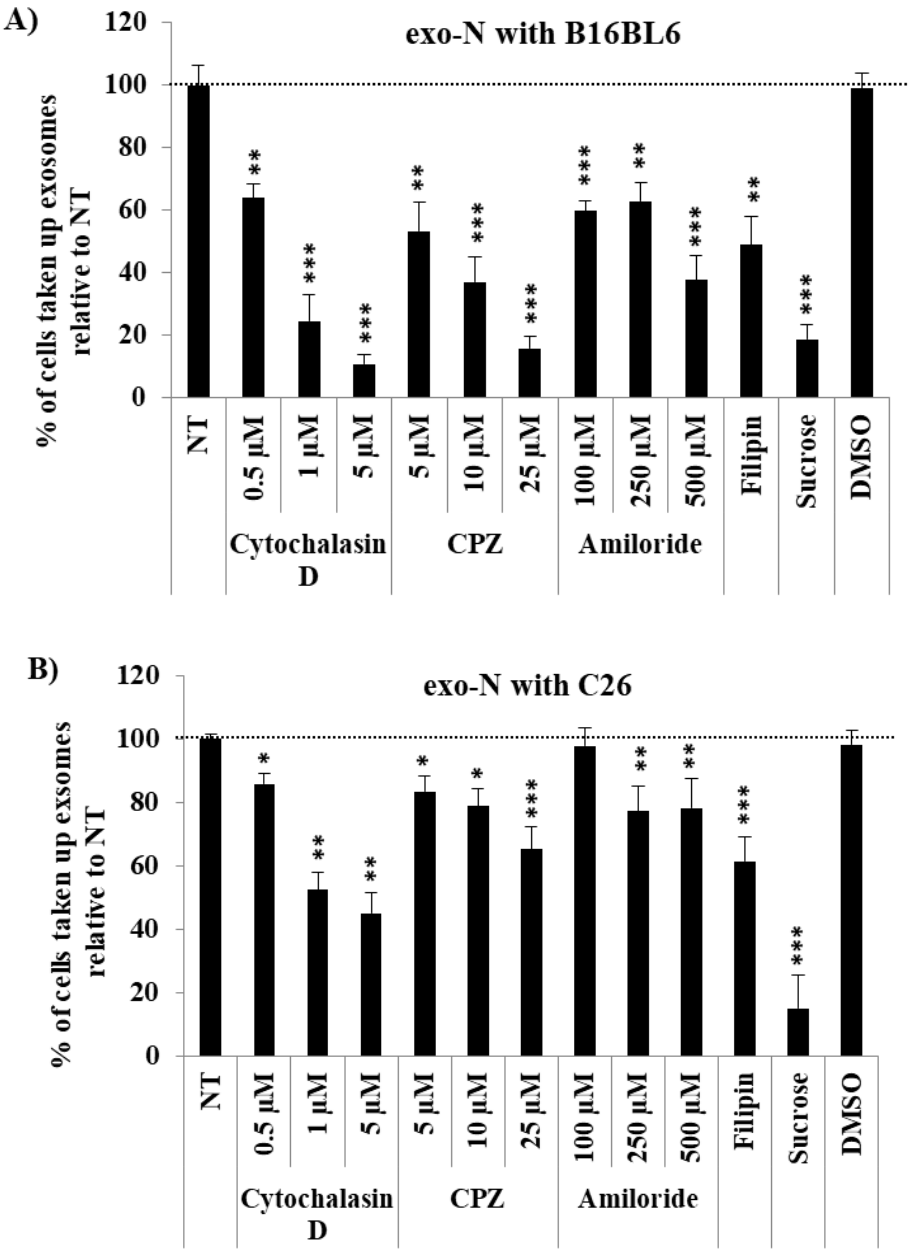

Figure 3.10. Identifying the uptake mechanisms for exo-N internalization by donor cells B16BL6 and other allogeneic cells C26 via flow cytometry analysis.

B16BL6 (A) and C26 (B) cancer cell lines were incubated in the presence of different uptake inhibitors for 30 min and then labeled exo-N were added. After 4 h incubation, cancer cells were harvested for analysis by flow cytometry. All data represent the mean ± SD of triplicates. An unpaired t test was applied for each value relative to untreated (NT) cancer cell, asterisks indicate different levels of significant difference; * $p < 0.05$, ** $p < 0.01$ and *** $p < 0.001$. NT, untreated cancer cells.

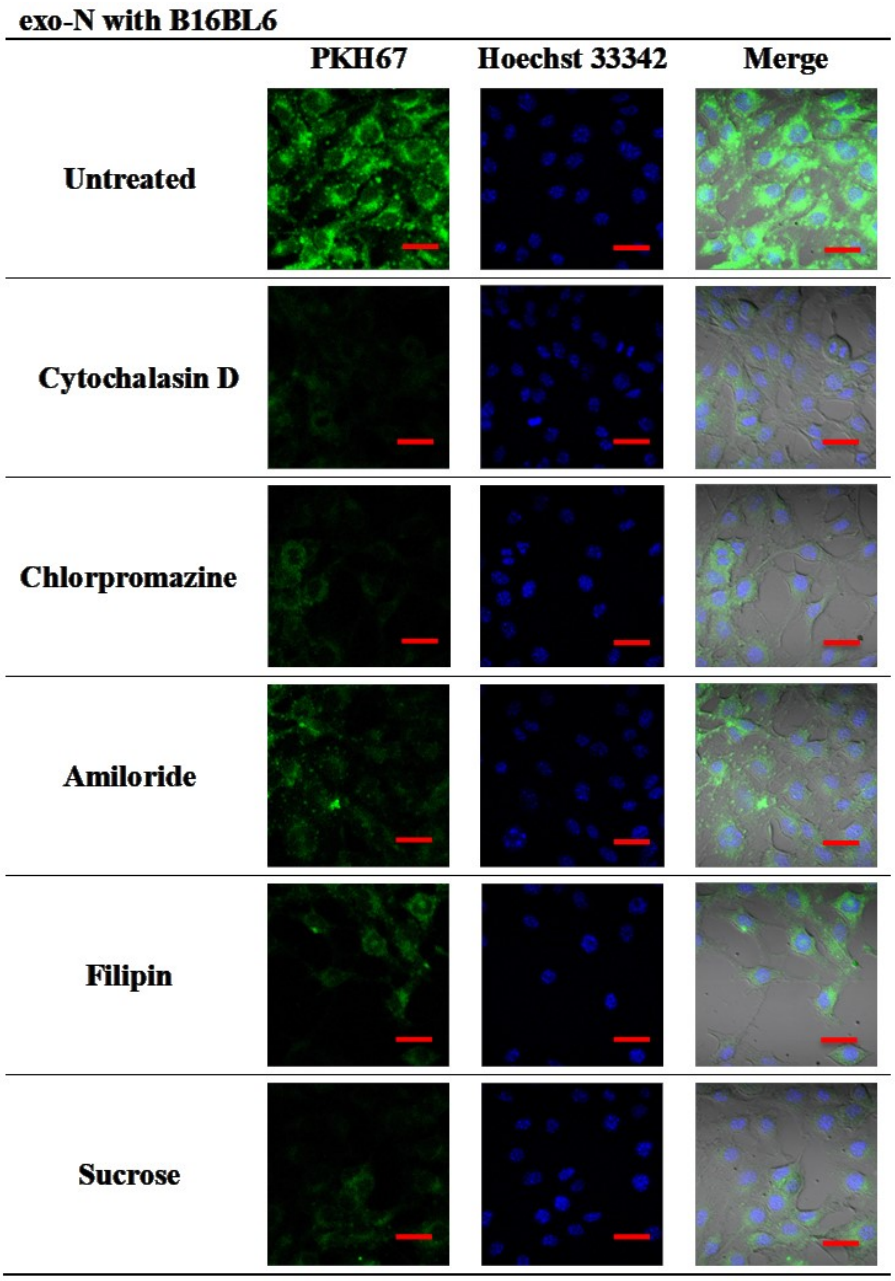

Figure 3.11. Identifying the uptake mechanisms for exo-N internalization by donor cells B16BL6 via confocal laser scanning microscopy.

B16BL6 cancer cells were incubated in the presence of different uptake inhibitors for 30 min and then labeled exo-N were added. After 4 h incubation, cancer cells were imaged by laser scanning confocal microscopy after staining the DNA core with Hoechst 33342. All data represent one set of triplicates. Exos were labeled with PHK67 (green) and the DNA. Scale bar indicates 20 μm.

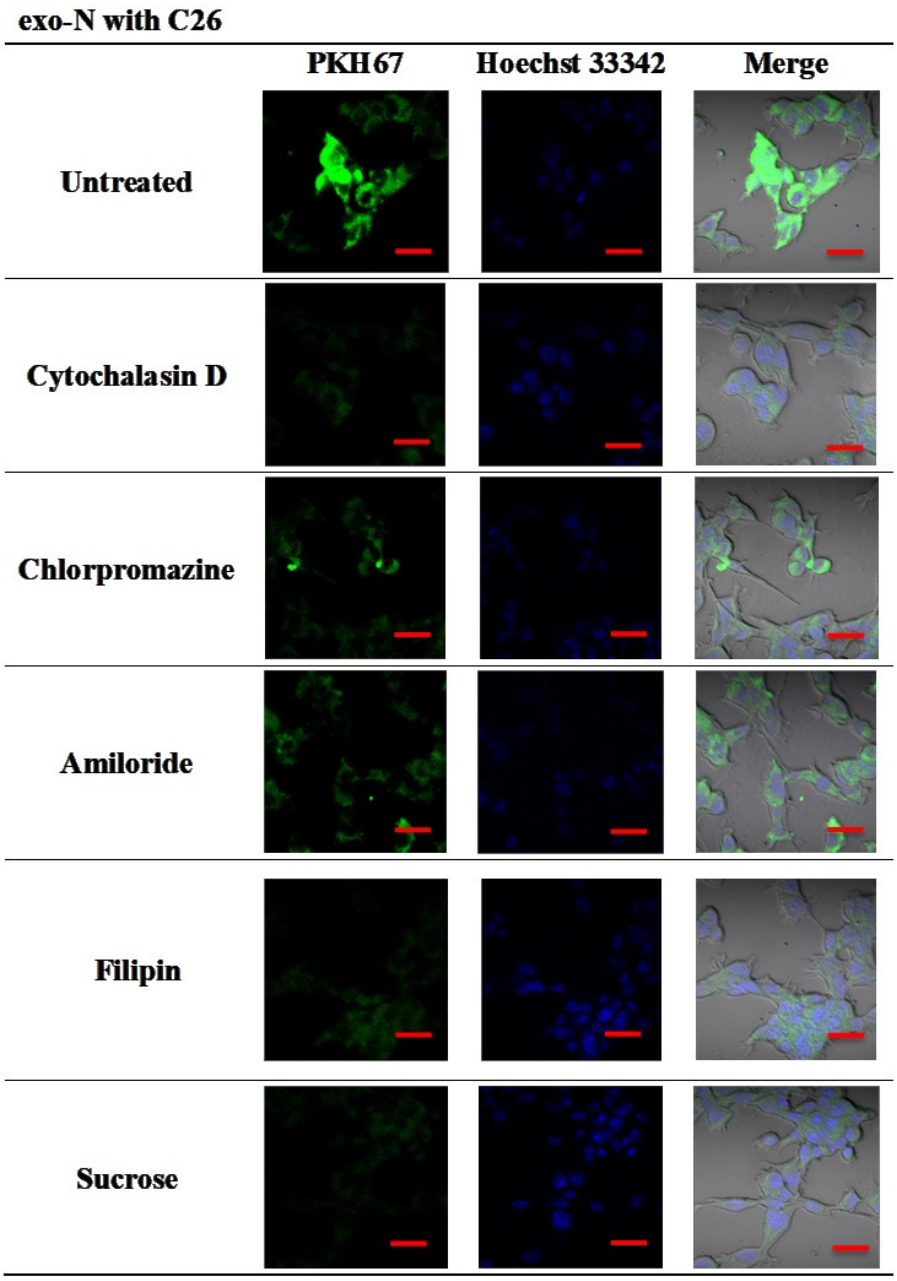

Figure 3.12. Identifying the uptake mechanisms for exo-N internalization by allogeneic cells C26 via confocal laser scanning microscopy.

C26 cancer cells were incubated in the presence of different uptake inhibitors for 30 min and then labeled exo-N were added. After 4 h incubation, cancer cells were imaged by laser scanning confocal microscopy after staining the DNA core with Hoechst 33342. All data represent one set of triplicates. Exos were labeled with PHK67 (green) and the DNA. Scale bar indicates 20 μm.

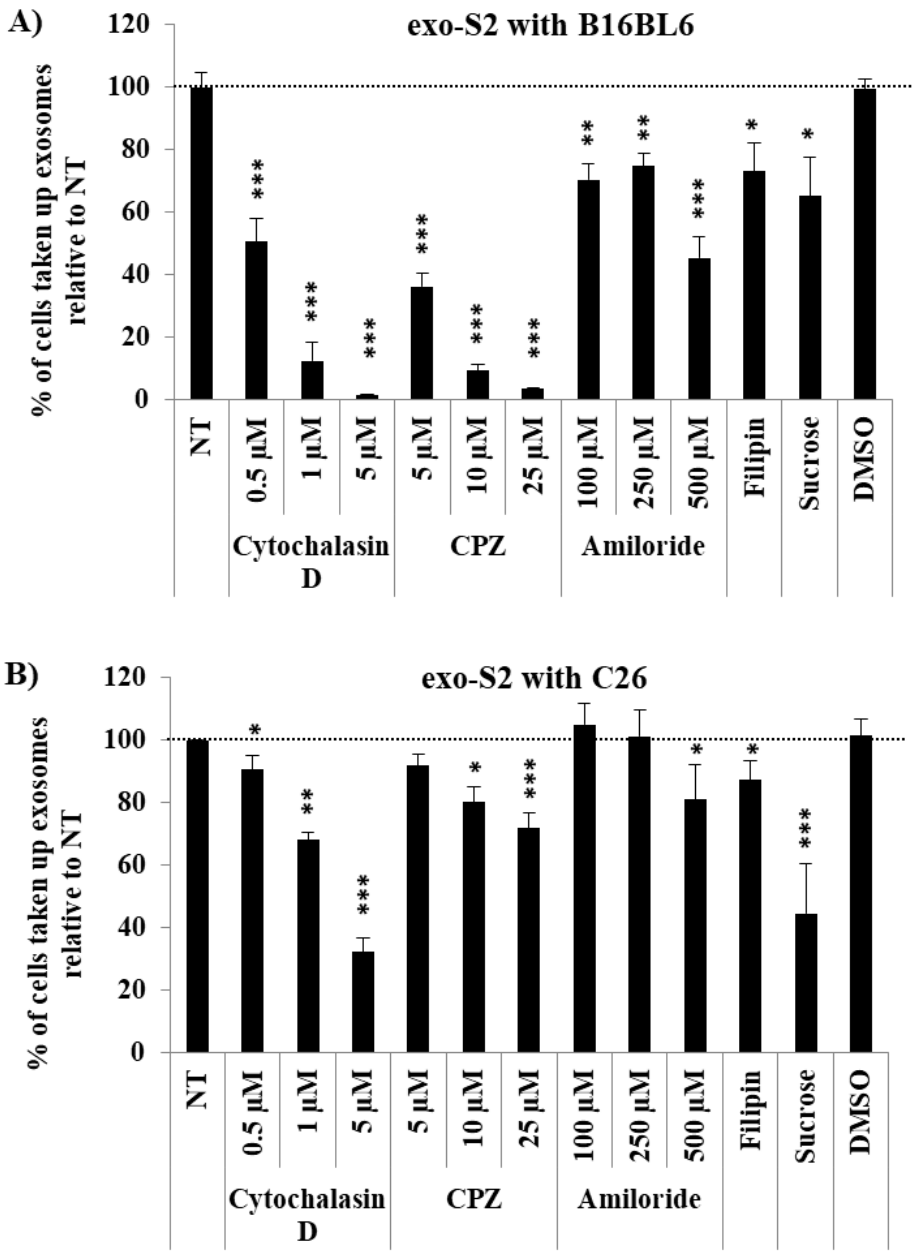

Figure 3.13. Identifying the uptake mechanisms for exo-S2 internalization by donor cells B16BL6 and other allogeneic cells C26 via flow cytometry analysis.

B16BL6 (A) and C26 (B) cancer cell lines were incubated in the presence of different uptake inhibitors for 30 min and then labeled exo-S2 were added. After 4 h incubation, cancer cells were harvested for analysis by flow cytometry. All data represent the mean ± SD of triplicates. An unpaired t test was applied for each value relative to untreated (NT) cancer cell, asterisks indicate different levels of significant difference; * $p < 0.05$, ** $p < 0.01$ and *** $p < 0.001$. NT, untreated cancer cells.

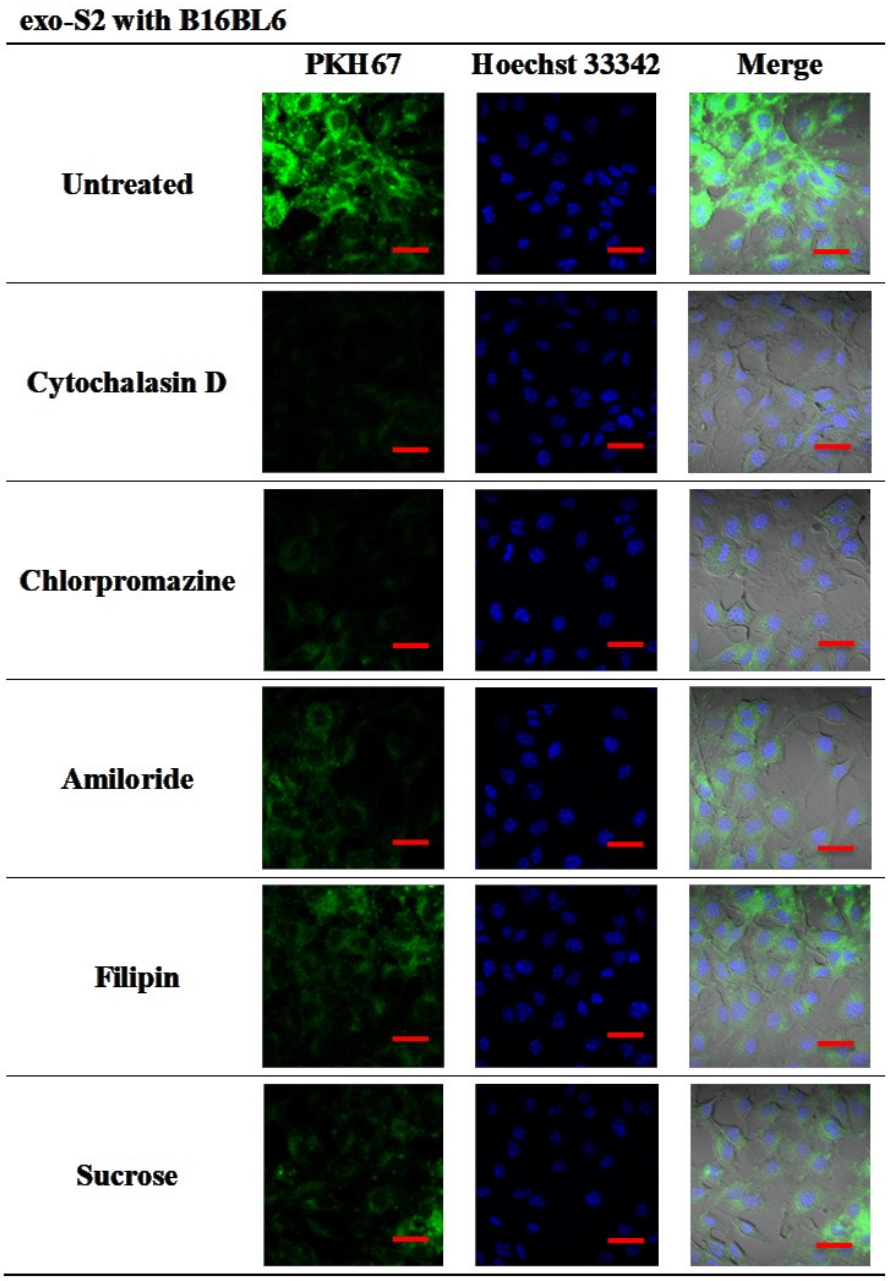

Figure 3.14. Identifying the uptake mechanisms for exo-S2 internalization by donor cells B16BL6 via confocal laser scanning microscopy.

B16BL6 cancer cells were incubated in the presence of different uptake inhibitors for 30 min and then labeled exo-S2 were added. After 4 h incubation, cancer cells were imaged by laser scanning confocal microscopy after staining the DNA core with Hoechst 33342. All data represent one set of triplicates. Exos were labeled with PHK67 (green) and the DNA. Scale bar indicates 20 µm.

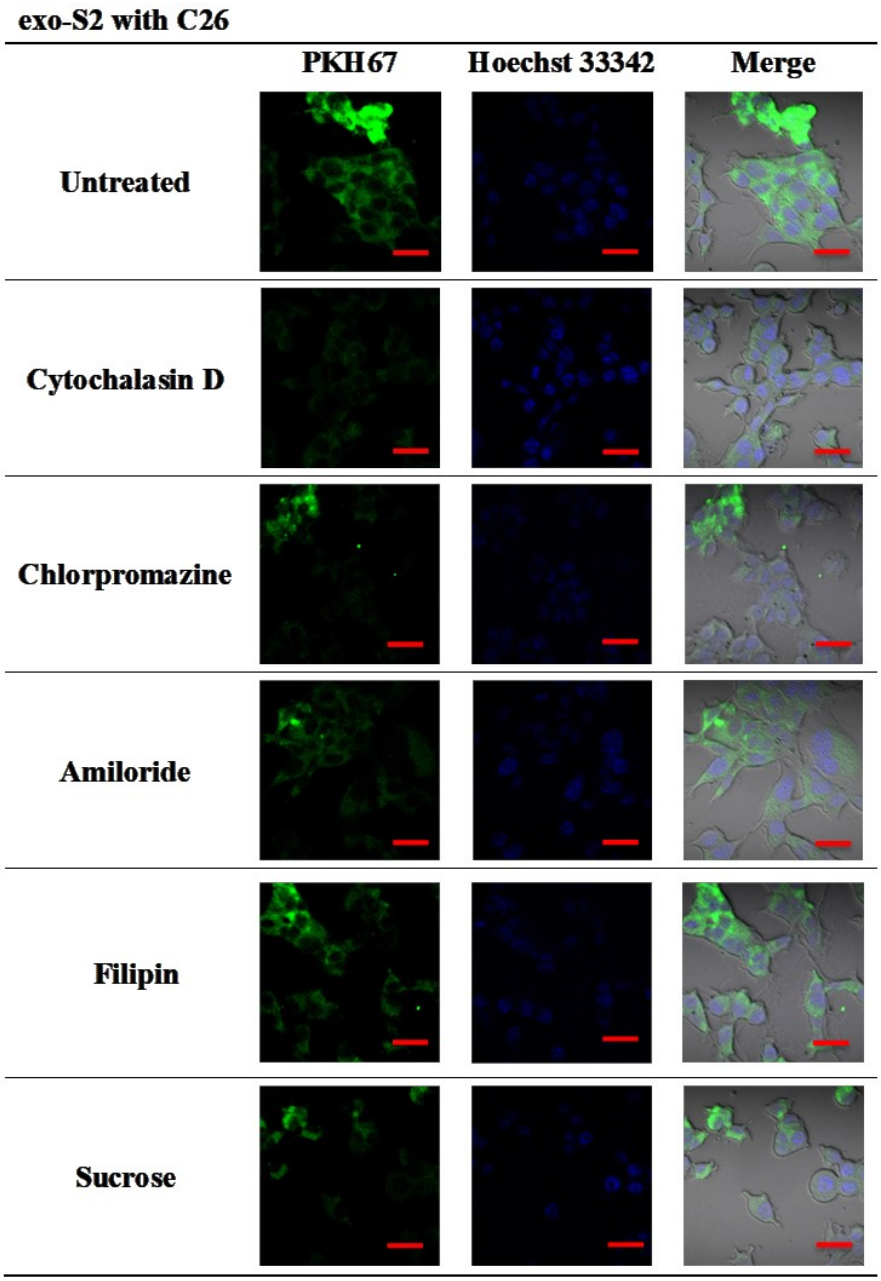

Figure 3.15. Identifying the uptake mechanisms for exo-S2 internalization by allogeneic cells C26 via confocal laser scanning microscopy.

C26 cancer cells were incubated in the presence of different uptake inhibitors for 30 min and then labeled exo-S2 were added. After 4 h incubation, cancer cells were imaged by laser scanning confocal microscopy after staining the DNA core with Hoechst 33342. All data represent one set of triplicates. Exos were labeled with PHK67 (green) and the DNA. Scale bar indicates 20 μm.

3.4. Discussion

In this chapter, I found that Exos incubated with different liposome preparations expressed different types of proteins **(Table 3.1)**. Among the three types of Exos I tested, exo-S1 showed the lowest level of protein expression and lacked several Exo marker proteins (**Fig. 3.3**). CD9, annexin-A2, flotillin-1 and EGF are known to contribute to Exo uptake by target cells via various mechanisms **(Morelli et al., 2004; Glebov et al., 2006; Feng et al., 2010; T. Tian et al., 2010; Liu et al., 2011; Montecalvo et al., 2012; Meister and Tikkanen, 2014; Mulcahy et al., 2014; S. Wang et al., 2016b; French et al., 2017)**. The lack of relevant proteins in the exo-S1 might be related to the low levels of Exo uptake by the donor cancer cell line (**Figs. 2.11 and 2.12**). Heterogeneous collections of Exos, each with different protein expression, may contribute to the differences in apparent uptake mechanisms observed in this study (**Figs. 3.10-3.15**) and various other studies **(Mulcahy et al., 2014; van Dongen et al., 2016; French et al., 2017)**. My current study showed that liposome incubation with donor cells, depending on liposome composition, can lead to substantial changes in the protein expression in the Exos, although the mechanism for this is unknown. My finding suggests a reliable method to control the characteristics of derived Exos by changing physicochemical property of liposomes used for incubation with the donor cells, allowing the fine-tuning of induced Exos.

The current study indicated that, not only a single exosomal marker protein, but several proteins are involved in the interaction of Exos with cancer cells (**Figs. 3.4-3.7**) and the subsequent cellular uptake of Exos (**Figs. 3.8-3.15**). As I showed in this study, the involvement of CD9, flotillins and EGF in the adhesion and targeting of Exos to the recipient cells has been highlighted in a number of previous reports **(Morelli et al., 2004; Otto and Nichols, 2011; Ohno et al., 2013; Banning et al., 2014)**. Morelli and colleagues illustrated that Exos taken up by bone marrow dendritic

cells is mediated by CD9 **(Morelli et al., 2004)**. Flotillin-1, lipid raft marker of Exos, is involved in the clathrin-independent endocytosis pathway **(Otto and Nichols, 2011; Banning et al., 2014)**. Furthermore, EGF-positive Exos are efficiently internalized by breast cancer cells in an EGFR-dependent manner **(Ohno et al., 2013)**. Although the contribution of other proteins, not investigated in this study, to the Exo interaction with recipient cells should not be excluded, the exosomal interaction seems to follow a general pattern already reported.

Of note, in the interaction of exo-S2 samples with the donor cell line (B16BL6) or an unrelated cell line (C26), different marker proteins contributed to the interaction of the Exos with the recipient cell lines, i.e., CD-9, flotillin-1 and EGF for B16BL6 cells, and flotillin-1 and EGF for C26 cells **(Figs. 3.6 and 3.7)**. This finding indicates that different cells may recognize Exos via different Exo surface markers. Hence, the specificity of Exos for target cells may be determined not only by characteristics such as the expression pattern of surface marker proteins on the induced Exos but also by the expression pattern of the membrane receptors on the surface of the recipient cells. It has been reported that the Exos that are released by cancer cells **(Tickner et al., 2014)** can promote tumor development and are involved in mediating intercellular communication within the tumor microenvironment **(Tickner et al., 2014; Whiteside, 2016)**. Despite the expected predominance of cancer-derived Exos in tumors, several studies have indicated poor *in vivo* tumor targetability of tumor-derived Exos **(Ohno et al., 2013; Y. Tian et al., 2014b; T. Smyth et al., 2015)**. Differential protein expression, as well as rapid clearance, may account for poor targetability of Exos *in vivo* **(Ohno et al., 2013; Y. Tian et al., 2014b; T. Smyth et al., 2015)**.

Confocal laser scanning microscopy allowed visualizing the internalization of Exo samples into B16BL6 or C26 cells in the absence of inhibitory Abs (**Figs. 3.5 and 3.7**). The result **(Figs. 3.8 and 3.9)** indicates that the internalization is an energy-dependent process, consistent with other studies **(Morelli et al., 2004; T. Tian et al., 2010; Escrevente et al., 2011)**. Several endocytosis inhibitors significantly reduced, but didn't completely inhibit, the uptake of Exos in this study **(Figs. 3.10 and 3.13)**. Taken together, these results suggest that the endocytosis of Exos occurs through more than one mechanism, again consistent with previous studies **(Feng et al., 2010; T. Tian et al., 2010; Escrevente et al., 2011)**. The heterogeneity of Exo samples may be one reason for the differential uptake (internalization), in addition to the lack of single clear uptake mechanism. It is possible that a population of Exos can be taken up into cells via a number of different entry pathways with the initial entry steps depending on the cell type and Exo composition.

Endocytosis inhibitors inhibited the uptake of exo-N and exo-S2 to a greater degree in donor B16BL6 cells than in C26 cells **(Figs. 3.10 and 3.13)**. This may suggest that donor cells interact strongly with the Exo samples via their surface marker proteins, which in turn trigger rapid internalization. It has been reported that the uptake of Exos *in vitro* occurs as early as 15 min after addition **(Feng et al., 2010)**, depending on cell type. Exos may bind to "autocrine" receptors on donor cells that trigger rapid internalization, although further studies would be required to show this.

Nowadays, there is interest in applications of Exos as vehicles for the delivery of therapeutics to diseased cells **(Alvarez-Erviti et al., 2011; Zhuang et al., 2011; Ohno et al., 2013; Y. Tian et al., 2014b; Batrakova and Kim, 2015; Haney et al., 2015)**. However, their use is presently restricted by low Exo yields and Exo heterogeneity, leading to low targetability. In the chapter II, I showed how the release

of Exos from donor cancer cells is increased when they are incubated with liposome preparations of varying compositions. In the current study, I report that incubating the donor cancer cells with liposome preparations changes the protein content in the induced Exos, which raises the possibility of fine tuning Exo properties and making them more useful in drug delivery applications. Accordingly, my strategy, to employ and select liposome preparations as stimulators for the production of Exos expressing different surface protein markers, may be useful for engineering Exos for selective targeting to different diseases.

4.1. Background

Exos have several promising characteristics highlighting their potential exploitation in drug delivery **(Johnsen et al., 2014)**. However, unpredictable Exo (EV) biodistribution and poor specific cell-targeting of systemically administered Exos (EVs) hinders their implication in drug delivery to tumor **(Tominaga et al., 2015; Vader et al., 2016)**. In addition, Exos (EVs) are supposed to have a privileged immune response through bypassing the clearance by MPS because of their endogenous origin particularly allogeneic Exos (EVs). However, recent investigations, along with my current observations, oppose this assumption. Systemically administered Exos (EVs) are found to be rapidly cleared from blood circulation **(Takahashi et al., 2013; Lai et al., 2014; T. Smyth et al., 2015)**. Therefore, solutions of this hurdle are of utmost importance to expand Exo (EV) implications in drug delivery. Accordingly, to overcome the short circulation time and/or off target effect of Exos (EVs), Exo (EV) modification is emerged via several approaches **(Ohno et al., 2013; Y. Tian et al., 2014b; S. A. A. Kooijmans et al., 2016; Armstrong et al., 2017; Gilligan and Dwyer, 2017; Y. Wang et al., 2017)**.

One of the popular approaches for Exo (EV) modifications is Exo (EV) decoration with targeting ligands via transfecting their donor cells. Despite of its effectiveness, it is time-consuming process and restrained by challenging technical difficulties **(Hung and Leonard, 2015)**. Another potential approach is coating Exo surface with polyethylene glycol (PEG), PEGylation. The latter is considered one of the ubiquitous approaches to prolong the circulation time of the nanoparticles (including natural ones) and reduce their immunogenicity **(Allen et al., 1991; S. A. A. Kooijmans et al., 2016; Suk et al., 2016)**. This approach is characterized by its simplicity and PEG safety. In addition, it is amenable for modification by targeting

ligands in what called post-insertion strategy **(Ishida et al., 1999; Allen et al., 2002; Moreira et al., 2002)**. Unfortunately, PEGylation of Exos (EVs) doesn't produce any remarkable change in their targeting to tumor, despite extending the circulation time of Exos (EVs) **(S. A. A. Kooijmans et al., 2016)**. Therefore, I believe that there is still a missed key factor to fruitfully exploit PEGylated Exos (EVs) in cancer therapy. Presumably, this missed puzzle piece is closely related to cell-type tropism, autologous Exos (EVs). Accordingly, in this study, autologous and allogeneic cancer cell-derived Exos with/without PEGylation, were investigated to evaluate their *in vitro* uptake by cancer cells as well as their biodistribution in murine colorectal tumor-bearing mice. In addition, I evaluated the efficiency of PEGylated autologous cancer cell-derived Exos in targeting either cancer cells or tumor-infiltrating immune cells to reveal whether Exos can be employed as DDS for various cancer therapeutic strategies including chemotherapy, gene therapy, immunotherapy and cancer vaccines.

4.2. Materials and Methods

4.2.1. Materials and antibodies

1,1'-Dioctadecyl-3,3,3',3'-Tetramethylindotricarbocyanine Iodide (DiR; DiIC18(7)), 1,1'-Dioctadecyl-3,3,3',3'-Tetramethylindocarbocyanine Perchlorate (DiI; DiIC18(3)), F4/80 monoclonal antibody (BM8, eFluor 660, eBioscience™) and CD11c monoclonal antibody (N418, FITC, eBioscience™) were purchased from Thermo Fisher Science, (MA, US). CD3 antibody (17A2, APC) was purchased from BioLegend (CA, US). IgM antibody (A135FS, FITC) was purchased from American Qualex (CA, US). The reagents, $mPEG_{2000}$-DSPE, PKH67 Green Fluorescent Cell Linker kit, exo-FBS and FBS, are previously described in the chapter II. All other reagents were of analytical grade.

4.2.2. Experimental animals and cell lines

BALB/c mice (male, 5 weeks old) were purchased from Japan SLC (Shizuoka, Japan). The experimental animals were allowed free access to water and mouse chow, and were housed under controlled environmental conditions (constant temperature, humidity, and a 12-h dark–light cycle). All animal experiments were evaluated and approved by the Animal and Ethics Review Committee of Tokushima University.

C26 and B16BL6 were supplied, maintained and cultured as previously described in the chapter II.

4.2.3. Collection and PEGylation of Exos

Both cell lines were adopted for collecting Exos, C26-Exos from C26 and B16BL6-Exos from B16BL6, as previously described in the chapter II. PEGylation of Exos was conducted after Exo labeling step via co-incubation of labeled Exos with PEG micelles. Briefly, PEG micelles were prepared via dissolving mPEG2000-DSPE

in PBS. Then, Exos were incubated at 37 °C for 1 h in the presence of different ratios of PEG micelles (μg Exo protein : μg PEG lipid).

4.2.4. Evaluation of the *in vitro* cellular uptake of collected Exos

The cellular uptake of both Exo types (C26-Exos and B16BL6-Exos) was evaluated via two cancer cell lines, C26 and B16BL6, using a flow cytometer as previously described in the chapter II.

4.2.5. Evaluation of biodistribution and tumor accumulation of Exos in tumor-bearing mice

The biodistribution and tumor accumulation of both Exo types was evaluated using C26 tumor-bearing BALB/c mice. To track Exo biodistribution, DiR and DiI were employed for Exo labeling according to the manufacturer's protocol. Both dyes were incorporated to Exos at a final concentration 0.5 % (μg dye/μg Exo protein) via incubation at 37 °C for 1 h and then Exos were washed twice with PBS. To evaluate Exo biodistribution in C26 tumor-bearing mice, C26 cells (2×10^6 cell/200 μL PBS) were subcutaneously inoculated into the back region of 5-week-old male BALB/c mice. Tumor bearing mice were divided into five cohorts; one with PBS (control), two treated with non-PEGylated Exos (C26-Exos and B16BL6-Exos) and two treated with PEGylated Exos (PEGylated C26- Exos and PEGylated B16BL6-Exos). For the treated groups, on the day 9 post-inoculation, a dose (70 μg/200 μl PBS/mouse) of fluorescently labeled Exos was intravenously injected via the tail vein of C26 tumor-bearing mice. At predetermined time points post-injection (4, 8, 24, 48, 72, 96, 120, 144 and 168 h), the mice were anesthetized and then the biodistribution of DiR-labled Exos was visualized using an *in vivo* imaging system (IVIS, Xenogen, CA, US). To evaluate tumor accumulation of Exos, mice were sacrificed after 24 h of Exo injection and then tumor tissue was collected. The accumulation of DiR-labeled Exos in the

collected tumors was monitored via *ex vivo* imaging using IVIS. In addition, tumor cells were harvested from the collected tumors and then the uptake of DiI-labeled Exos by these cells was evaluated via flow cytometry analysis using a specified gate for tumor cells.

4.2.6. Evaluation of Exo uptake by tumor-infiltrating immune cells

The uptake of both Exo types by tumor-associated immune cells was evaluated using C26 tumor-bearing BALB/c mice. Briefly, DiI-labeled PEGylated Exos (70 µg/200 µl PBS/mouse) were intravenously injected via the tail vein of tumor-bearing mice. At 24 h post-injection, C26 tumors were collected and then tumor-associated cells were harvested. The uptake of DiI-labeled Exos by each cell population was measured using a flow cytometer adjusted for a specified gate of tumor-associated immune cells after labeling with fluorescently labeled antibodies such as F4/80, CD3, CD11c and IgM for tumor-associated macrophage (TAM), T cell, dendritic cell (DC) and B cell, respectively.

4.2.7. Statistical analysis

Statistical analysis was performed via either an unpaired t test or an one way ANOVA test (Tukey's test) using Graphpad Prism 6.01 software (GraphPad Software Inc., CA, US). The level of significance was set at $p<0.05$.

4.3. Results

4.3.1. *In vitro* cross uptake of unmodified Exos

Currently, the potential use of cancer cell-derived Exos as drug delivery platform in cancer therapy is extensively investigated. The growing interest of that emerging field is driven by the innate ability of Exos to move from cell to cell transferring their cargo. That substantial ability is fundamentally determined by the type of donor and recipient cells **(Mulcahy et al., 2014; Hoshino et al., 2015)**. To investigate such factor, a cross uptake of different types of Exos by different cancer cells was conducted. In this study, two types of Exos, C26-Exos and B16BL6-Exos, were individually incubated with two types of cancer cells, C26 and B16BL6, under the same experimental conditions.

Fig. 4.1 showed that the uptake of C26-Exos with C26 was higher than that with B16BL6, in values of 31.14 % and 23.55 %, respectively. While, the uptake of B16BL6-Exos with C26 was lower than that with B16BL6, in values of 42.62 % and 59.58 % respectively. On the other hand, within each cancer cell type, the uptake of B16BL6-Exos was higher than that of C26-Exos. These observations reveal the predominant uptake of cancer cell-derived Exos by autologous cells, compared with other allogeneic cells. In addition, the uptake propensity of B16BL6-Exos is more prominent than C26-Exos, regardless of the type of target cancer cell.

4.3.2. PEGylation of Exos

PEGylation is one of the predominant strategies for coating different nanoparticles to evade their clearance by MPS and extend their circulation time **(Allen et al., 1991; Jokerst et al., 2011; Suk et al., 2016)**. To determine which concentration of PEG micelles could efficiently coat Exo surface, PEG-lipid micelles with three different concentrations were applied to both types of Exos. PEG layer has

been known to mask the surface of nanoparticles, hinder the contact between nanoparticles and target cells *in vitro* and accordingly restrict the cellular uptake of nanoparticles *in vitro*. The efficient level of PEG coating to Exos was evaluated on the basis of the resulted inhibition in their uptake by autologous cells.

Fig. 4.2 illustrated that all the tested ratios inhibited Exo uptake for both Exo types. The observed decrease in C26-Exo uptake was by 79.81 %, 83.95 % and 82.77 % for (1:10), (1:50) and (1:100) ratios respectively, while these ratios caused an inhibition in B16BL6-Exos by 89.43 %, 94.43 % and 90.36 % respectively. No significant difference in Exo particle size was detected after PEGylation, the particle size was about 200 nm **(Fig. 4.3)**. These data imply that $mPEG_{2000}$-DSPE micelles can efficiently mask Exo surface under current experimental condition. Conclusively, the ratio (1:50) was selected for Exo PEGylation in further study.

4.3.3. Biodistribution of non-PEGylated and PEGylated Exos in tumor-bearing mice

PEGylation is a well-established strategy in enhancing nanoparticle delivery to tumor through the enhanced permeation and retention (EPR) effect via bypassing the MPS clearance and extending the circulation time of nanoparticles **(Allen et al., 1991; Jokerst et al., 2011; Suk et al., 2016)**. Accordingly, I hypothesized that PEGylation of Exos will result in similar effects *in vivo*. To determine whether Exos with/without PEGylation could be employed for tumor delivery, biodistribution of Exos was evaluated in a tumor-bearing mouse. A C26 tumor model was selected due to its high vascular permeability. In this study, four types of DiR-labeled Exos, namely C26-Exos, B16BL6-Exos and their PEGylated forms, were intravenously injected in the tail vein of C26 tumor-bearing mice. Then their tumor accumulation was monitored using IVIS at the predetermined time points.

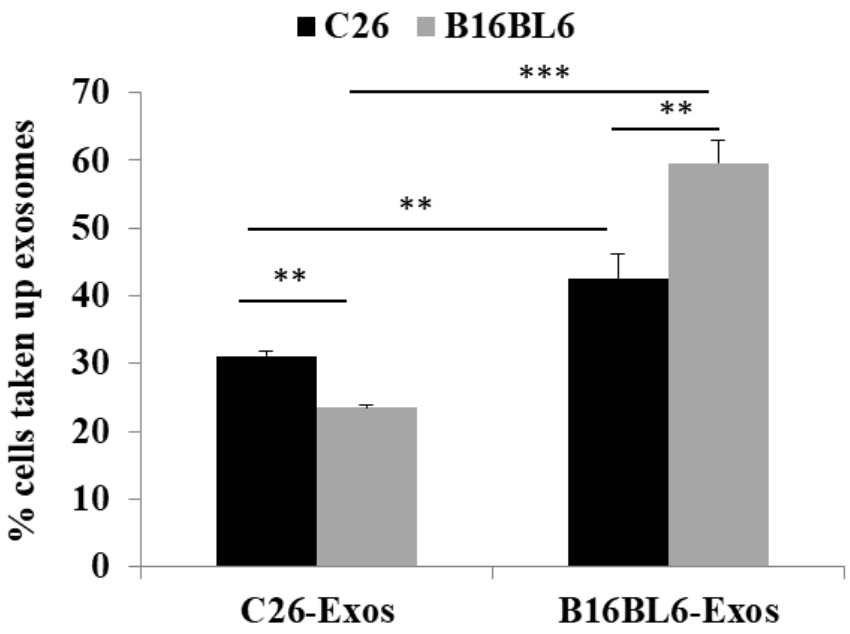

Figure 4.1. *In vitro* cross uptake of unmodified Exos

Two types of PKH67- labeled Exos, C26-Exos and B16BL6-Exos, were individually incubated with two cancer cell lines, C26 and B16BL6. After 4 h-incubation, cells were harvested and analyzed using a flow cytometer to evaluate Exo uptake %. All data represent the mean ± SD. An one way ANOVA test (Tukey's test) was applied. ** $p < 0.01$ and *** $p < 0.001$.

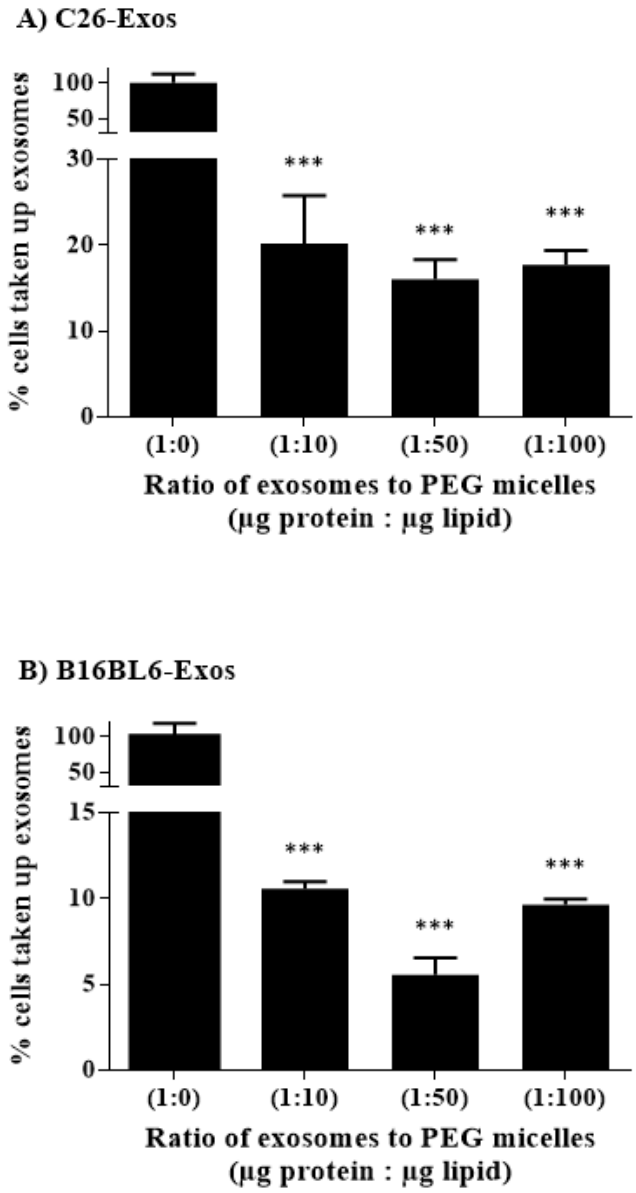

Figure 4.2. *In vitro* uptake of Exos before and after PEGylation

Two types of PKH67- labeled Exos, C26-Exos and B16BL6-Exos, were PEGylated using different PEG ratios and then incubated with autologous cells. After 4 h-incubation, cells were harvested and analyzed using a flow cytometer to evaluate Exo uptake %. All data represent the mean ± SD. An one way ANOVA test (Dunnett's test) was applied for each Exo type by comparing each PEG ratio with non-PEGylated treated group. *** $p < 0.001$.

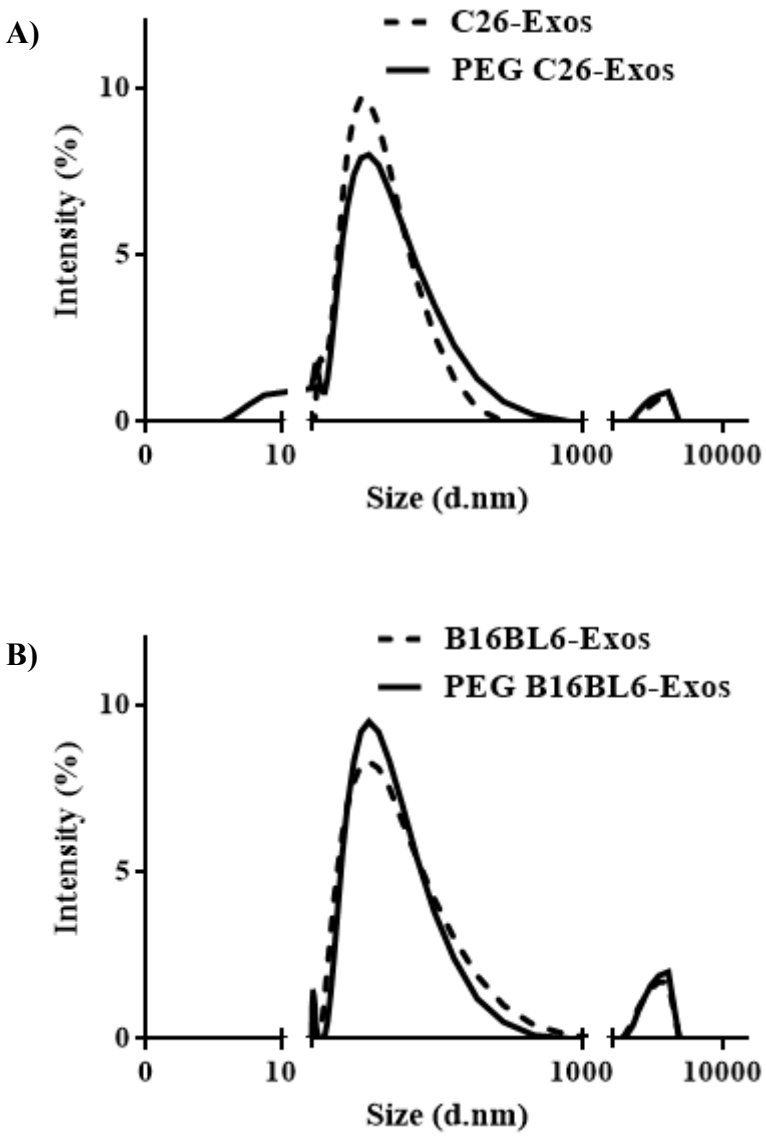

Figure 4.3. Size distribution of Exos versus PEGylated Exos

Two types of Exos, C26-Exos (A) and B16BL6-Exos (B), were PEGylated via incubating with PEG micelles in a ratio 1:50 (µg Exo protein : µg PEG lipid) and then particle size of either non-PEGylated or PEGylated Exos was evaluated using a zetasizer Nano ZS.

Figs. 4.4 and 4.5 demonstrated that both of non-PEGylated C26-Exos and B16BL6-Exos were rapidly cleared from blood circulation and did not show any detectable fluorescence in C26 tumor tissue. These results indicate that both unmodified autologous and allogeneic cancer cell-derived Exos can't target tumor tissue due to rapid clearance by MPS. On the other hand, PEGylated forms of both Exo types showed a remarkable fluorescence signal in C26 tumor tissue **(Figs. 4.4 and 4.5)**, indicating the accumulation of these types within C26 tumor tissue. The fluorescence signal of both of Exo types within C26 tumor tissue increased with time until reaching its peak at 48 h post-injection. The fluorescence of these accumulated Exos remained detectable at tumor site up to 7 days post-injection. Intriguingly, at all the predetermined time points, the fluorescence signal of PEGylated C26-Exos at C26 tumor site was more prominent than that of PEGylated B16BL6-Exos. These observations elucidate that PEGylation of cancer cell-derived Exos enhances their accumulation and retention within tumor tissue. This enhancing effect may be more predominant with PEGylated autologous Exos than PEGylated allogeneic Exos, probably due to the cell-type tropism.

4.3.4. Tumor accumulation and tumor cell uptake of PEGylated Exos

To further investigate the propensity of PEGylated Exos to accumulate within C26 tumor and their uptake by tumor cells, tumors from the treated mice were collected and further analyzed via *ex vivo* imaging and flow cytometry analysis. In this study, two different fluorescent dyes (DiR and DiI) were employed to label PEGylated Exos. For *ex vivo* imaging study, on Day 1, 2, 4 and 7 post-injection, the tumors were collected and monitored using IVIS to evaluate the accumulation of DiR-labeled Exos. For flow cytometry study, at 24 h post-injection, tumors were collected

and then tumor cells were harvested and examined using a flow cytometer to evaluate the uptake of DiI-labeled Exos.

The collected tumors did not show any detectable fluorescence in case of mice treated with PBS or non-PEGylated Exos, while show a detectable fluorescence in case of mice treated with PEGylated Exos **(Figs. 4.6A)**. Furthermore, the fluorescence signal with PEGylated C26-Exos was entirely higher than that with PEGylated B16BL6-Exos **(Figs. 4.6A and B)**. Regarding tumor cells, it was found that the Exo uptake by tumor cells was 1.54 ± 0.36 % and 0.02 ± 0.26 % with PEGylated C26-Exos and PEGylated B16BL6-Exos respectively **(Fig. 4.6C)**. These data are in consistence with the results of previous imaging experiment using the whole mice. This shows that Exo PEGylation may enhance their tumor accumulation and cell-type tropism may promote such enhancement. Combining these effects may address the poor tumor targetability of unmodified cancer cell-derived Exos. Accordingly, PEGylation as well as cell-type tropism may be considered promising targets in expanding the field of Exo-based drug delivery.

4.3.5. PEGylated Exos as a potential delivery system to tumor-associated immune populations

Cancer immunotherapy is considered one of the substantial strategies in cancer treatment via establishing an immunosurveillance effect in tumor microenvironment. To study whether PEGylated Exos could be adopted in cancer immunotherapy, the uptake of PEGylated Exos by certain tumor-infiltrating immune cells was evaluated. In this study, DiI-labeled PEGylated Exos were intravenously injected in the tail vein of C26 tumor-bearing mice. At 24 h post-injection, the tumors were collected and then tumor-associated cells were harvested and examined using a flow cytometer after

labeling with different fluorescently labeled antibodies for TAMs, T cells, DCs and B cells.

The uptake of PEGylated C26-Exos by TAMs, T cells, DCs and B cells were by 0.635, 0.258, 0.018 and 0.017 % of each population, respectively **(Fig. 4.7)**. While the uptake of PEGylated B16BL6-Exos by these immune cells were by 0.204, 0.105, 0.020 and 0.023 % of each population, respectively **(Fig. 4.7)**. These reveal that both types of PEGylated Exos can be taken up by these tumor-infiltrating immune cells. In addition, the uptake propensity of PEGylated C26-Exos by TAMs and T cells was higher than that of PEGylated B16BL6-Exos, while there was no significant difference in their uptake by DCs and B cells. Thus, PEGylation as well as cell-type tropism showed the ability to boost not only Exo uptake by tumor cells but also Exo uptake by tumor-associated immune cells. Accordingly, PEGylated Exos may be employed in cancer immunotherapy, especially TAMs and T cells which are promising targets immunotherapy **(Eyileten et al., 2016; Petty and Yang, 2017; Zanganeh et al., 2017)** because they are one of the most abundant tumor-infiltrating immune cells.

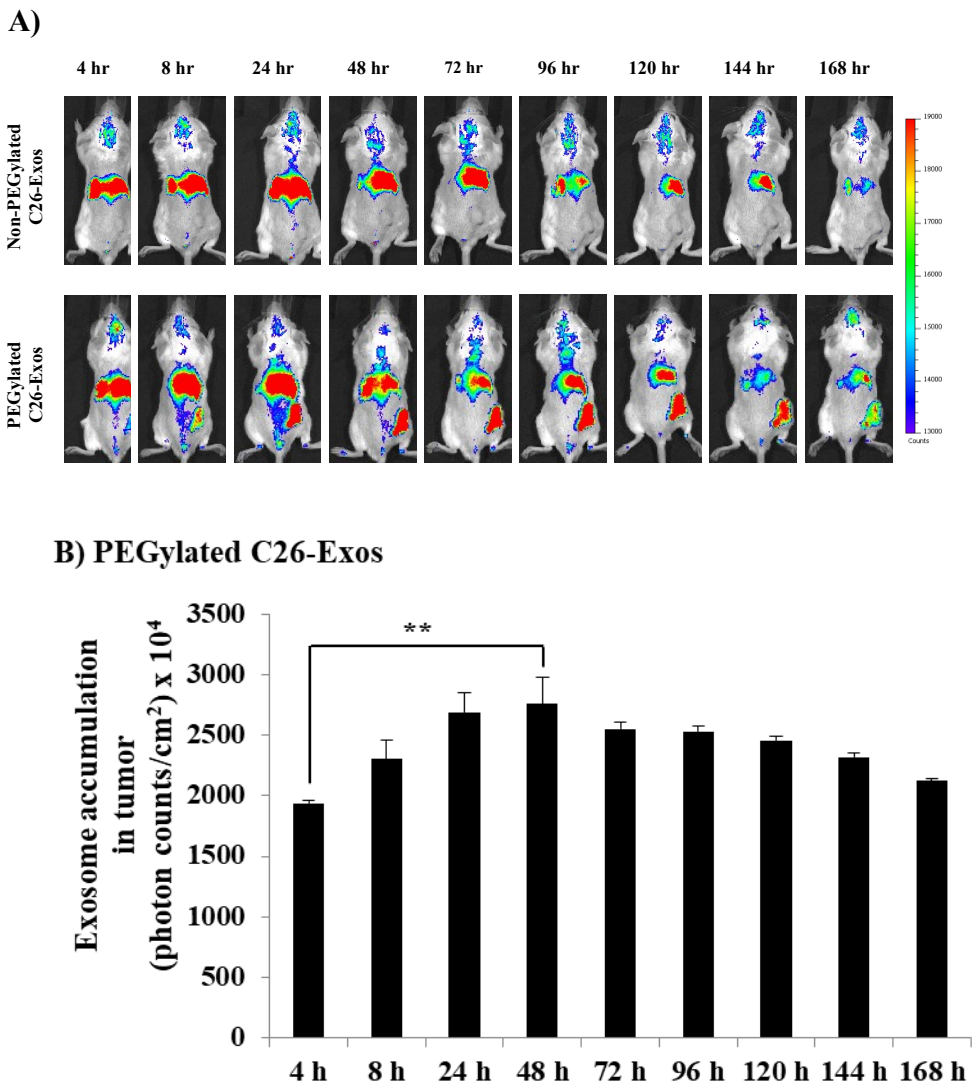

Figure 4.4. Biodistribution of C26-Exos before and after PEGylation in C26-tumor bearing mice

Two types of DiR- labeled Exos, C26-Exos, PEGylated C26-Exos), were intravenously injected into the tail vein of C26 tumor-bearing BALB/c mice. At the predetermined time points post-injection, the mice were anesthetized and monitored using IVIS to evaluate the biodistribution of Exos. All data (B, D and E) represent the mean ± SEM. An one way ANOVA test (Tukey's test) was applied. ** $p < 0.01$.

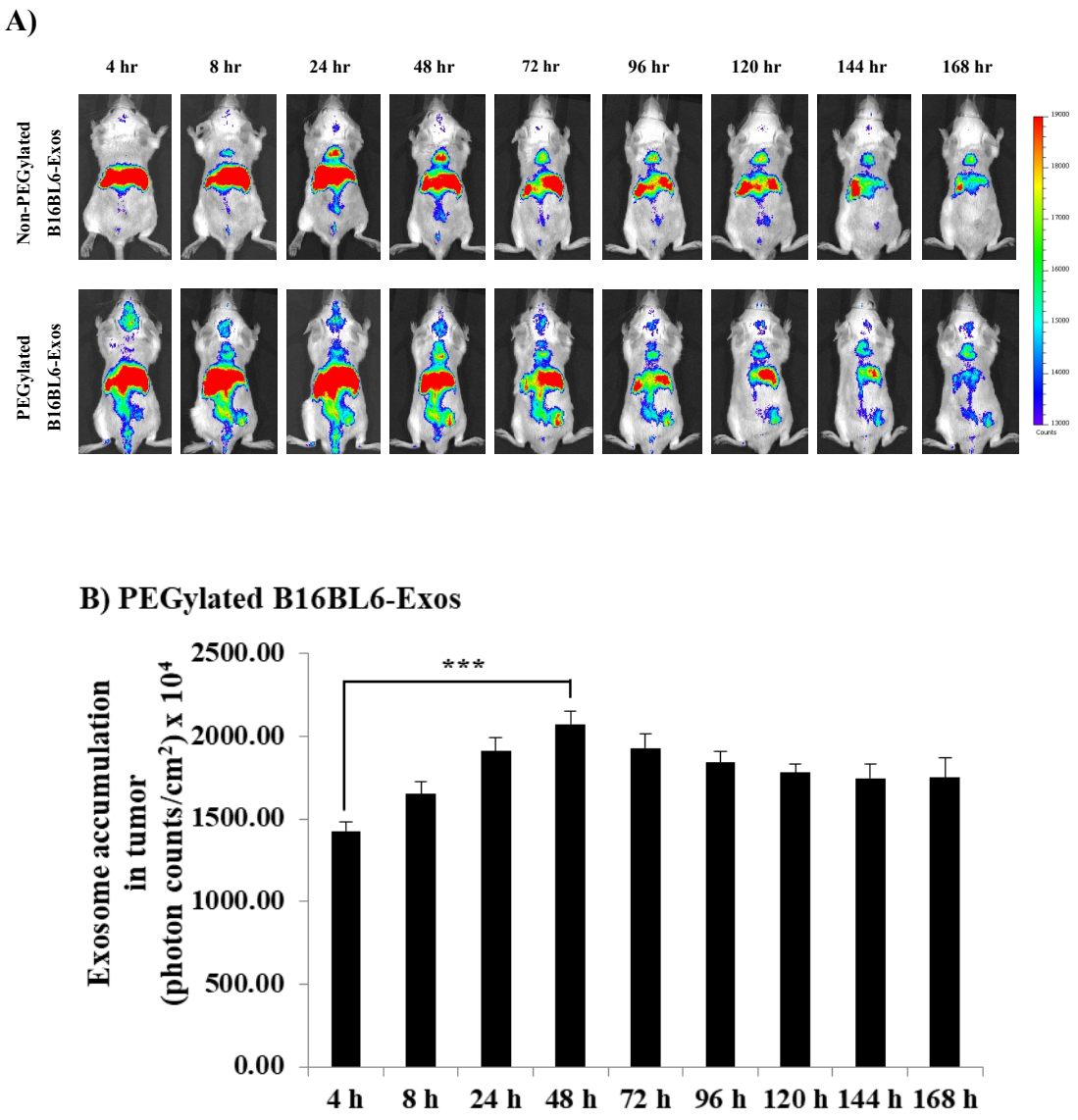

Figure 4.5. Biodistribution of B16BL6-Exos before and after PEGylation in C26-tumor bearing mice

Two types of DiR- labeled Exos, B16BL6-Exos and PEGylated B16BL6-Exos, were intravenously injected into the tail vein of C26 tumor-bearing BALB/c mice. At the predetermined time points post-injection, the mice were anesthetized and monitored using IVIS to evaluate the biodistribution of Exos. All data (B, D and E) represent the mean ± SEM. An one way ANOVA test (Tukey's test) was applied. *** $p < 0.001$.

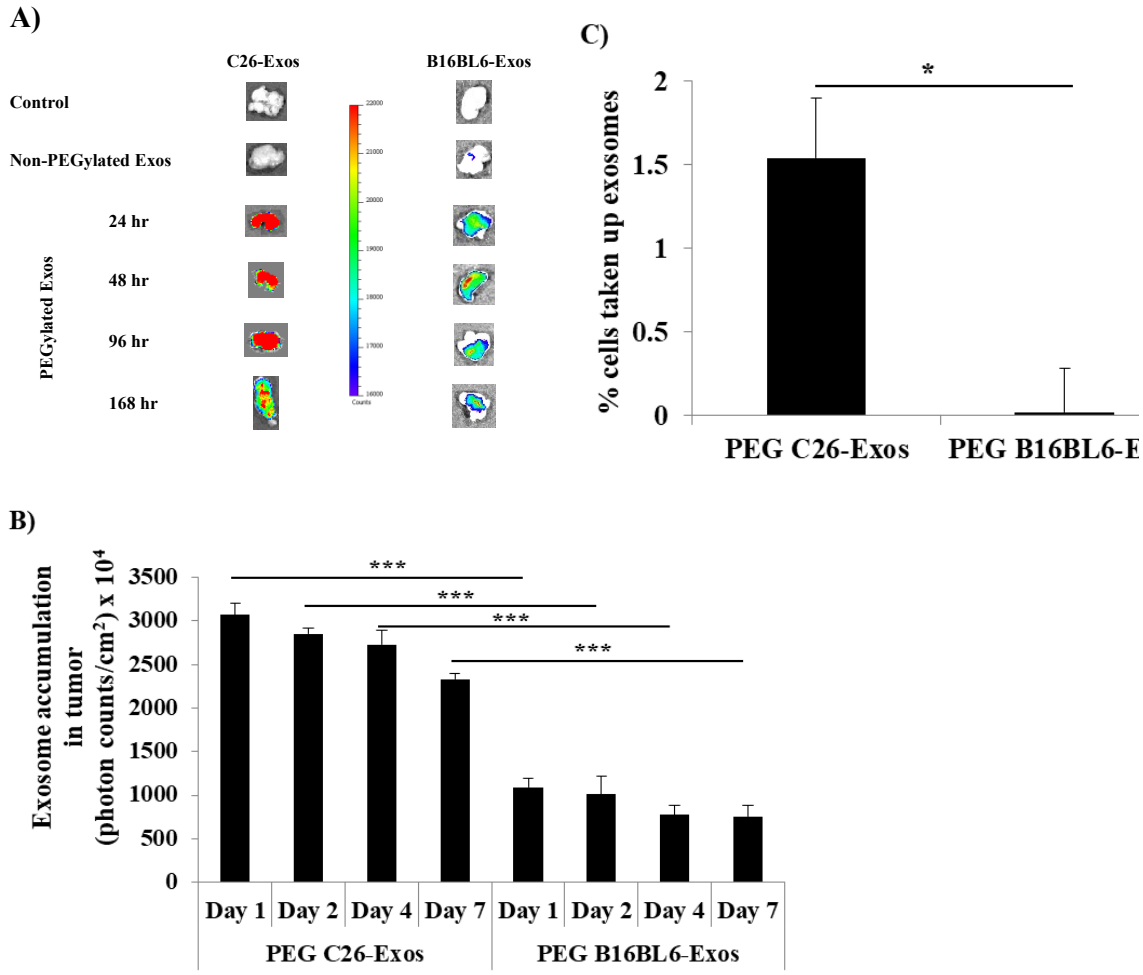

Figure 4.6. Tumor accumulation of PEGylated Exos.

Two types of labeled Exos, PEGylated C26-Exos and PEGylated B16BL6-Exos, were intravenously injected into the tail vein of C26 tumor-bearing BALB/c mice. Then, the mice were sacrificed and then tumors were collected at the predetermined time points post-injection. Two fluorescent dyes were employed, DiR for *ex vivo* imaging (A and B) and DiI for flow cytometry (C). For the former, the collected tumors were monitored using IVIS to evaluate the accumulation of DiR-labeled Exos. For the latter, tumor cells were harvested from the collected tumors and analyzed using a flow cytometer to evaluate the uptake of DiI-labeled Exos by tumor cells. All data (B and C) represent the mean ± SEM. An one way ANOVA test (Tukey's test) was applied to compare between the two Exo types at each time point (B). An unpaired t test was applied for C. * $p < 0.05$ and *** $p < 0.001$.

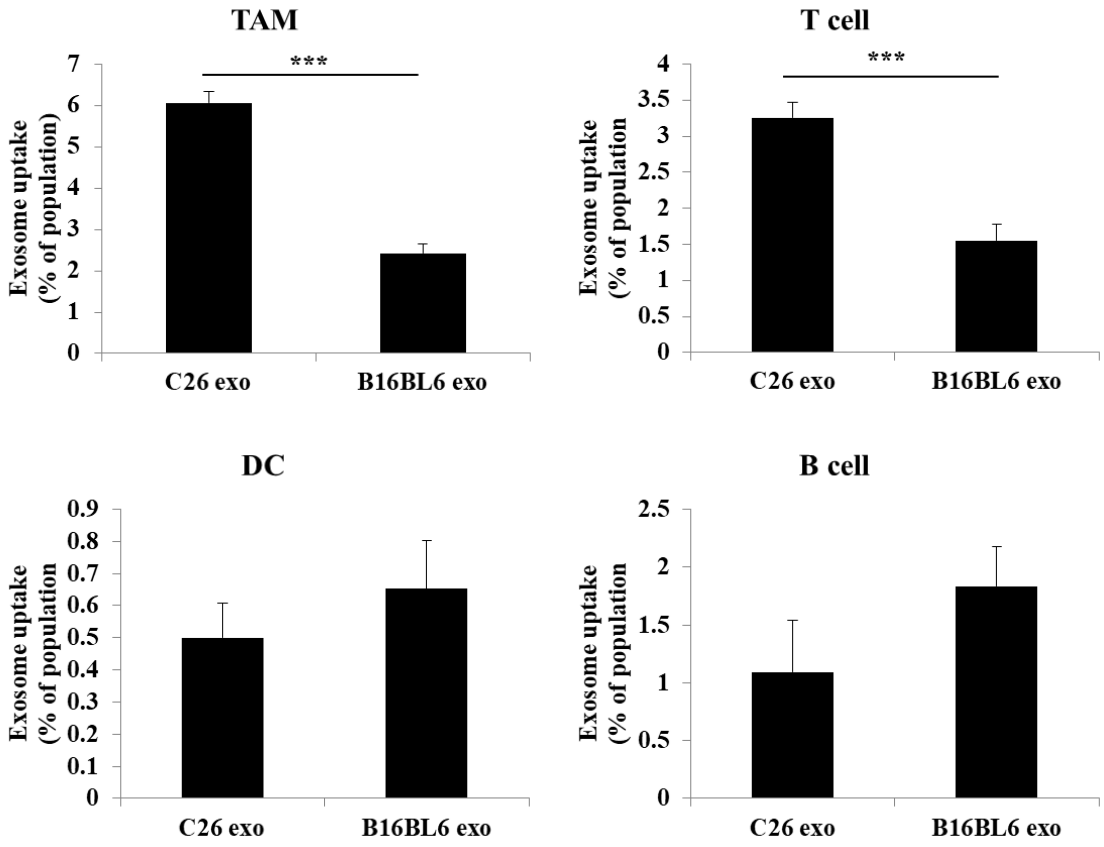

Figure 4.7. PEGylated Exo delivery to certain tumor-associated immune populations

Two types of DiI-labeled Exos, PEGylated C26-Exos and PEGylated B16BL6-Exos, were intravenously injected into the tail vein of C26 tumor-bearing BALB/c mice. At 24 h post-injection, tumors were collected and tumor-associated cells were harvested. Then, certain tumor-infiltrating immune populations were analyzed using a flow cytometer via labeling with different fluorescently labeled antibodies to TAMs, T cells, DCs and B cells to evaluate Exo uptake by each population. All data represent the mean ± SEM. An unpaired t test was applied for each immune cell population. *** $p < 0.001$.

4.4. Discussion

The emerging field of Exo-based drug delivery to cancer has been widely studied aiming to improve the limited Exo (EV) delivery to tumor. To overcome the unexpected poor tumor targeting of unmodified Exos (EVs), various strategies have been conducted via Exo engineering **(Vader et al., 2016; Barile and Vassalli, 2017)**. In this chapter, I introduced a simpler paradigm of a successful passive tumor-targeting tool using PEGylated Exos. I hypothesized that combining PEGylation and cell-type tropism effects overcome the problem of poor tumor targeting. *In vitro* study indicated the possibility of a preferential Exo uptake to autologous cancer cells, compared to allogeneic cancer cells **(Fig. 4.1)**. In addition, it was demonstrated the feasibility of Exo PEGylation using the selected ratios of PEG micelles to add **(Fig. 4.2)**. While, the animal study revealed that PEGylation improved Exo accumulation into C26 tumor **(Figs. 4.4, 4.5 and 4.6)**. Furthermore, PEGylated autologous cancer cell-derived Exos have interestingly shown a preferential accumulation into C26 tumor **(Figs. 4.4, 4.5, 4.6 and 4.7)** and consequently might be exploited in different strategies of C26 cancer treatment such as chemotherapy, gene therapy and immunotherapy. Accordingly, the synergism of PEGylation and cell-type tropism may be a potential solution for the poor tumor targeting of Exos.

Exo-based drug delivery has been emerged as a potential approach for cancer therapy. This potential implementation is substantially motivated by the inherent ability of Exos (EVs) in mediating cell – cell communication and transferring their cargo to recipient cells **(Colombo et al., 2014; Lo Cicero et al., 2015)**. Accordingly, understanding Exo (EV) uptake process is of utmost importance to expand this emerging field. In the chapter III, it was revealed that the *in vitro* uptake of cancer-derived Exos is mediated by exosomal surface proteins and different uptake

mechanisms, which their contribution in uptake process is remarkablely influenced by the type of recipient cell. Along with my previous observations, it was shown that Exo (EV) uptake is a controversial, complicated and ambiguous process which occurs via various pathways and is controlled by many factors such as surface proteins, membrane lipid or other components of both Exos (EVs) and recipient cells **(Mulcahy et al., 2014; Hoshino et al., 2015)**. Consequently, the complications and lack of consensus regarding Exo (EV) uptake process will hinder the implementations of Exo-based drug delivery. To address this problem, cell-type tropism has been investigated as an important factor to boost Exo (EV) internalization by their parental cancer cells. Presumably, cell-type tropism can ensure the matching between Exos (EVs) and target cells facilitating the uptake process. In this chapter, it is noticed that each type of cancer cell probably have avidity for their autologous Exos **(Fig. 4.1)**. This is inconsistence with others' observations which show that cell-type tropism confers the preponderance of cancer cell-derived Exo (EV) uptake by their parental cancer cells *in vitro*. Saari et al. indicated that prostate cancer cell-derived EVs could effectively deliver paclitaxel to their parental cells **(Saari et al., 2015)**. Toda et al. illustrated that glioblastoma cell-derived Exos could preferentially target cancer cells especially their parent cells **(Toda et al., 2015)**. Taken together, cell-type tropism is substantial to foster Exo (EV) uptake by cancer cell *in vitro*.

The enhancing effect of cell-type tropism on Exo uptake by cancer cells *in vitro* motivated thinking how this could affect Exo delivery to tumor *in vivo*. Unfortunately, achieving that target was restricted by the MPS which has been known to rapidly clear nanoparticles from blood circulation. Similarly, MPS has been responsible for the clearance of unmodified Exos (EVs), preventing them from reaching the tumor site. PEGylation has been known to inhibit the binding of plasma

proteins to nanoparticle surface, consequently reduce nanoparticle clearance by MPS and increase nanoparticle circulation time **(Allen et al., 1991; Jokerst et al., 2011; Suk et al., 2016)**. Accordingly, PEGylation of Exos was conducted **(Fig. 4.2)** to extend the circulation time of Exos and allow them to extravasate though the leaky vasculature of tumor and passively accumulate in tumor tissue via the EPR effect. The current study showed that the long-circulating (PEGylated) autologous and allogeneic cancer cell-derived Exos accumulate in C26 tumor tissue with an extended retention time inside tumor tissue **(Figs. 4.4, 4.5 and 4.6)**. In addition, the results illustrate that cell-type tropism may help PEGylated Exos to accumulate into C26 tumor tissue **(Figs. 4.4, 4.5 and 4.6)**. The effect of cell-type tropism may be responsible for the detected improvement in tumor targeting in this study, compared with others' investigations. Kooijmans et al. revealed that PEGylation of mouse neuroblastoma cell-derived EVs results in a remarkable increase in their circulation time, but this does not result in a significant increase in their accumulation in human epidermoid carcinoma xenograft **(S. A. A. Kooijmans et al., 2016)**. While Tian et al. stated that immature dendritic cell-derived iRGD-Exos succeed in targeting the tumor tissue in mice model of human breast cancer, but with a short retention time within tumor (about 8 h) **(Y. Tian et al., 2014b)**. The former study used mouse cancer cell-derived EVs with human cancer model. While, the latter study employed non cancer cell-derived Exos (engineered with a targeting ligand, iRGD) to target human cancer model. Thus, the detected poor tumor accumulation of Exos (EVs) and their short retention time within tumor might be related to the missed enhancing effect of cell-type tropism in these studies. Furthermore, it is noteworthy that the preferential tumor accumulation of PEGylated autologous cancer cell-derived Exos may be related to the potential Exo uptake by C26 tumor cells and certain C26 tumor-infiltrating immune

cells especially TAMs and T cells within C26 tumor tissue **(Fig. 4.7)**. On the basis of these results, the synergistic effect of cell-type tropism with PEGylation becomes indispensable for an effective Exo delivery to tumor in this study.

The outcomes of this thesis could be summarized as following:

- *In vitro* incubation with liposomes enhanced/suppressed Exo secretion derived from cancer cells. The stimulatory/inhibitory effect of liposomes was dependent on their dose, surface charge, membrane fluidity, and PEG modification, as well as on the type and viability of treated cancer cells. My approach may be a new strategy to stimulate/inhibit the secretion of Exos if the physicochemical properties of liposomes can be correctly controlled.
- Different liposome preparations induced Exos with different protein expressions which relate different uptake pathways probably via different exosomal marker proteins. Liposomes may become one of promising tools to fine-tune the Exos, which achieve targeting of Exos *in vitro* and *in vivo*.
- PEGylation of cancer cell-derived Exos extended their circulation time and cell-type tropism fosters the accumulation and retention of these long-circulating Exos within allogeneic tumor tissue.
- PEGylated autologous cancer cell-derived Exos had the predominant ability to target not only tumor cells but also tumor-associated immune cells within allogeneic tumor tissue. This targeting capability can be effectively exploited for drug delivery to allogeneic tumor and hopefully, this paradigm can be implemented with other cancers.

Accordingly, in this thesis, I could expand Exo yield, identify the role of certain Exo surface proteins in Exo uptake and enhance the tumor accumulation of Exos. These are considered potential solutions of some hurdles of Exo field and may push forward the different Exo implementations.

Liposomes have been widely used as carriers for chemotherapeutic agents and nucleic acids **(Huang, 2008; Zhang et al., 2012; Torchilin, 2014)**. Doxil®, doxorubicin-containing PEGylated liposome, has been approved for clinical use **(Chang and Yeh, 2012)**. Recently, many studies have indicated that Exos have specialized functions and play a key role in processes such as intercellular signaling and waste management **(Théry et al., 2002)**. Consequently, there is growing interest in the clinical applications of Exos. In the chapter II, it was shown that liposomes have the ability to upregulate and/or downregulate Exo secretion in response to the surface modification of liposomes. After intravenous injection of long-circulating PEGylated liposomes, the liposomes reach solid tumors via the EPR effect **(Park, 2002)** and might stimulate the tumor cells, resulting in a decrease in tumor-related Exo secretion *in vivo*. Exos are known to partially contribute to tumor metastasis **(Théry et al., 2002; Hedlund et al., 2011)**. Therefore, chemotherapeutic agents containing PEGylated liposomes may provide a synergistic effect to tumor growth suppression as well as to the prevention of tumor metastasis.

Furthermore, Exos gain the attention of many researchers to be employed in various applications especially drug delivery **(Alvarez-Erviti et al., 2011; Zhuang et al., 2011; Ohno et al., 2013; Y. Tian et al., 2014b; Batrakova and Kim, 2015; Haney et al., 2015)**. However, such applications are restricted by the low Exo yield and Exo heterogeneity leading low targetability. In the chapter II, I introduced the incubation with liposome preparations increases the release of Exos from the donor cancer cells. In the chapter III, I realized that incubating the donor cancer cells with liposome preparations has an ability to change the protein contents in the induced Exos, which leads a possibility to tune-up the Exos if I could understand how the liposomes affect the donor cells. Accordingly, my strategy, to employ the liposome

preparations as a stimulator for Exo production, may be useful for engineering Exos to implement specific targeting and treat several diseases, although further detailed studies must be required to achieve this goal.

In addition, one of the substantial applications of Exo-based drug delivery is to employ Exos (EVs) in cancer therapy. Unfortunately, the achieved success in this area is limited as well as several hurdles still restrict expanding this field such as the poor pharmacokinetics and tumor-targeted delivery of Exos. In the chapter IV, I succeeded in improving Exo (EV) delivery to C26 tumor tissue (including C26 tumor cells and C26 tumor-associated immune cells) via the synergism between PEGylation and cell-type tropism effects. Besides that, PEG layer of PEGylated Exos (EVs) can be further decorated with targeting ligands via post-insertion technique for more specific applications **(Ishida et al., 1999; Allen et al., 2002; Moreira et al., 2002)**. Together with the ability of Exos (EVs) in delivering several therapeutics agents such as chemotherapeutics, therapeutic proteins, genetic materials and siRNA **(Johnsen et al., 2014; Inamdar et al., 2017)**, PEGylated autologous cancer cell-derived Exos (EVs) can be employed in various therapeutic approaches of cancer such as chemotherapy, gene therapy, immunotherapy and cancer vaccination.

Furthermore, other strategies have been conducted to overcome the unexpected poor tumor targeting of unmodified Exos (EVs) such as modifying Exo (EV) surface characteristics via targeting ligands **(Ohno et al., 2013; Y. Tian et al., 2014b; S. A. A. Kooijmans et al., 2016; Y. Wang et al., 2017)** and the use of certain route of administration (intratumoral and intranasal) **(T. Smyth et al., 2015; Kim et al., 2016)**. Despite of these dedicated efforts, many limitations still exist such as the non-significant improvement in tumor targeting **(S. A. A. Kooijmans et al., 2016)**, the improper expression as well as the instability of targeting ligands **(Hung and**

Leonard, 2015), the short retention time of Exos (EVs) within the tumor tissue **(Y. Tian et al., 2014b)** and finally the limited target tissue due to the limited route of administration.

Finding the appropriate isolation method that ensures the collection of high quantity of the secreted Exos of a high purity level is an urgent and challenging issue. Accordingly, efforts have been devoted to achieve these criteria. Several Exo isolation methods of varying yields and purities of Exo samples have been developed to collect Exos form either cell culture medium or biological, such as ultracentrifugation, density gradient centrifugation, synthetic polymer precipitation, immuno-isolation (immunoaffinity capture), ultrafiltration, size-exclusion chromatography and microfluidic devices **(Théry et al., 2006; Stremersch et al., 2016; Sunkara et al., 2016; Whiteside, 2016; Xu et al., 2016; Contreras-Naranjo et al., 2017; Coumans et al., 2017; P. Li et al., 2017; Lu et al., 2017)**, however, none of them have shown the enough credentials for clinical applications and large scale production.

Despite of my and other efforts to reveal the underlying mechanisms of Exo uptake and the role of their surface ligands in this process, there is no consensus on what are the determinants for Exo uptake. Exo mimetics are one of the promising implementations to mirror the privileged characteristics of Exos via designing nanocarriers having the same composition of Exos, however, the outcomes are still limited probably due to the complexity of Exo composition and missing the full definition of the potential Exo components required to mimic Exo characteristics **(S. A. Kooijmans et al., 2012)**. Accordingly, unraveling the complete set of Exo surface proteins and lipids are required to drive Exo uptake, is of utmost importance to design an efficient drug delivery systems using Exos or even artificial Exo-mimic nanocarriers.

Finally, the implementations of Exo-based drug delivery are still in the beginning and unraveling the black box of Exo release, composition and uptake will tremendously expand their use not only in drug delivery but also in various therapeutic and diagnostic purposes. More is still expected from these tiny vesicles.

Allen, T. M., Hansen, C., Martin, F., Redemann, C., and Yau-Young, A. (1991). Liposomes containing synthetic lipid derivatives of poly(ethylene glycol) show prolonged circulation half-lives in vivo. *Biochim Biophys Acta, 1066*(1), 29-36.

Allen, T. M., Sapra, P., and Moase, E. (2002). Use of the post-insertion method for the formation of ligand-coupled liposomes. *Cell Mol Biol Lett, 7*(3), 889-894.

Alvarez-Erviti, L., Seow, Y., Yin, H., Betts, C., Lakhal, S., and Wood, M. J. (2011). Delivery of siRNA to the mouse brain by systemic injection of targeted exosomes. *Nat Biotechnol, 29*(4), 341-345. doi: 10.1038/nbt.1807

Andre, F., Chaput, N., Schartz, N. E., Flament, C., Aubert, N., Bernard, J., Lemonnier, F., Raposo, G., Escudier, B., Hsu, D. H., Tursz, T., Amigorena, S., Angevin, E., and Zitvogel, L. (2004). Exosomes as potent cell-free peptide-based vaccine. I. Dendritic cell-derived exosomes transfer functional MHC class I/peptide complexes to dendritic cells. *J Immunol, 172*(4), 2126-2136.

Armstrong, J. P., Holme, M. N., and Stevens, M. M. (2017). Re-Engineering Extracellular Vesicles as Smart Nanoscale Therapeutics. *ACS Nano, 11*(1), 69-83. doi: 10.1021/acsnano.6b07607

Atienzar-Aroca, S., Flores-Bellver, M., Serrano-Heras, G., Martinez-Gil, N., Barcia, J. M., Aparicio, S., Perez-Cremades, D., Garcia-Verdugo, J. M., Diaz-Llopis, M., Romero, F. J., and Sancho-Pelluz, J. (2016). Oxidative stress in retinal pigment epithelium cells increases exosome secretion and promotes angiogenesis in endothelial cells. *J Cell Mol Med, 20*(8), 1457-1466. doi: 10.1111/jcmm.12834

Auriac, A., Willemetz, A., and Canonne-Hergaux, F. (2010). Lipid raft-dependent endocytosis: a new route for hepcidin-mediated regulation of ferroportin in macrophages. *Haematologica, 95*(8), 1269-1277. doi: 10.3324/haematol.2009.019992

Banning, A., Kurrle, N., Meister, M., and Tikkanen, R. (2014). Flotillins in receptor tyrosine kinase signaling and cancer. *Cells, 3*(1), 129-149. doi: 10.3390/cells3010129

Barile, L., and Vassalli, G. (2017). Exosomes: Therapy delivery tools and biomarkers of diseases. *Pharmacol Ther, 174*, 63-78. doi: 10.1016/j.pharmthera.2017.02.020

Bartlett, G. R. (1959). Colorimetric assay methods for free and phosphorylated glyceric acids. *J Biol Chem, 234*(3), 469-471.

Batrakova, E. V., and Kim, M. S. (2015). Using exosomes, naturally-equipped nanocarriers, for drug delivery. *J Control Release, 219*, 396-405. doi: 10.1016/j.jconrel.2015.07.030

Batrakova, E. V., and Kim, M. S. (2016). Development and regulation of exosome-based therapy products. *Wiley Interdiscip Rev Nanomed Nanobiotechnol, 8*(5), 744-757. doi: 10.1002/wnan.1395

Bell, B. M., Kirk, I. D., Hiltbrunner, S., Gabrielsson, S., and Bultema, J. J. (2016). Designer exosomes as next-generation cancer immunotherapy. *Nanomedicine, 12*(1), 163-169. doi: 10.1016/j.nano.2015.09.011

Carpentier, J. L., Sawano, F., Geiger, D., Gorden, P., Perrelet, A., and Orci, L. (1989). Potassium depletion and hypertonic medium reduce "non-coated" and clathrin-coated pit formation, as well as endocytosis through these two gates. *J Cell Physiol, 138*(3), 519-526. doi: 10.1002/jcp.1041380311

Carrière, J., Barnich, N., and Nguyen, H. T. (2016). Exosomes: From Functions in Host-Pathogen Interactions and Immunity to Diagnostic and Therapeutic Opportunities. *Rev Physiol Biochem Pharmacol, 172*, 39-75. doi: 10.1007/112_2016_7

Chang, H. I., and Yeh, M. K. (2012). Clinical development of liposome-based drugs: formulation, characterization, and therapeutic efficacy. *Int J Nanomedicine, 7*, 49-60. doi: 10.2147/IJN.S26766

Chaput, N., Schartz, N. E., Andre, F., Taieb, J., Novault, S., Bonnaventure, P., Aubert, N., Bernard, J., Lemonnier, F., Merad, M., Adema, G., Adams, M., Ferrantini, M., Carpentier, A. F., Escudier, B., Tursz, T., Angevin, E., and Zitvogel, L. (2004).

Exosomes as potent cell-free peptide-based vaccine. II. Exosomes in CpG adjuvants efficiently prime naive Tc1 lymphocytes leading to tumor rejection. *J Immunol, 172*(4), 2137-2146.

Chaput, N., Taieb, J., Andre, F., and Zitvogel, L. (2005). The potential of exosomes in immunotherapy. *Expert Opin Biol Ther, 5*(6), 737-747. doi: 10.1517/14712598.5.6.737

Chou, T. H., Liang, C. H., Lee, Y. C., and Yeh, L. H. (2014). Effects of lipid composition on physicochemical characteristics and cytotoxicity of vesicles composed of cationic and anionic dialkyl lipids. *Phys Chem Chem Phys, 16*(4), 1545-1553. doi: 10.1039/c3cp54176b

Christianson, H. C., Svensson, K. J., van Kuppevelt, T. H., Li, J. P., and Belting, M. (2013). Cancer cell exosomes depend on cell-surface heparan sulfate proteoglycans for their internalization and functional activity. *Proc Natl Acad Sci U S A, 110*(43), 17380-17385. doi: 10.1073/pnas.1304266110

Colombo, M., Raposo, G., and Théry, C. (2014). Biogenesis, Secretion, and Intercellular Interactions of Exosomes and Other Extracellular Vesicles. *Annu Rev Cell Dev Biol, 30*(1), 255-289. doi: 10.1146/annurev-cellbio-101512-122326

Conner, S. D., and Schmid, S. L. (2003). Regulated portals of entry into the cell. *Nature, 422*(6927), 37-44. doi: 10.1038/nature01451

Contreras-Naranjo, J. C., Wu, H. J., and Ugaz, V. M. (2017). Microfluidics for exosome isolation and analysis: enabling liquid biopsy for personalized medicine. *Lab Chip, 17*(21), 3558-3577. doi: 10.1039/c7lc00592j

Cooper, J. A. (1987). Effects of cytochalasin and phalloidin on actin. *J Cell Biol, 105*(4), 1473-1478.

Coumans, F. A. W., Brisson, A. R., Buzas, E. I., Dignat-George, F., Drees, E. E. E., El-Andaloussi, S., Emanueli, C., Gasecka, A., Hendrix, A., Hill, A. F., Lacroix, R., Lee, Y., van Leeuwen, T. G., Mackman, N., Mager, I., Nolan, J. P., van der Pol, E., Pegtel, D. M., Sahoo, S., Siljander, P. R. M., Sturk, G., de Wever, O., and Nieuwland, R. (2017). Methodological Guidelines to Study Extracellular Vesicles. *Circ Res, 120*(10), 1632-1648. doi: 10.1161/CIRCRESAHA.117.309417

Cui, Z., Han, S. J., Vangasseri, D. P., and Huang, L. (2005). Immunostimulation mechanism of LPD nanoparticle as a vaccine carrier. *Mol Pharm, 2*(1), 22-28. doi: 10.1021/mp049907k

Doeppner, T. R., Bahr, M., Hermann, D. M., and Giebel, B. (2017). Concise Review: Extracellular Vesicles Overcoming Limitations of Cell Therapies in Ischemic Stroke. *Stem Cells Transl Med, 6*(11), 2044-2052. doi: 10.1002/sctm.17-0081

Doherty, G. J., and McMahon, H. T. (2009). Mechanisms of endocytosis. *Annu Rev Biochem, 78*, 857-902. doi: 10.1146/annurev.biochem.78.081307.110540

Dutta, D., and Donaldson, J. G. (2012). Search for inhibitors of endocytosis: Intended specificity and unintended consequences. *Cell Logist, 2*(4), 203-208. doi: 10.4161/cl.23967

Ekstrom, K., Valadi, H., Sjostrand, M., Malmhall, C., Bossios, A., Eldh, M., and Lotvall, J. (2012). Characterization of mRNA and microRNA in human mast cell-derived exosomes and their transfer to other mast cells and blood CD34 progenitor cells. *J Extracell Vesicles, 1*. doi: 10.3402/jev.v1i0.18389

El Andaloussi, S., Mäger, I., Breakefield, X. O., and Wood, M. J. A. (2013). Extracellular vesicles: biology and emerging therapeutic opportunities. *Nature Reviews Drug Discovery, 12*, 347. doi: 10.1038/nrd3978

Elsabahy, M., and Wooley, K. L. (2013). Cytokines as biomarkers of nanoparticle immunotoxicity. *Chem Soc Rev, 42*(12), 5552-5576. doi: 10.1039/c3cs60064e

Escrevente, C., Keller, S., Altevogt, P., and Costa, J. (2011). Interaction and uptake of exosomes by ovarian cancer cells. *BMC Cancer, 11*, 108. doi: 10.1186/1471-2407-11-108

Eyileten, C., Majchrzak, K., Pilch, Z., Tonecka, K., Mucha, J., Taciak, B., Ulewicz, K., Witt, K., Boffi, A., Krol, M., and Rygiel, T. P. (2016). Immune Cells in Cancer Therapy and Drug Delivery. *Mediators Inflamm, 2016*, 5230219. doi: 10.1155/2016/5230219

Feng, D., Zhao, W. L., Ye, Y. Y., Bai, X. C., Liu, R. Q., Chang, L. F., Zhou, Q., and Sui, S. F. (2010). Cellular internalization of exosomes occurs through phagocytosis. *Traffic, 11*(5), 675-687. doi: 10.1111/j.1600-0854.2010.01041.x

Fitzner, D., Schnaars, M., van Rossum, D., Krishnamoorthy, G., Dibaj, P., Bakhti, M., Regen, T., Hanisch, U. K., and Simons, M. (2011). Selective transfer of exosomes from oligodendrocytes to microglia by macropinocytosis. *J Cell Sci, 124*(Pt 3), 447-458. doi: 10.1242/jcs.074088

French, K. C., Antonyak, M. A., and Cerione, R. A. (2017). Extracellular vesicle docking at the cellular port: Extracellular vesicle binding and uptake. *Semin Cell Dev Biol, 67*, 48-55. doi: 10.1016/j.semcdb.2017.01.002

Fruhbeis, C., Frohlich, D., Kuo, W. P., Amphornrat, J., Thilemann, S., Saab, A. S., Kirchhoff, F., Mobius, W., Goebbels, S., Nave, K. A., Schneider, A., Simons, M., Klugmann, M., Trotter, J., and Kramer-Albers, E. M. (2013). Neurotransmitter-triggered transfer of exosomes mediates oligodendrocyte-neuron communication. *PLoS Biol, 11*(7), e1001604. doi: 10.1371/journal.pbio.1001604

Fujimoto, L. M., Roth, R., Heuser, J. E., and Schmid, S. L. (2000). Actin assembly plays a variable, but not obligatory role in receptor-mediated endocytosis in mammalian cells. *Traffic, 1*(2), 161-171.

Gilligan, K. E., and Dwyer, R. M. (2017). Engineering Exosomes for Cancer Therapy. *Int J Mol Sci, 18*(6). doi: 10.3390/ijms18061122

Glebov, O. O., Bright, N. A., and Nichols, B. J. (2006). Flotillin-1 defines a clathrin-independent endocytic pathway in mammalian cells. *Nat Cell Biol, 8*(1), 46-54. doi: 10.1038/ncb1342

Haney, M. J., Klyachko, N. L., Zhao, Y., Gupta, R., Plotnikova, E. G., He, Z., Patel, T., Piroyan, A., Sokolsky, M., Kabanov, A. V., and Batrakova, E. V. (2015). Exosomes as drug delivery vehicles for Parkinson's disease therapy. *J Control Release, 207*, 18-30. doi: 10.1016/j.jconrel.2015.03.033

Hannafon, B. N., and Ding, W. Q. (2013). Intercellular communication by exosome-derived microRNAs in cancer. *Int J Mol Sci, 14*(7), 14240-14269. doi: 10.3390/ijms140714240

Hedlund, M., Nagaeva, O., Kargl, D., Baranov, V., and Mincheva-Nilsson, L. (2011). Thermal- and oxidative stress causes enhanced release of NKG2D ligand-bearing immunosuppressive exosomes in leukemia/lymphoma T and B cells. *PLoS One, 6*(2), e16899. doi: 10.1371/journal.pone.0016899

Holder, B., Jones, T., Sancho Shimizu, V., Rice, T. F., Donaldson, B., Bouqueau, M., Forbes, K., and Kampmann, B. (2016). Macrophage Exosomes Induce Placental Inflammatory Cytokines: A Novel Mode of Maternal-Placental Messaging. *Traffic, 17*(2), 168-178. doi: 10.1111/tra.12352

Hoshino, A., Costa-Silva, B., Shen, T. L., Rodrigues, G., Hashimoto, A., Tesic Mark, M., Molina, H., Kohsaka, S., Di Giannatale, A., Ceder, S., Singh, S., Williams, C., Soplop, N., Uryu, K., Pharmer, L., King, T., Bojmar, L., Davies, A. E., Ararso, Y., Zhang, T., Zhang, H., Hernandez, J., Weiss, J. M., Dumont-Cole, V. D., Kramer, K., Wexler, L. H., Narendran, A., Schwartz, G. K., Healey, J. H., Sandstrom, P., Labori, K. J., Kure, E. H., Grandgenett, P. M., Hollingsworth, M. A., de Sousa, M., Kaur, S., Jain, M., Mallya, K., Batra, S. K., Jarnagin, W. R., Brady, M. S., Fodstad, O., Muller, V., Pantel, K., Minn, A. J., Bissell, M. J., Garcia, B. A., Kang, Y., Rajasekhar, V. K., Ghajar, C. M., Matei, I., Peinado, H.,

Bromberg, J., and Lyden, D. (2015). Tumour exosome integrins determine organotropic metastasis. *Nature, 527*(7578), 329-335. doi: 10.1038/nature15756

Hu, Y., Xie, J., Tong, Y. W., and Wang, C. H. (2007). Effect of PEG conformation and particle size on the cellular uptake efficiency of nanoparticles with the HepG2 cells. *J Control Release, 118*(1), 7-17. doi: 10.1016/j.jconrel.2006.11.028

Huang, S. L. (2008). Liposomes in ultrasonic drug and gene delivery. *Adv Drug Deliv Rev, 60*(10), 1167-1176. doi: 10.1016/j.addr.2008.03.003

Hung, M. E., and Leonard, J. N. (2015). Stabilization of exosome-targeting peptides via engineered glycosylation. *J Biol Chem, 290*(13), 8166-8172. doi: 10.1074/jbc.M114.621383

Inamdar, S., Nitiyanandan, R., and Rege, K. (2017). Emerging applications of exosomes in cancer therapeutics and diagnostics. *Bioeng Transl Med, 2*(1), 70-80. doi: 10.1002/btm2.10059

Inder, K. L., Ruelcke, J. E., Petelin, L., Moon, H., Choi, E., Rae, J., Blumenthal, A., Hutmacher, D., Saunders, N. A., Stow, J. L., Parton, R. G., and Hill, M. M. (2014). Cavin-1/PTRF alters prostate cancer cell-derived extracellular vesicle content and internalization to attenuate extracellular vesicle-mediated osteoclastogenesis and osteoblast proliferation. *J Extracell Vesicles, 3*. doi: 10.3402/jev.v3.23784

Ishida, T., Harada, M., Wang, X. Y., Ichihara, M., Irimura, K., and Kiwada, H. (2005). Accelerated blood clearance of PEGylated liposomes following preceding liposome injection: effects of lipid dose and PEG surface-density and chain length of the first-dose liposomes. *J Control Release, 105*(3), 305-317. doi: 10.1016/j.jconrel.2005.04.003

Ishida, T., Harashima, H., and Kiwada, H. (2001). Interactions of liposomes with cells in vitro and in vivo: opsonins and receptors. *Curr Drug Metab, 2*(4), 397-409.

Ishida, T., Harashima, H., and Kiwada, H. (2002). Liposome clearance. *Biosci Rep, 22*(2), 197-224.

Ishida, T., Iden, D. L., and Allen, T. M. (1999). A combinatorial approach to producing sterically stabilized (Stealth) immunoliposomal drugs. *FEBS Lett, 460*(1), 129-133.

Jiang, X. C., and Gao, J. Q. (2017). Exosomes as novel bio-carriers for gene and drug delivery. *Int J Pharm, 521*(1-2), 167-175. doi: 10.1016/j.ijpharm.2017.02.038

Johnsen, K. B., Gudbergsson, J. M., Skov, M. N., Pilgaard, L., Moos, T., and Duroux, M. (2014). A comprehensive overview of exosomes as drug delivery vehicles - endogenous nanocarriers for targeted cancer therapy. *Biochim Biophys Acta, 1846*(1), 75-87. doi: 10.1016/j.bbcan.2014.04.005

Jokerst, J. V., Lobovkina, T., Zare, R. N., and Gambhir, S. S. (2011). Nanoparticle PEGylation for imaging and therapy. *Nanomedicine (Lond), 6*(4), 715-728. doi: 10.2217/nnm.11.19

Kamerkar, S., LeBleu, V. S., Sugimoto, H., Yang, S., Ruivo, C. F., Melo, S. A., Lee, J. J., and Kalluri, R. (2017). Exosomes facilitate therapeutic targeting of oncogenic KRAS in pancreatic cancer. *Nature, 546*(7659), 498-503. doi: 10.1038/nature22341

Kawanishi, M., Hashimoto, Y., Shimizu, T., Sagawa, I., Ishida, T., and Kiwada, H. (2015). Comprehensive analysis of PEGylated liposome-associated proteins relating to the accelerated blood clearance phenomenon by combination with shotgun analysis and conventional methods. *Biotechnol Appl Biochem, 62*(4), 547-555. doi: 10.1002/bab.1291

Keerthikumar, S., Chisanga, D., Ariyaratne, D., Al Saffar, H., Anand, S., Zhao, K., Samuel, M., Pathan, M., Jois, M., Chilamkurti, N., Gangoda, L., and Mathivanan, S. (2016). ExoCarta: A Web-Based Compendium of Exosomal Cargo. *J Mol Biol, 428*(4), 688-692. doi: 10.1016/j.jmb.2015.09.019

Kim, M. S., Haney, M. J., Zhao, Y., Mahajan, V., Deygen, I., Klyachko, N. L., Inskoe, E., Piroyan, A., Sokolsky, M., Okolie, O., Hingtgen, S. D., Kabanov, A. V., and Batrakova, E. V. (2016). Development of exosome-encapsulated paclitaxel to overcome MDR in cancer cells. *Nanomedicine, 12*(3), 655-664. doi: 10.1016/j.nano.2015.10.012

Kočišová, E., Antalík, A., and Procházka, M. (2013). Drop coating deposition Raman spectroscopy of liposomes: role of cholesterol. *Chem Phys Lipids, 172-173*, 1-5. doi: 10.1016/j.chemphyslip.2013.04.002

Koivusalo, M., Welch, C., Hayashi, H., Scott, C. C., Kim, M., Alexander, T., Touret, N., Hahn, K. M., and Grinstein, S. (2010). Amiloride inhibits macropinocytosis by lowering submembranous pH and preventing Rac1 and Cdc42 signaling. *J Cell Biol, 188*(4), 547-563. doi: 10.1083/jcb.200908086

Kooijmans, S. A., Vader, P., van Dommelen, S. M., van Solinge, W. W., and Schiffelers, R. M. (2012). Exosome mimetics: a novel class of drug delivery systems. *Int J Nanomedicine, 7*, 1525-1541. doi: 10.2147/IJN.S29661

Kooijmans, S. A. A., Fliervoet, L. A. L., van der Meel, R., Fens, M., Heijnen, H. F. G., van Bergen En Henegouwen, P. M. P., Vader, P., and Schiffelers, R. M. (2016). PEGylated and targeted extracellular vesicles display enhanced cell specificity and circulation time. *J Control Release, 224*, 77-85. doi: 10.1016/j.jconrel.2016.01.009

Lachenal, G., Pernet-Gallay, K., Chivet, M., Hemming, F. J., Belly, A., Bodon, G., Blot, B., Haase, G., Goldberg, Y., and Sadoul, R. (2011). Release of exosomes from differentiated neurons and its regulation by synaptic glutamatergic activity. *Mol Cell Neurosci, 46*(2), 409-418. doi: 10.1016/j.mcn.2010.11.004

Lai, C. P., Mardini, O., Ericsson, M., Prabhakar, S., Maguire, C., Chen, J. W., Tannous, B. A., and Breakefield, X. O. (2014). Dynamic biodistribution of extracellular vesicles in vivo using a multimodal imaging reporter. *ACS Nano, 8*(1), 483-494. doi: 10.1021/nn404945r

Lakhal, S., and Wood, M. J. (2011). Exosome nanotechnology: an emerging paradigm shift in drug delivery: exploitation of exosome nanovesicles for systemic in vivo delivery of RNAi heralds new horizons for drug delivery across biological barriers. *Bioessays, 33*(10), 737-741. doi: 10.1002/bies.201100076

Lane, R. E., Korbie, D., Anderson, W., Vaidyanathan, R., and Trau, M. (2015). Analysis of exosome purification methods using a model liposome system and tunable-resistive pulse sensing. *Sci Rep, 5*, 7639. doi: 10.1038/srep07639

Lee, Y., El Andaloussi, S., and Wood, M. J. (2012). Exosomes and microvesicles: extracellular vesicles for genetic information transfer and gene therapy. *Hum Mol Genet, 21*(R1), R125-134. doi: 10.1093/hmg/dds317

Lespagnol, A., Duflaut, D., Beekman, C., Blanc, L., Fiucci, G., Marine, J. C., Vidal, M., Amson, R., and Telerman, A. (2008). Exosome secretion, including the DNA damage-induced p53-dependent secretory pathway, is severely compromised in TSAP6/Steap3-null mice. *Cell Death Differ, 15*(11), 1723-1733. doi: 10.1038/cdd.2008.104

Li, J., Lee, Y., Johansson, H. J., Mager, I., Vader, P., Nordin, J. Z., Wiklander, O. P., Lehtio, J., Wood, M. J., and Andaloussi, S. E. (2015). Serum-free culture alters the quantity and protein composition of neuroblastoma-derived extracellular vesicles. *J Extracell Vesicles, 4*, 26883. doi: 10.3402/jev.v4.26883

Li, P., Kaslan, M., Lee, S. H., Yao, J., and Gao, Z. (2017). Progress in Exosome Isolation Techniques. *Theranostics, 7*(3), 789-804. doi: 10.7150/thno.18133

Liu, L., Shi, H., Chen, X., and Wang, Z. (2011). Regulation of EGF-stimulated EGF receptor endocytosis during M phase. *Traffic, 12*(2), 201-217. doi: 10.1111/j.1600-0854.2010.01141.x

Lo Cicero, A., Stahl, P. D., and Raposo, G. (2015). Extracellular vesicles shuffling intercellular messages: for good or for bad. *Curr Opin Cell Biol, 35*, 69-77. doi: 10.1016/j.ceb.2015.04.013

Lu, M., Xing, H., Yang, Z., Sun, Y., Yang, T., Zhao, X., Cai, C., Wang, D., and Ding, P. (2017). Recent advances on extracellular vesicles in therapeutic delivery: Challenges, solutions, and opportunities. *Eur J Pharm Biopharm, 119*, 381-395. doi: 10.1016/j.ejpb.2017.07.010

McKelvey, K. J., Powell, K. L., Ashton, A. W., Morris, J. M., and McCracken, S. A. (2015). Exosomes: Mechanisms of Uptake. *J Circ Biomark, 4*, 7. doi: 10.5772/61186

Meister, M., and Tikkanen, R. (2014). Endocytic trafficking of membrane-bound cargo: a flotillin point of view. *Membranes (Basel), 4*(3), 356-371. doi: 10.3390/membranes4030356

Montecalvo, A., Larregina, A. T., Shufesky, W. J., Stolz, D. B., Sullivan, M. L., Karlsson, J. M., Baty, C. J., Gibson, G. A., Erdos, G., Wang, Z., Milosevic, J., Tkacheva, O. A., Divito, S. J., Jordan, R., Lyons-Weiler, J., Watkins, S. C., and Morelli, A. E. (2012). Mechanism of transfer of functional microRNAs between mouse dendritic cells via exosomes. *Blood, 119*(3), 756-766. doi: 10.1182/blood-2011-02-338004

Moreira, J. N., Ishida, T., Gaspar, R., and Allen, T. M. (2002). Use of the post-insertion technique to insert peptide ligands into pre-formed stealth liposomes with retention of binding activity and cytotoxicity. *Pharm Res, 19*(3), 265-269.

Morelli, A. E., Larregina, A. T., Shufesky, W. J., Sullivan, M. L., Stolz, D. B., Papworth, G. D., Zahorchak, A. F., Logar, A. J., Wang, Z., Watkins, S. C., Falo, L. D., Jr., and Thomson, A. W. (2004). Endocytosis, intracellular sorting, and processing of exosomes by dendritic cells. *Blood, 104*(10), 3257-3266. doi: 10.1182/blood-2004-03-0824

Mulcahy, L. A., Pink, R. C., and Carter, D. R. (2014). Routes and mechanisms of extracellular vesicle uptake. *J Extracell Vesicles, 3*. doi: 10.3402/jev.v3.24641

Narayanan, A., Iordanskiy, S., Das, R., Van Duyne, R., Santos, S., Jaworski, E., Guendel, I., Sampey, G., Dalby, E., Iglesias-Ussel, M., Popratiloff, A., Hakami, R., Kehn-Hall, K., Young, M., Subra, C., Gilbert, C., Bailey, C., Romerio, F., and Kashanchi, F. (2013). Exosomes derived from HIV-1-infected cells contain trans-activation response element RNA. *J Biol Chem, 288*(27), 20014-20033. doi: 10.1074/jbc.M112.438895

Ohno, S., Takanashi, M., Sudo, K., Ueda, S., Ishikawa, A., Matsuyama, N., Fujita, K., Mizutani, T., Ohgi, T., Ochiya, T., Gotoh, N., and Kuroda, M. (2013). Systemically injected exosomes targeted to EGFR deliver antitumor microRNA to breast cancer cells. *Mol Ther, 21*(1), 185-191. doi: 10.1038/mt.2012.180

Otto, G. P., and Nichols, B. J. (2011). The roles of flotillin microdomains--endocytosis and beyond. *J Cell Sci, 124*(Pt 23), 3933-3940. doi: 10.1242/jcs.092015

Park, J. W. (2002). Liposome-based drug delivery in breast cancer treatment. *Breast Cancer Res, 4*(3), 95-99.

Parolini, I., Federici, C., Raggi, C., Lugini, L., Palleschi, S., De Milito, A., Coscia, C., Iessi, E., Logozzi, M., Molinari, A., Colone, M., Tatti, M., Sargiacomo, M., and Fais, S. (2009). Microenvironmental pH is a key factor for exosome traffic in tumor cells. *J Biol Chem, 284*(49), 34211-34222. doi: 10.1074/jbc.M109.041152

Patel, D. B., Gray, K. M., Santharam, Y., Lamichhane, T. N., Stroka, K. M., and Jay, S. M. (2017). Impact of cell culture parameters on production and vascularization bioactivity of mesenchymal stem cell-derived extracellular vesicles. *Bioeng Transl Med, 2*(2), 170-179. doi: 10.1002/btm2.10065

Petty, A. J., and Yang, Y. (2017). Tumor-associated macrophages: implications in cancer immunotherapy. *Immunotherapy, 9*(3), 289-302. doi: 10.2217/imt-2016-0135

Raposo, G., and Stoorvogel, W. (2013). Extracellular vesicles: exosomes, microvesicles, and friends. *J Cell Biol, 200*(4), 373-383. doi: 10.1083/jcb.201211138

Riches, A., Campbell, E., Borger, E., and Powis, S. (2014). Regulation of exosome release from mammary epithelial and breast cancer cells - a new regulatory pathway. *Eur J Cancer, 50*(5), 1025-1034. doi: 10.1016/j.ejca.2013.12.019

Saari, H., Lazaro-Ibanez, E., Viitala, T., Vuorimaa-Laukkanen, E., Siljander, P., and Yliperttula, M. (2015). Microvesicle- and exosome-mediated drug delivery enhances the cytotoxicity of Paclitaxel in autologous prostate cancer cells. *J Control Release, 220*(Pt B), 727-737. doi: 10.1016/j.jconrel.2015.09.031

Sampath, P., and Pollard, T. D. (1991). Effects of cytochalasin, phalloidin, and pH on the elongation of actin filaments. *Biochemistry, 30*(7), 1973-1980.

Savina, A., Fader, C. M., Damiani, M. T., and Colombo, M. I. (2005). Rab11 promotes docking and fusion of multivesicular bodies in a calcium-dependent manner. *Traffic, 6*(2), 131-143. doi: 10.1111/j.1600-0854.2004.00257.x

Shrestha, R., Elsabahy, M., Florez-Malaver, S., Samarajeewa, S., and Wooley, K. L. (2012). Endosomal escape and siRNA delivery with cationic shell crosslinked knedel-like nanoparticles with tunable buffering capacities. *Biomaterials, 33*(33), 8557-8568. doi: 10.1016/j.biomaterials.2012.07.054

Smyth, T., Kullberg, M., Malik, N., Smith-Jones, P., Graner, M. W., and Anchordoquy, T. J. (2015). Biodistribution and delivery efficiency of unmodified tumor-derived exosomes. *J Control Release, 199*, 145-155. doi: 10.1016/j.jconrel.2014.12.013

Smyth, T. J., Redzic, J. S., Graner, M. W., and Anchordoquy, T. J. (2014). Examination of the specificity of tumor cell derived exosomes with tumor cells in vitro. *Biochim Biophys Acta, 1838*(11), 2954-2965. doi: 10.1016/j.bbamem.2014.07.026

Socaciu, C., Jessel, R., and Diehl, H. A. (2000). Competitive carotenoid and cholesterol incorporation into liposomes: effects on membrane phase transition, fluidity, polarity and anisotropy. *Chem Phys Lipids, 106*(1), 79-88.

Stremersch, S., De Smedt, S. C., and Raemdonck, K. (2016). Therapeutic and diagnostic applications of extracellular vesicles. *J Control Release, 244*(Pt B), 167-183. doi: 10.1016/j.jconrel.2016.07.054

Suk, J. S., Xu, Q., Kim, N., Hanes, J., and Ensign, L. M. (2016). PEGylation as a strategy for improving nanoparticle-based drug and gene delivery. *Adv Drug Deliv Rev, 99*(Pt A), 28-51. doi: 10.1016/j.addr.2015.09.012

Sunkara, V., Woo, H. K., and Cho, Y. K. (2016). Emerging techniques in the isolation and characterization of extracellular vesicles and their roles in cancer diagnostics and prognostics. *Analyst, 141*(2), 371-381. doi: 10.1039/c5an01775k

Svensson, K. J., Christianson, H. C., Wittrup, A., Bourseau-Guilmain, E., Lindqvist, E., Svensson, L. M., Morgelin, M., and Belting, M. (2013). Exosome uptake depends on ERK1/2-heat shock protein 27 signaling and lipid Raft-mediated endocytosis negatively regulated by caveolin-1. *J Biol Chem, 288*(24), 17713-17724. doi: 10.1074/jbc.M112.445403

Taieb, J., Chaput, N., Schartz, N., Roux, S., Novault, S., Menard, C., Ghiringhelli, F., Terme, M., Carpentier, A. F., Darrasse-Jeze, G., Lemonnier, F., and Zitvogel, L. (2006). Chemoimmunotherapy of tumors: cyclophosphamide synergizes with exosome based vaccines. *J Immunol, 176*(5), 2722-2729.

Takahashi, Y., Nishikawa, M., Shinotsuka, H., Matsui, Y., Ohara, S., Imai, T., and Takakura, Y. (2013). Visualization and in vivo tracking of the exosomes of murine melanoma B16-BL6 cells in mice after intravenous injection. *J Biotechnol, 165*(2), 77-84. doi: 10.1016/j.jbiotec.2013.03.013

Tan, A., De La Pena, H., and Seifalian, A. M. (2010). The application of exosomes as a nanoscale cancer vaccine. *Int J Nanomedicine, 5*, 889-900. doi: 10.2147/IJN.S13402

Tan, A., Rajadas, J., and Seifalian, A. M. (2013). Exosomes as nano-theranostic delivery platforms for gene therapy. *Adv Drug Deliv Rev, 65*(3), 357-367. doi: 10.1016/j.addr.2012.06.014

Théry, C., Amigorena, S., Raposo, G., and Clayton, A. (2006). Isolation and Characterization of Exosomes from Cell Culture Supernatants and Biological Fluids. *Current Protocols in Cell Biology, 30*(1), 3.22.21-23.22.29. doi: 10.1002/0471143030.cb0322s30

Théry, C., Zitvogel, L., and Amigorena, S. (2002). Exosomes: composition, biogenesis and function. *Nature Reviews Immunology, 2*, 569. doi: 10.1038/nri855

Tian, T., Wang, Y., Wang, H., Zhu, Z., and Xiao, Z. (2010). Visualizing of the cellular uptake and intracellular trafficking of exosomes by live-cell microscopy. *J Cell Biochem, 111*(2), 488-496. doi: 10.1002/jcb.22733

Tian, T., Zhu, Y. L., Zhou, Y. Y., Liang, G. F., Wang, Y. Y., Hu, F. H., and Xiao, Z. D. (2014a). Exosome uptake through clathrin-mediated endocytosis and macropinocytosis and mediating miR-21 delivery. *J Biol Chem, 289*(32), 22258-22267. doi: 10.1074/jbc.M114.588046

Tian, Y., Li, S., Song, J., Ji, T., Zhu, M., Anderson, G. J., Wei, J., and Nie, G. (2014b). A doxorubicin delivery platform using engineered natural membrane vesicle exosomes for targeted tumor therapy. *Biomaterials, 35*(7), 2383-2390. doi: 10.1016/j.biomaterials.2013.11.083

Tickner, J. A., Urquhart, A. J., Stephenson, S. A., Richard, D. J., and O'Byrne, K. J. (2014). Functions and therapeutic roles of exosomes in cancer. *Front Oncol, 4*, 127. doi: 10.3389/fonc.2014.00127

Toda, Y., Takata, K., Nakagawa, Y., Kawakami, H., Fujioka, S., Kobayashi, K., Hattori, Y., Kitamura, Y., Akaji, K., and Ashihara, E. (2015). Effective internalization of U251-MG-secreted exosomes into cancer cells and characterization of their lipid components. *Biochem Biophys Res Commun, 456*(3), 768-773. doi: 10.1016/j.bbrc.2014.12.015

Tominaga, N., Yoshioka, Y., and Ochiya, T. (2015). A novel platform for cancer therapy using extracellular vesicles. *Adv Drug Deliv Rev, 95*, 50-55. doi: 10.1016/j.addr.2015.10.002

Torchilin, V. P. (2014). Multifunctional, stimuli-sensitive nanoparticulate systems for drug delivery. *Nat Rev Drug Discov, 13*(11), 813-827. doi: 10.1038/nrd4333

Uz, M., Bulmus, V., and Alsoy Altinkaya, S. (2016). The Effect of PEG Grafting Density and Hydrodynamic Volume on Gold Nanoparticle-Cell Interactions: An Investigation on Cell Cycle, Apoptosis and DNA Damage. *Langmuir*. doi: 10.1021/acs.langmuir.6b01289

Vader, P., Mol, E. A., Pasterkamp, G., and Schiffelers, R. M. (2016). Extracellular vesicles for drug delivery. *Adv Drug Deliv Rev, 106*(Pt A), 148-156. doi: 10.1016/j.addr.2016.02.006

Van Deun, J., Mestdagh, P., Sormunen, R., Cocquyt, V., Vermaelen, K., Vandesompele, J., Bracke, M., De Wever, O., and Hendrix, A. (2014). The impact of disparate isolation methods for extracellular vesicles on downstream RNA profiling. *J Extracell Vesicles, 3*. doi: 10.3402/jev.v3.24858

van Dongen, H. M., Masoumi, N., Witwer, K. W., and Pegtel, D. M. (2016). Extracellular Vesicles Exploit Viral Entry Routes for Cargo Delivery. *Microbiol Mol Biol Rev, 80*(2), 369-386. doi: 10.1128/MMBR.00063-15

Vulpis, E., Cecere, F., Molfetta, R., Soriani, A., Fionda, C., Peruzzi, G., Caracciolo, G., Palchetti, S., Masuelli, L., Simonelli, L., D'Oro, U., Abruzzese, M. P., Petrucci, M. T., Ricciardi, M. R., Paolini, R., Cippitelli, M., Santoni, A., and Zingoni, A. (2017). Genotoxic stress modulates the release of exosomes from multiple myeloma cells capable of activating NK cell cytokine production: Role of HSP70/TLR2/NF-kB axis. *Oncoimmunology, 6*(3), e1279372. doi: 10.1080/2162402X.2017.1279372

Wang, J., Zheng, Y., and Zhao, M. (2016a). Exosome-Based Cancer Therapy: Implication for Targeting Cancer Stem Cells. *Front Pharmacol, 7*, 533. doi: 10.3389/fphar.2016.00533

Wang, L. H., Rothberg, K. G., and Anderson, R. G. (1993). Mis-assembly of clathrin lattices on endosomes reveals a regulatory switch for coated pit formation. *J Cell Biol, 123*(5), 1107-1117.

Wang, S., Sun, H., Tanowitz, M., Liang, X. H., and Crooke, S. T. (2016b). Annexin A2 facilitates endocytic trafficking of antisense oligonucleotides. *Nucleic Acids Res, 44*(15), 7314-7330. doi: 10.1093/nar/gkw595

Wang, Y., Chen, X., Tian, B., Liu, J., Yang, L., Zeng, L., Chen, T., Hong, A., and Wang, X. (2017). Nucleolin-targeted Extracellular Vesicles as a Versatile Platform for Biologics Delivery to Breast Cancer. *Theranostics, 7*(5), 1360-1372. doi: 10.7150/thno.16532

Whiteside, T. L. (2016). Tumor-Derived Exosomes and Their Role in Cancer Progression. *Adv Clin Chem, 74*, 103-141. doi: 10.1016/bs.acc.2015.12.005

Whiteside, T. L. (2017). Exosomes in Cancer: Another Mechanism of Tumor-Induced Immune Suppression. *Adv Exp Med Biol, 1036*, 81-89. doi: 10.1007/978-3-319-67577-0_6

Wolfers, J., Lozier, A., Raposo, G., Regnault, A., Thery, C., Masurier, C., Flament, C., Pouzieux, S., Faure, F., Tursz, T., Angevin, E., Amigorena, S., and Zitvogel, L. (2001). Tumor-derived exosomes are a source of shared tumor rejection antigens for CTL cross-priming. *Nat Med, 7*(3), 297-303. doi: 10.1038/85438

Xu, R., Greening, D. W., Zhu, H. J., Takahashi, N., and Simpson, R. J. (2016). Extracellular vesicle isolation and characterization: toward clinical application. *J Clin Invest, 126*(4), 1152-1162. doi: 10.1172/JCI81129

Yang, T., Martin, P., Fogarty, B., Brown, A., Schurman, K., Phipps, R., Yin, V. P., Lockman, P., and Bai, S. (2015). Exosome delivered anticancer drugs across the blood-brain barrier for brain cancer therapy in Danio rerio. *Pharm Res, 32*(6), 2003-2014. doi: 10.1007/s11095-014-1593-y

Yao, Y., Wei, W., Sun, J., Chen, L., Deng, X., Ma, L., and Hao, S. (2015). Proteomic analysis of exosomes derived from human lymphoma cells. *Eur J Med Res, 20*(1), 8. doi: 10.1186/s40001-014-0082-4

Yim, N., Ryu, S. W., Choi, K., Lee, K. R., Lee, S., Choi, H., Kim, J., Shaker, M. R., Sun, W., Park, J. H., Kim, D., Heo, W. D., and Choi, C. (2016). Exosome engineering for efficient intracellular delivery of soluble proteins using optically reversible protein-protein interaction module. *Nat Commun, 7*, 12277. doi: 10.1038/ncomms12277

Zanganeh, S., Spitler, R., Hutter, G., Ho, J. Q., Pauliah, M., and Mahmoudi, M. (2017). Tumor-associated macrophages, nanomedicine and imaging: the axis of success in the future of cancer immunotherapy. *Immunotherapy, 9*(10), 819-835. doi: 10.2217/imt-2017-0041

Zhang, Y., Satterlee, A., and Huang, L. (2012). In vivo gene delivery by nonviral vectors: overcoming hurdles? *Mol Ther, 20*(7), 1298-1304. doi: 10.1038/mt.2012.79

Zhou, Y., Xu, H., Xu, W., Wang, B., Wu, H., Tao, Y., Zhang, B., Wang, M., Mao, F., Yan, Y., Gao, S., Gu, H., Zhu, W., and Qian, H. (2013). Exosomes released by human umbilical cord mesenchymal stem cells protect against cisplatin-induced renal oxidative stress and apoptosis in vivo and in vitro. *Stem Cell Res Ther, 4*(2), 34. doi: 10.1186/scrt194

Zhuang, X., Xiang, X., Grizzle, W., Sun, D., Zhang, S., Axtell, R. C., Ju, S., Mu, J., Zhang, L., Steinman, L., Miller, D., and Zhang, H. G. (2011). Treatment of brain inflammatory diseases by delivering exosome encapsulated anti-inflammatory drugs from the nasal region to the brain. *Mol Ther, 19*(10), 1769-1779. doi: 10.1038/mt.2011.164

Zitvogel, L., Regnault, A., Lozier, A., Wolfers, J., Flament, C., Tenza, D., Ricciardi-Castagnoli, P., Raposo, G., and Amigorena, S. (1998). Eradication of established murine tumors

using a novel cell-free vaccine: dendritic cell-derived exosomes. *Nat Med, 4*(5), 594-600.

Zlotogorski-Hurvitz, A., Dayan, D., Chaushu, G., Korvala, J., Salo, T., Sormunen, R., and Vered, M. (2015). Human saliva-derived exosomes: comparing methods of isolation. *J Histochem Cytochem, 63*(3), 181-189. doi: 10.1369/0022155414564219